REPORT A405
6 January 1964

92p.

UNPUBLISHED PRELIMINARY DATA

OPTIMUM DIGITAL ADAPTIVE ATTITUDE CONTROL SYSTEM FOR SPACE VEHICLES

Final Report

NASw -614(SC-4734)

MCDONNELL
ELECTRONIC EQUIPMENT DIVISION

REPORT A405
6 January 1964

OPTIMUM DIGITAL ADAPTIVE ATTITUDE CONTROL SYSTEM FOR SPACE VEHICLES

Final Report

(NASA NASw-614(SC-4734))

(NASA CR-53109; A405) OTS: $ 8.60 ph, $ 2.96 mf

James C. Bowers 6 Jan. 1964 92p

[2]

[X] OTS

Copy No. 1

Prepared by:

James C. Bowers
Senior Group Engineer, Electronics

Approved by:

E. C. Lindenberg
Manager, Guidance and Control

Approved by:

W. I. Harris
Section Manager
Control and Instrumentation

Approved by:

John C. Cosby
Manager, Engineering

McDONNELL Aircraft Corp., St. Louis, Mo.

(2) ELECTRONIC EQUIPMENT DIVISION

TABLE OF CONTENTS

TABLE OF CONTENTS

FIGURES

FIGURES

FIGURES

TABLES

1. INTRODUCTION

This Final Report summarizes the Electronic Equipment Division (EED) investigation of the Optimum Digital Adaptive Attitude Control System (ODAACS). The System is discussed in detail in McDonnell Report A005, the first progress report submitted in accordance with contract NASw-614(SC-4734).

Section 2 discusses program design changes which have been incorporated since the submission of McDonnell Report A005. The modifications resulted in improved performance of both the optimum switching and limit cycle programs.

The feasibility of the ODAACS concept is demonstrated in Section 3 which includes plots of simulated trajectories and the effects of all parameter variations to which the system is expected to adapt. Limit cycle performance in the presence of bias and disturbance torques is presented in Paragraph 3.4. Paragraph 3.5 discusses the effect of the quantizing step on system stability. Switching accuracy in the optimum switching program is analyzed in Paragraph 3.6.

A parametric study of fuel consumption and speed of response as a function of system configuration is contained in Section 4. The effects of sensor accuracy are investigated in Section 5 which establishes minimum accuracy requirements for successful control program performance.

Airborne computer requirements and pertinent program characteristics affecting the requirements are discussed in Section 6 while overall program results and a summary of future work and program additions are considered in Section 7.

2. PROGRAM MODIFICATIONS

2.1 General. Several improvements in system performance were accomplished through program changes during this reporting period.

2.2 Optimum Switching Program Modifications. The optimum switching program adapts to alterations in the torque to inertia ratio caused by changes in inertia, torque or a combination of both through derivation of effective plant acceleration. If acceleration changes drastically, there is a possibility that the limit cycle will not be acquired after the first switchover if the K_n or K_p which defines the switching line has not been updated. Exact updating of the constant cannot be accomplished until appropriate polarity torque has been applied.

One of the principal control objectives is acquisition of the limit cycye on the first switch, irrespective of drastic changes in system parameters. Since torque changes caused by changes in length of the moment arm, motion of the center of gravity, partial thruster malfunction and thruster misalignment are relatively minor, it is reasoned that any large deviation in the torque to inertia ratio results from changes in the inertia caused by acquisition or jettisoning of a large percentage of the initial mass of the plant. A modification based on this reasoning is incorporated into the optimum switching program.

After derivation of the acceleration and computation of K_n or K_p, the last computed constant is compared with the previous K_n or K_p to determine whether a deviation of more than 50 per cent has occurred. The inequality, written in terms of K_p, senses the change.

$$\left| (K_p)_n - (K_p)_{n-1} \right| - 0.5 (K_p)_{n-1} \geq 0 \qquad (1)$$

If Equation (1) is true, a change of 50 per cent or more has occurred in K_p. Since a large inertia deviation is responsible for the change, both the positive and negative accelerations are affected approximately equally. The constant in switching Equation (2) is then made equal to the K_p just computed.

$$\varphi(\theta + 2K\dot{\theta}|\dot{\theta}|) \leq 0 \qquad (2)$$

The substitution remains in effect until the actual value of K_n is computed on the next pass. In this case the last computed value of K_n is not affected, thus allowing for the possibility that the drastic change actually resulted from a malfunction of the positive torquer. If the change is caused by a thruster malfunction, the limit cycle will not be acquired on the first switchover; however, overall system stability is not affected.

When no significant deviation occurs in K_p, the constant in Equation (2) is K_n. This is the normal situation, the switching equation generally based upon the appropriate values of K_n or K_p. The program change is reflected in the flow diagram of Figure 1.

Logic also is incorporated in the optimum switching program to accommodate initial control acquisition at turn-on. It is anticipated that the initial state of the system can lie anywhere in the phase plane. The unmodified optimum switching program chooses the proper torque to be applied, proceeds with the acceleration derivation and seeks the proper switchover point.

Several effects detrimental to system performance result from this logic. If initial rates are high, the system may make the rates even higher before reducing them to zero. The derivation of acceleration is then inaccurate, affecting the constant employed in the switching equation and causing erroneous switching. It is therefore desirable to confine the acceleration derivation to relatively low rates and to make a thrust application decision which always

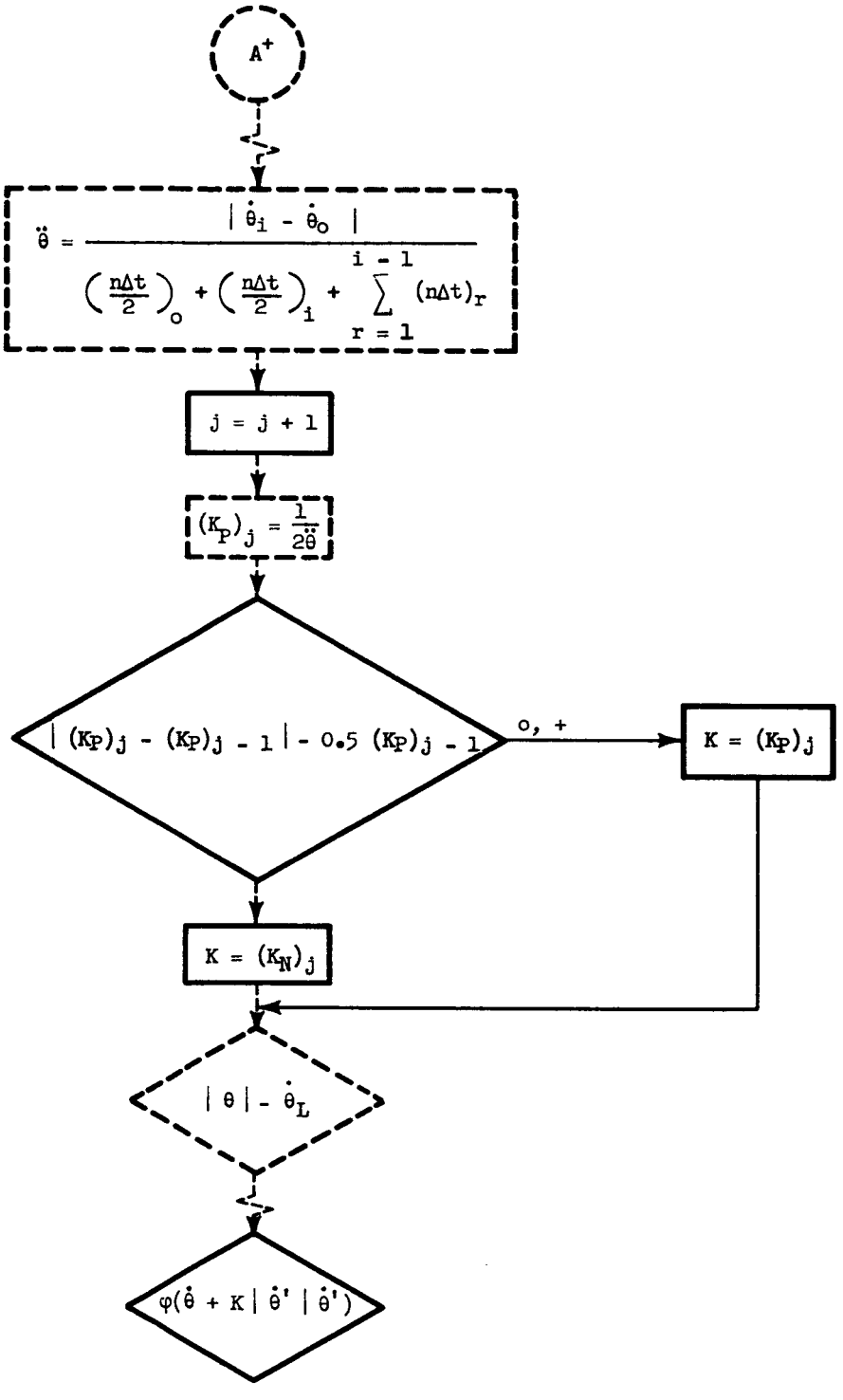

SWITCHING CONSTANT CHANGE
FIGURE 1

reduces the initial rates of the plant.

Additional logic incorporated into the optimum switching program to accomplish the improvements is presented in Figure 2. The logic basically subdivides the phase plane into the regions indicated in Figure 3. The program applies no torque when the rate is higher than $\dot{\theta}_L$ and of such polarity as to cause the plant to drift in the direction of the switching curve. If the initial rate is less than $\dot{\theta}_L$ but greater than $\dot{\theta}_c$, the acceleration derivation is bypassed, thus eliminating erroneous computations. Accordingly, acceleration is derived only if the magnitude of the rate is less than $\dot{\theta}_c$, a relatively low rate (e.g., one degree per second). If the initial rate is higher than $\dot{\theta}_L$ but of such polarity as to cause the system to drift away from the switching line, appropriate torque is applied, acceleration derivation is bypassed and the switchover point is computed on the basis of the best previous information. This is also the case when the rate is greater than $\dot{\theta}_c$ and less than $\dot{\theta}_L$.

2.3 Limit Cycle Program Modifications. Final limit cycle rates are established by the choice of $\dot{\theta}_p$ and $\dot{\theta}_n$. Values assigned to these quantities vary with application and are based upon anticipated minimum impulse available from the torquers. The minimum repeatable impulse causes a rate change equal to $\dot{\theta}_p - \dot{\theta}_n$. Thus, if the vehicle is in the limit cycle to a rate equal to $\dot{\theta}_p$, the minimum impulse reverses the motion of the vehicle at a rate of $\dot{\theta}_n$.

A provision is now made to take advantage of the possibility that the minimum repeatable impulse is smaller than that anticipated by the manufacturer. If the minimum impulse is regarded as a minimum rate change capability, it can be seen that the minimum impulse diminishes as the inertia of the plant increases. Therefore, the capability exists to establish lower limit cycle

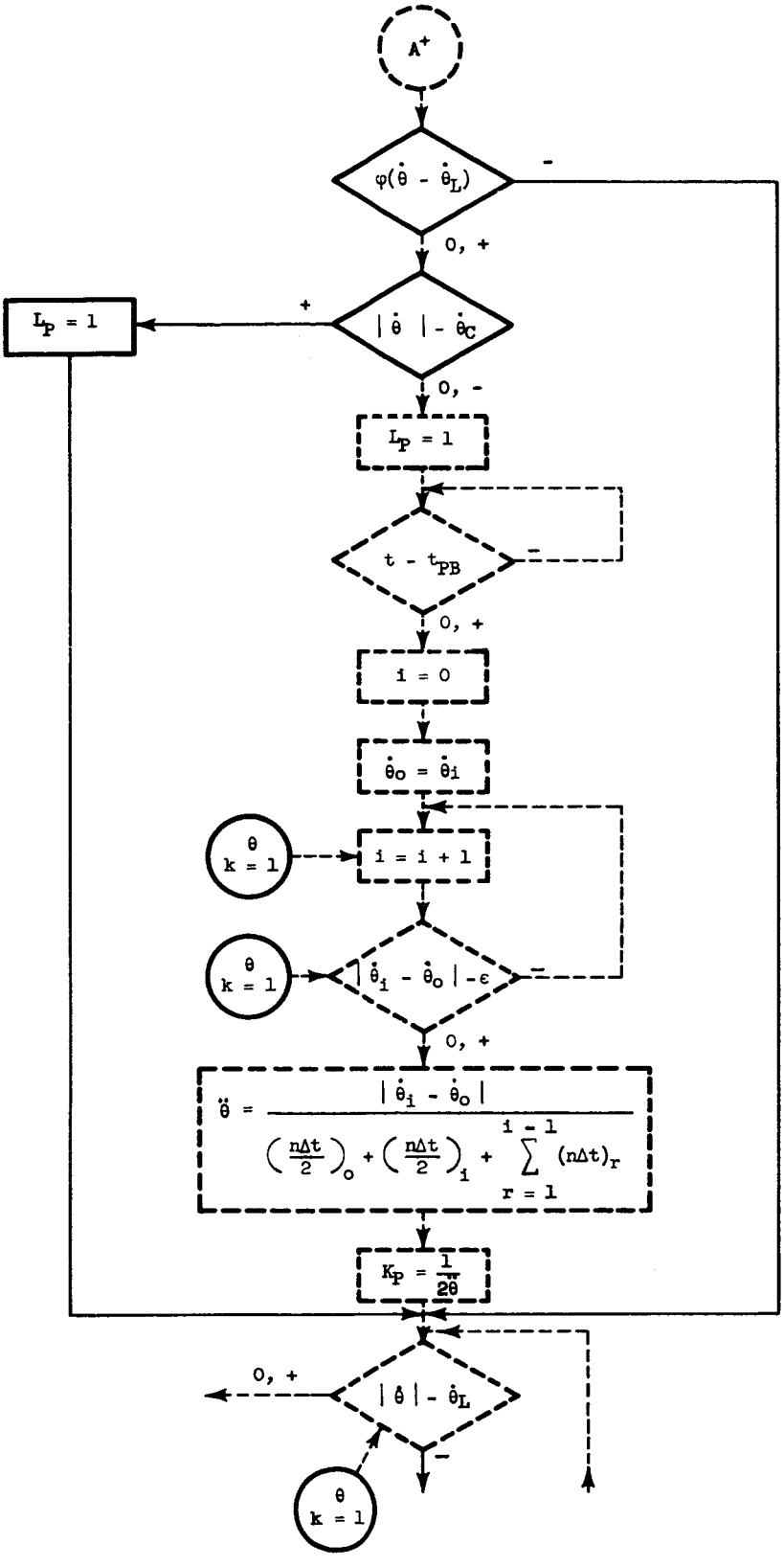

ACCELERATION DERIVATION LOGIC

FIGURE 2

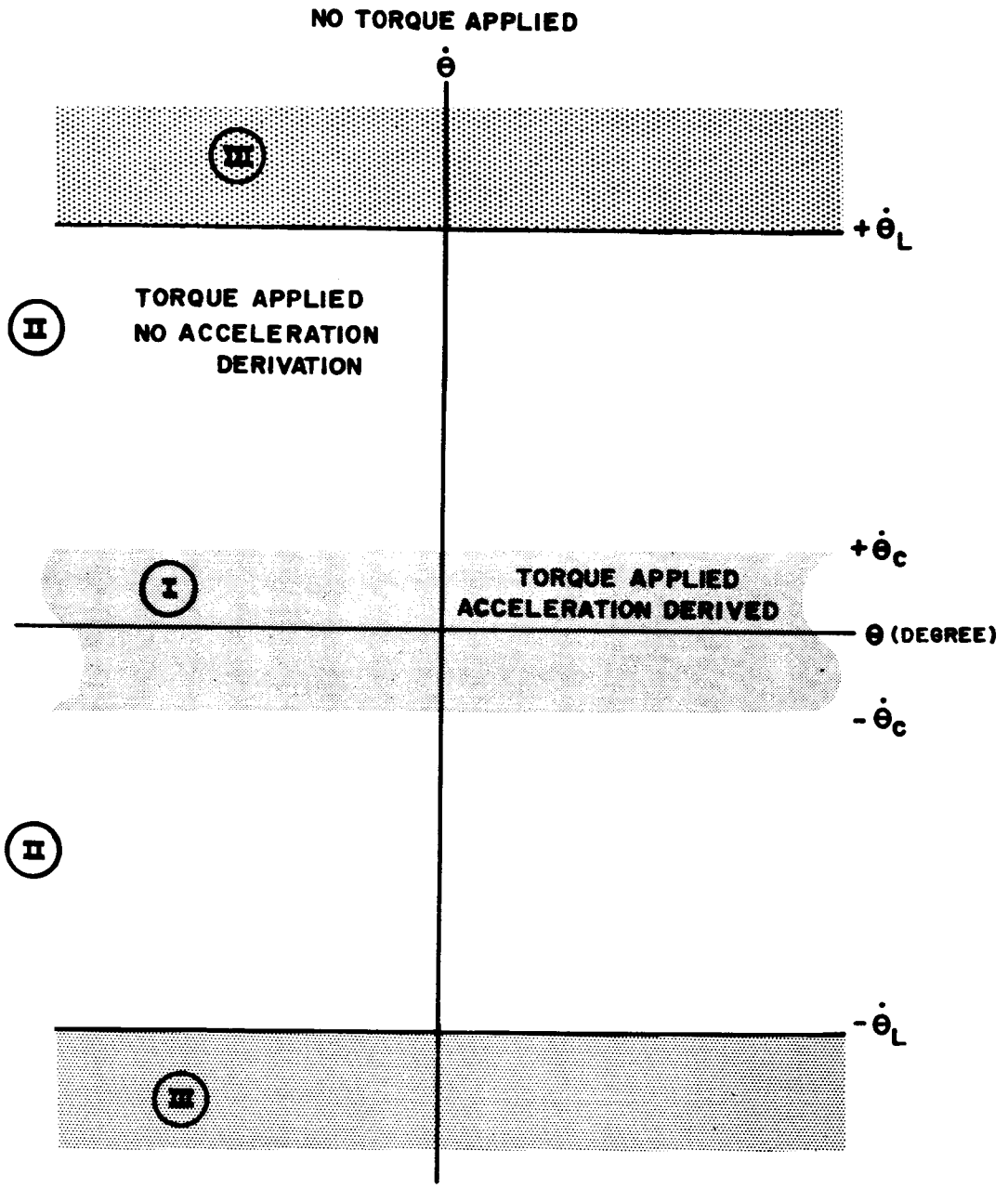

PHASE PLANE LOGIC FOR ACCELERATION DERIVATION

FIGURE 3

rates with the same torquers. A modification is incorporated in the limit cycle program to capitalize upon this capability.

Adaptation of the positive and negative impulse time constants is based upon the error created in attempting to establish $\dot{\theta}_n$ or $\dot{\theta}_p$. Application of a minimum impulse that results in a rate having a magnitude lower than $\dot{\theta}_n$ or $\dot{\theta}_p$ could be caused by a lower repeatable minimum impulse capability or a nonrepeatable smaller impulse. For larger inertia, this effect is definitely repeatable.

The limit cycle program now includes logic which basically interprets the thrust application results and decides whether to correct t_{px} or t_{nx}. If the resulting rate is of opposite sign to the rate before thrust application and of lower magnitude than the intended rate $\dot{\theta}_n$ or $\dot{\theta}_p$, t_{px} or t_{nx} is not corrected. Consequently, if the result was caused by a new repeatable minimum impulse, the limit cycle program establishes new lower rates. If the new impulse is not repeatable, no correction is made on the basis of nonrepeatable data. Logic tests to determine whether correction is necessary are given in Figure 4.

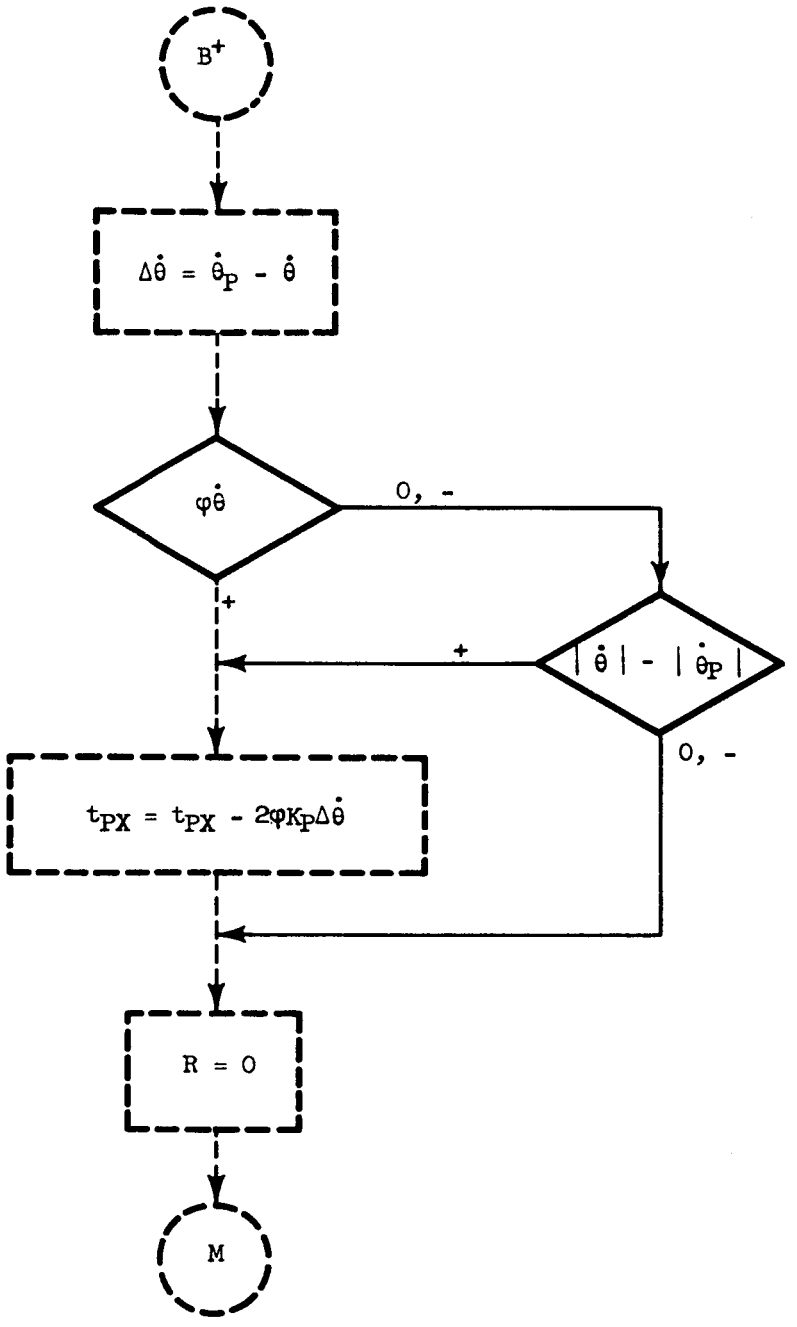

LIMIT CYCLE PROGRAM CHANGE

FIGURE 4

3. FEASIBILITY STUDY

3.1 Computer Simulation. The ODAACS control program is simulated on an IBM 7094 computer which also simulates the dynamics of the controlled plant. Tests performed to demonstrate ODAACS feasibility include programmed changes in inertia and torque, demonstrating control system stability and adaptability in the presence of such changes. Certain tests superimpose a bias torque on the system while others test the stability of the control system in the presence of impulse distrubance torques. Simulation runs demonstrate the effect of the theta subroutine quantizing step upon the accuracy and stability of the control program.

Switching accuracy of the optimum switching program as inertia increases is tested by removing the rate limit and permitting the initial error to increase to a full 180 degrees. The actual point in the phase plane at which switchover from positive to negative torque occurs is compared with the theoretical value at which switchover should have occurred. Analysis of the sources of error indicates which control parameters most affect accuracy.

3.2 Inertia Changes. Each test case begins with a plant inertia of 3,910 slug-feet squared, a thrust of 25 pounds and positive and negative thrust moment arms of 12 and 11 feet respectively. The following sequence of inputs is introduced.

(a) $\theta_o = 18^o$

(b) $\theta_o = -18^o$

(c) $\theta_o = 30^o$

(d) $\theta_o = -30^o$, $I = I_2$

(e) $\theta_o = 30^o$

(f) $\theta_o = -30^o$

The system is allowed to settle into the limit cycle oscillation between each input in the sequence. Step (d) in the input sequence is the point where inertia changes are introduced. Inputs (e) and (f) then demonstrate adaption to the new parameters. Figures 5 through 15 are plots of the phase plane trajectories which result from input changes. The large dynamic range of the variables, particularly the rate, necessitates splitting the trajectories into two plots. The optimum switching portion of the trajectory is presented separately from a greatly expanded plot of the resultant limit cycle. Numerical reference points on each pair of plots marry the two portions of each trajectory. Split presentations are used for all complete trajectories.

3.2.1 Test Results.

(a) Case Ia - The first three sequence inputs permit the ODAACS to adapt to the parameters which exist at the beginning of the run. The three inputs are repeated in each test case and for all future tests to prepare for the introduction of large parameter changes later in the program.

Initially, there is a small amount of nonsymmetry in the system. The positive moment arm is 12 feet and the negative moment arm 11 feet. Since the system commences operation symmetrically with nominal K_n and K_p stored in the program, the first three inputs in the sequence update the system.

The input at point a, Figure 5a, causes a negative torque to be applied and a negative acceleration is derived which establishes the proper switching curve for inputs of opposite polarity. After switchover has occurred at point b, the control program attempts to turn-off the acceleration, leaving the system with no residual rate. Results are evaluated and the turn-off time constant (t_{nc}) updated. Inputs at points c and d reflect this adaptation by

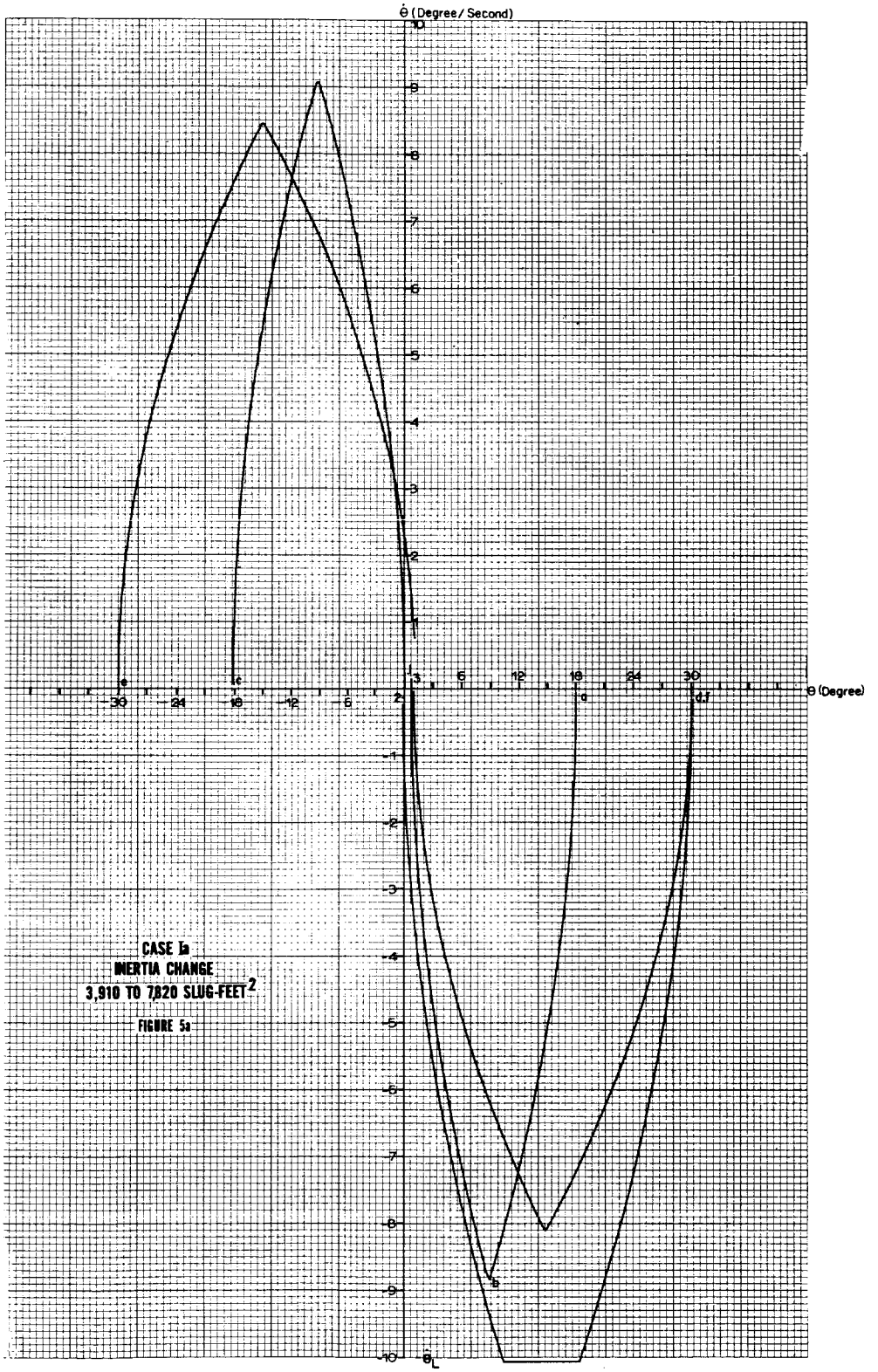

CASE 1a
INERTIA CHANGE
3,910 TO 7,820 SLUG-FEET^2
FIGURE 5a

switching at the proper time and turning off the system at a much lower rate.

A programmed change in the plant inertia is introduced at the time of the fourth input in the sequence. The inertia is increased from 3,910 to 7,820 slug-feet squared, point e in Figure 5a, which results in the immediate movement of the switching curve because of the magnitude of the change. The trajectory now enters the limit cycle logic box on the first attempt with an overshoot of 1.16 degrees. Since this is less than the two degrees at which θ_{L2} has been set for these tests, the limit cycle is acquired at once. The next input in the sequence starts the trajectory at point f. Switching now occurs at the proper place and, once again, the limit cycle is acquired.

Figure 5b illustrates the limit cycle trajectories resulting from successive inputs. The beginning points of the limit cycle paths are numbered sequentially to correspond to the appropriate optimum switching trajectory. In each limit cycle trajectory a limit cycle rate smaller than $\dot{\theta}_n$ or $\dot{\theta}_p$, entered into the control program as ±0.05 degree per second, is established.

(b) Case Ib - After the initial sequence of inputs updates the control parameters, an inertia increase from 3,910 to 15,664 slug-feet squared is introduced prior to the input at point d in Figure 6. The size of the increase again causes the switching curve to move prior to switchover. Switchover at point e now occurs at $\frac{\theta_o}{2}$ degrees from the origin and the negative torque portion of the trajectory terminates within the limit cycle control box at 0.825 degree and 1.1 degrees per second. The relatively large residual rate is caused by the error in turn-off timing introduced by the new acceleration.

In normal operation the limit cycle would be entered at this point. However, the limit cycle is not acquired because of simulation characteristics. The dynamic range of the rate necessitates a large integration time step at

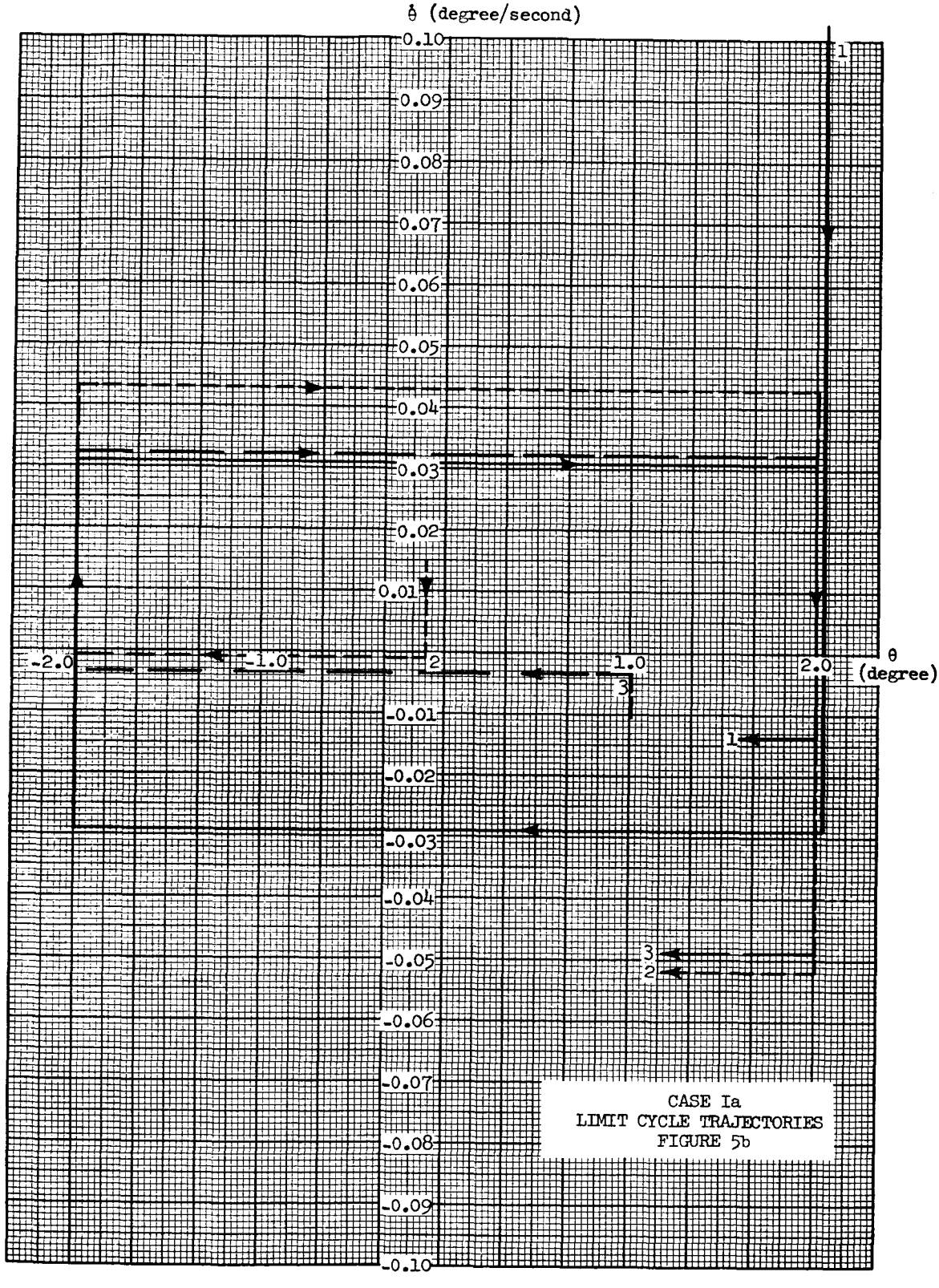

CASE Ia
LIMIT CYCLE TRAJECTORIES
FIGURE 5b

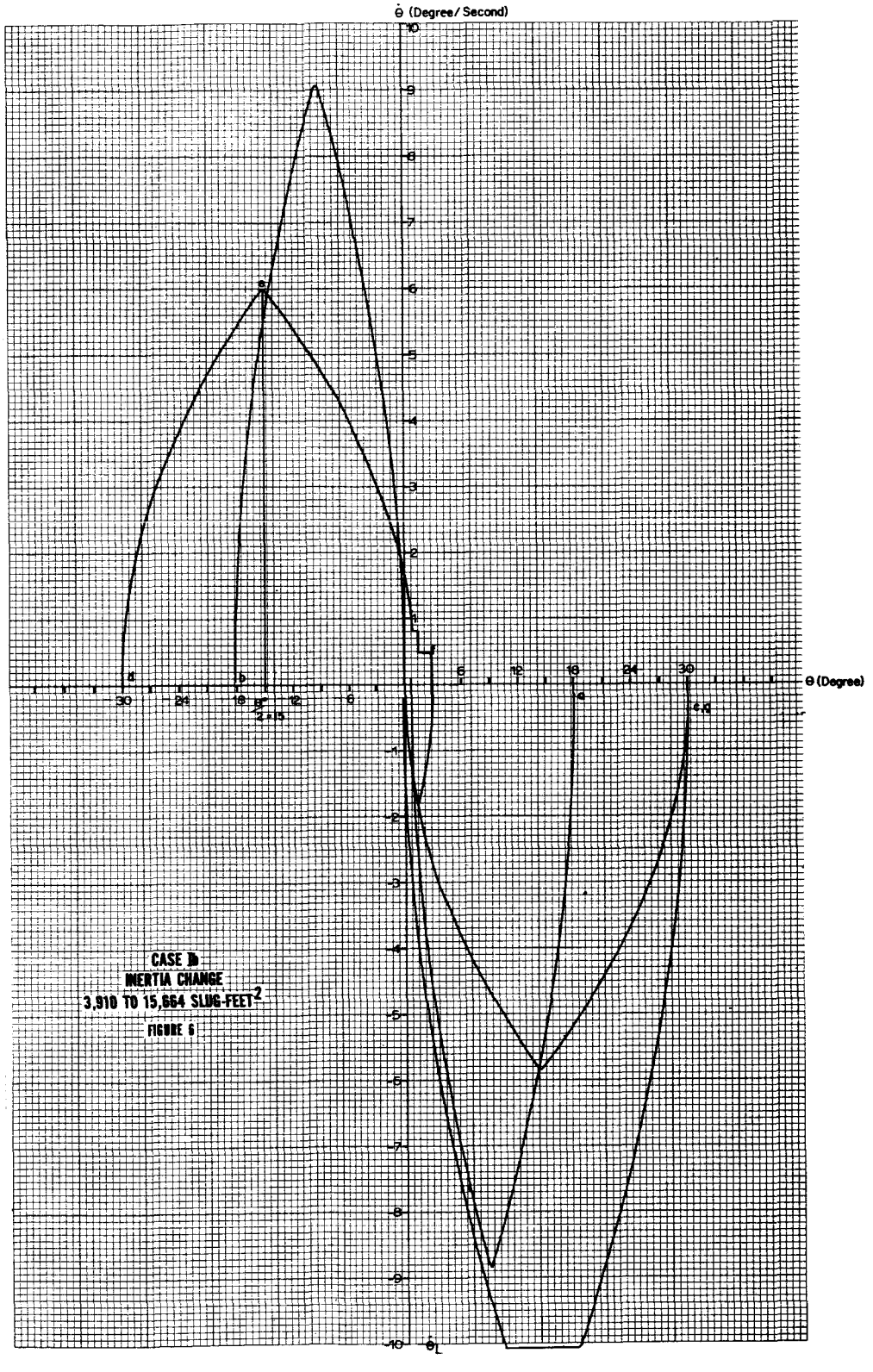

CASE Ib
INERTIA CHANGE
3,910 TO 15,664 SLUG-FEET^2
FIGURE 6

the low rates encountered in the limit cycle to prevent excessive machine time and print-out. When torque is not being applied, the integration step during portions of the limit cycle logic is 0.5 second. A rate is derived at the end of the A loop and in the main program to make the decision to enter the limit cycle logic. With the simulation integrating vehicle motion every 0.5 second and a rate of 1.1 degrees per second, the simulation has allowed the vehicle attitude to drift to two degrees before limit cycle logic is called. After an unsuccessful attempt to reverse vehicle motion in the B loop, the system has drifted sufficiently far to logically call for an A loop to correct the accumulated error. The short A loop trajectory with timing corrections, commencing at point e in Figure 6, now turns off very close to the origin at 0.2 degree and 0.0007 degree per second.

The next input of 30 degrees at point g switches at the proper instant and terminates inside the limit cycle box at -0.083 degree and -0.0012 degree per second, thus illustrating that the optimum switching portion of the control program has completely adapted to the new parameters. The design limit cycle rates also are immediately established because the limit cycle timing parameters (t_{nx}, t_{px}) are updated from the previous limit cycle entry.

(c) Case Ic - In this test the inertia was increased from 3,910 to 31,325 slug-feet squared at point d in Figure 7. The resulting trajectory is similar in many respects to that of Case Ib.

The timing errors and integration interval in the simulation cause the system to come to rest inside the limit cycle box at such a high rate that the limit cycle is not acquired. After timing correction, the input at point e results in a trajectory that switches at the proper point. Thrust is terminated at 0.06 degree and 0.0005 degree per second.

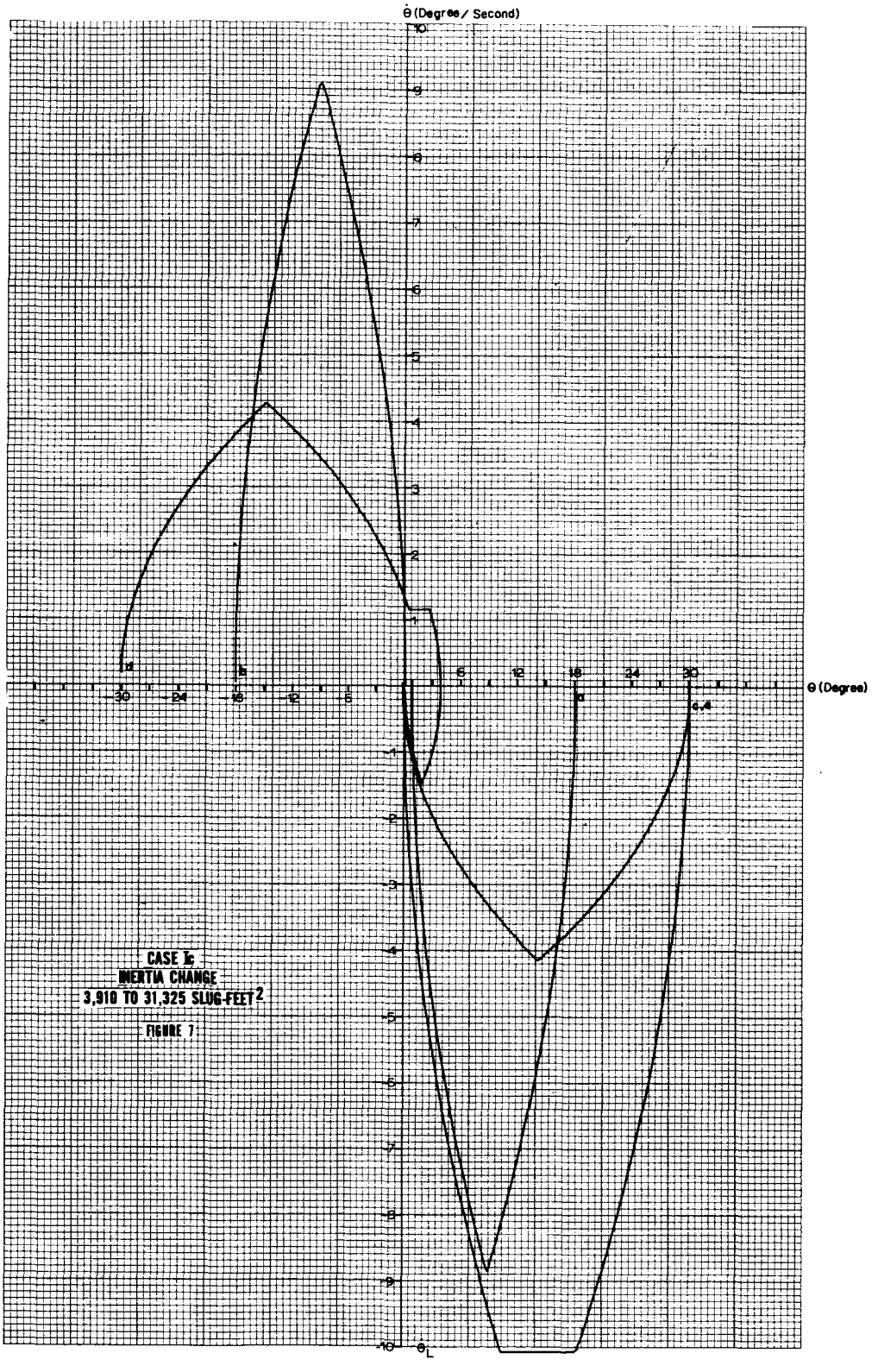
θ̇ (Degree / Second)
θ (Degree)
θL
CASE 1c
INERTIA CHANGE
3,910 TO 31,325 SLUG-FEET²

FIGURE 7

(d) Case Id - An inertia change from 3,910 to 62,658 slug-feet squared results in the same type trajectory as Cases Ib and Ic and the limit cycle is not acquired after the inertia change. The trajectory is shown in Figure 8.

3.2.2 Summary of Test Results. In all tests the control program resulted in the termination of thrust inside the limit cycle logic box. The cases where the limit cycle is not acquired because of plant simulation program characteristics acquire the limit cycle on the first attempt after an inertia change in actual practice.

The size of the inertia change is limited in that the new inertia cannot be so large as to cause the limit cycle box to be undershot because $\dot{\theta}_c$ is passed through before the system is inside the attitude control limits (θ_{L2}). Since $\dot{\theta}_c$ is a design decision, the choice should be based upon required attitude control limits and maximum anticipated inertia. The limitation does not, however, cause instability if exceeded but merely results in a sizable overshoot and hunting phase before the limit cycle is acquired.

None of the cases presented will have an overshoot in actual practice. There is no way for an instability to arise from any inertia change.

3.3 Torque Changes. The effects of nonsymmetric moment arm or torque changes were investigated by a series of test cases similar to those in which the inertia was changed. The input sequence is the same except that the moment arm of the positive or negative torquer is changed in place of the inertia. For positive torque, the moment arm begins at 12 feet and is altered to 3, 5, 10, 20 and 40 feet with one input sequence for each change. The same set of final values is used for the negative moment arm changes. The initial value of the negative thrust moment arm is 11 feet.

3.3.1 Test Results.

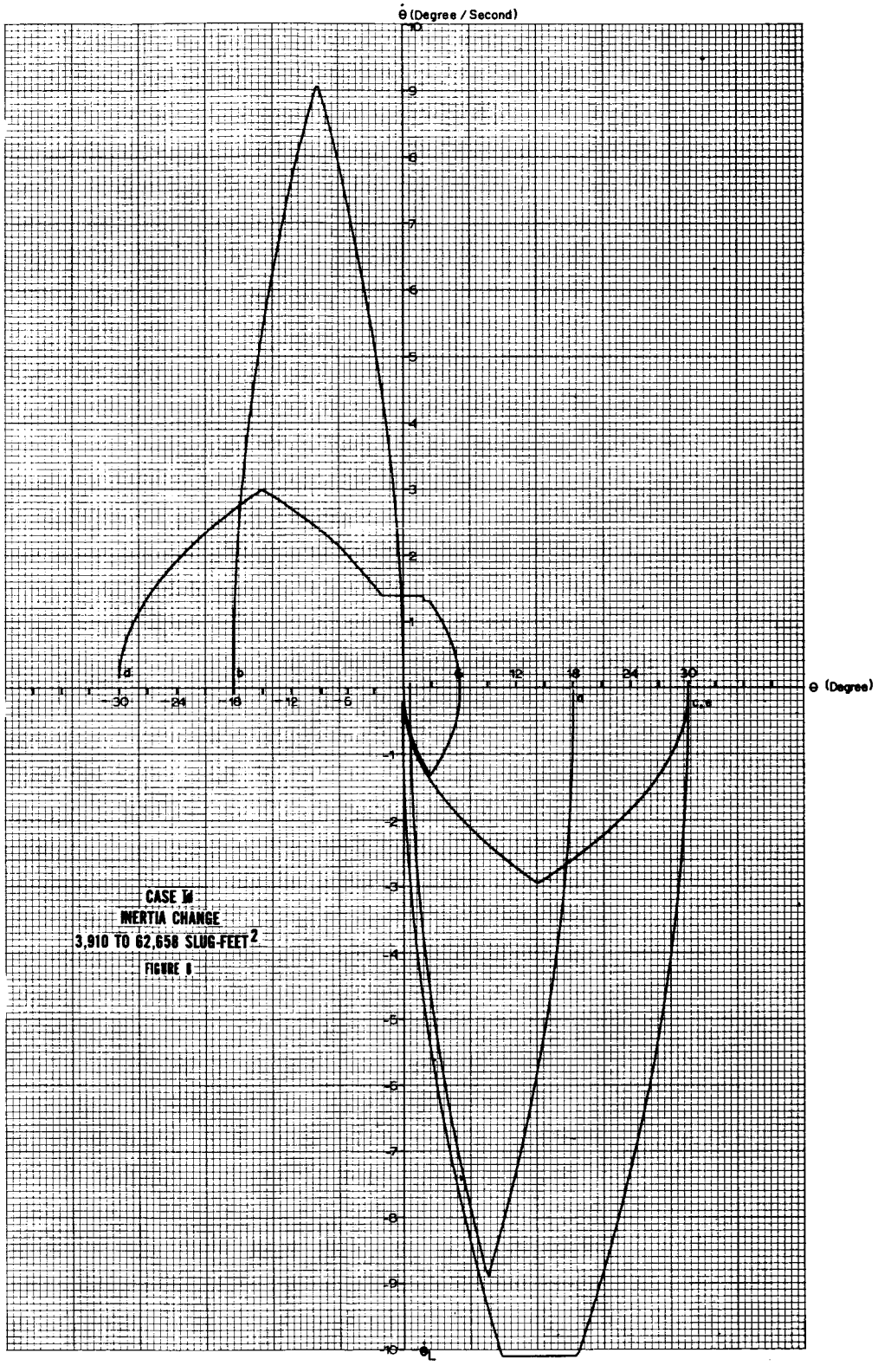
θ̇ (Degree / Second)
θ (Degree)
a
b
-30
-24
-18
-12
-6
6
12
18
24
30
10
9
8
7
6
5
4
3
2
1
-1
-2
-3
-4
-5
-6
-7
-8
-9
-10
CASE 14
INERTIA CHANGE
3,910 TO 62,658 SLUG-FEET²
FIGURE 8

(a) Case IIa - When the positive thrust moment arm is suddenly altered from 12 to 3 feet, just prior to the input labeled point d in Figure 9, the torque is reduced 75 per cent and the control program causes the switching curve to shift in accordance with the changes described in Paragraph 2.2. Since negative torque has not changed, switching should occur on the same switching line as previously defined. However, switching erroneously occurs at point e, with the result that the limit cycle box is undershot. The condition is immediately corrected by the switching logic which causes positive torque to be reapplied at point f. Switching now occurs on the original switching line and the limit cycle is acquired at point g. Because no change in negative acceleration has taken place, turn-off timing is still accurate and the turn-off at point f is at as low a rate as at point g.

(b) Case IIb - Trajectories resulting from the positive torque moment arm decrease from 12 to 5 feet are given in Figure 10. The first three inputs in the sequence are the same as previous runs to set up the system with the latest plant parameters prior to the change. Since the change from 12 to 5 feet causes a torque decrease of more than 50 per cent, the switching curve is moved, the resulting trajectory being the same type as the previous run.

(c) Case IIc - In the test presented in Figure 11, the positive torque moment arm is altered from 12 to 10 feet after the first three inputs in the sequence, effecting a torque change of less than 50 per cent. Since the switching curve is not moved, proper switching and immediate acquisition of the limit cycle result as soon as the change has occurred. The new value of K_p is derived properly and the system set to optimally control all future inputs. The next input causes rate limiting; positive torque is applied at the proper point so that the new trajectory passes through or nearly through the

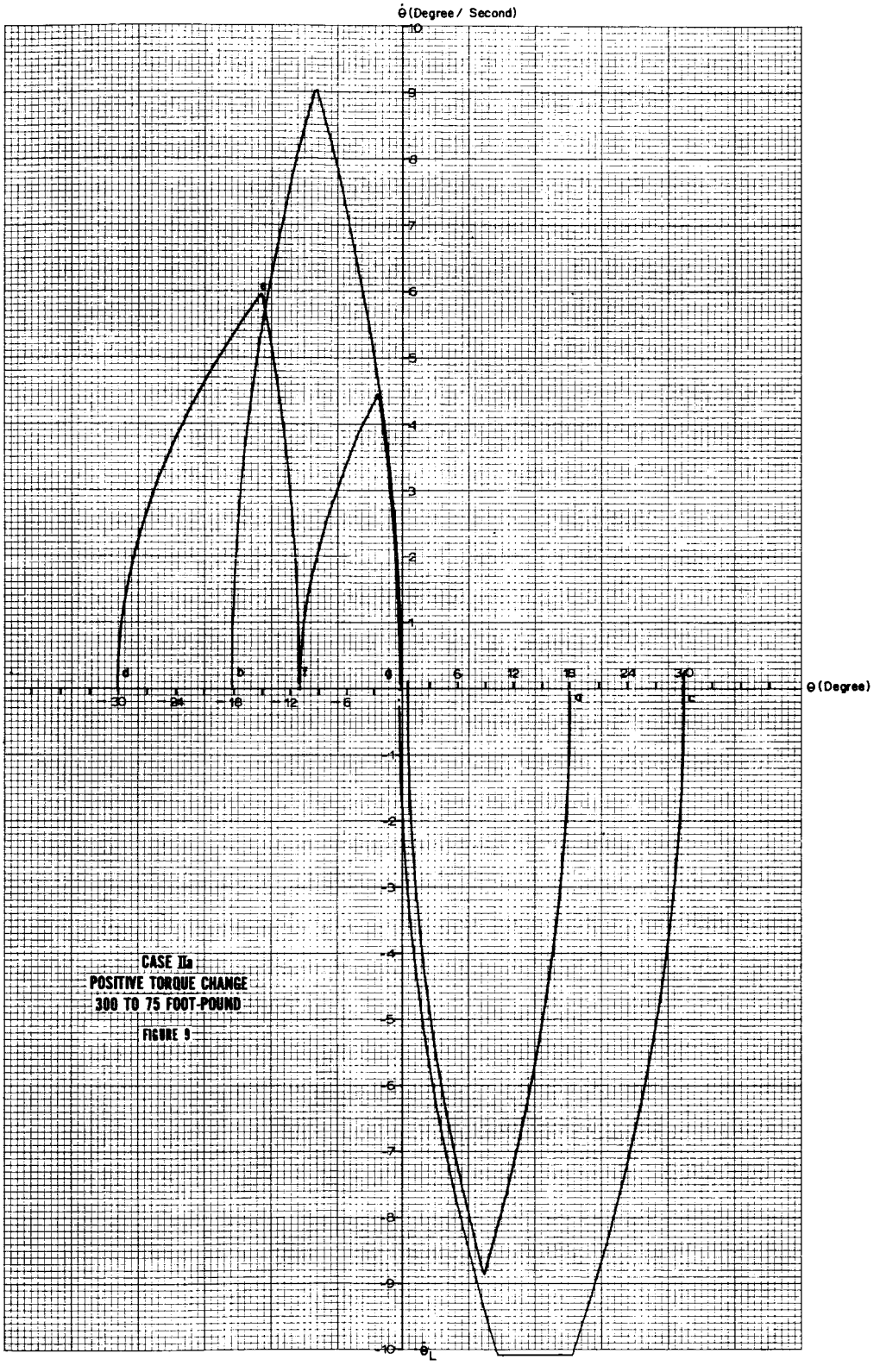

CASE IIa
POSITIVE TORQUE CHANGE
300 TO 75 FOOT-POUND

FIGURE 9

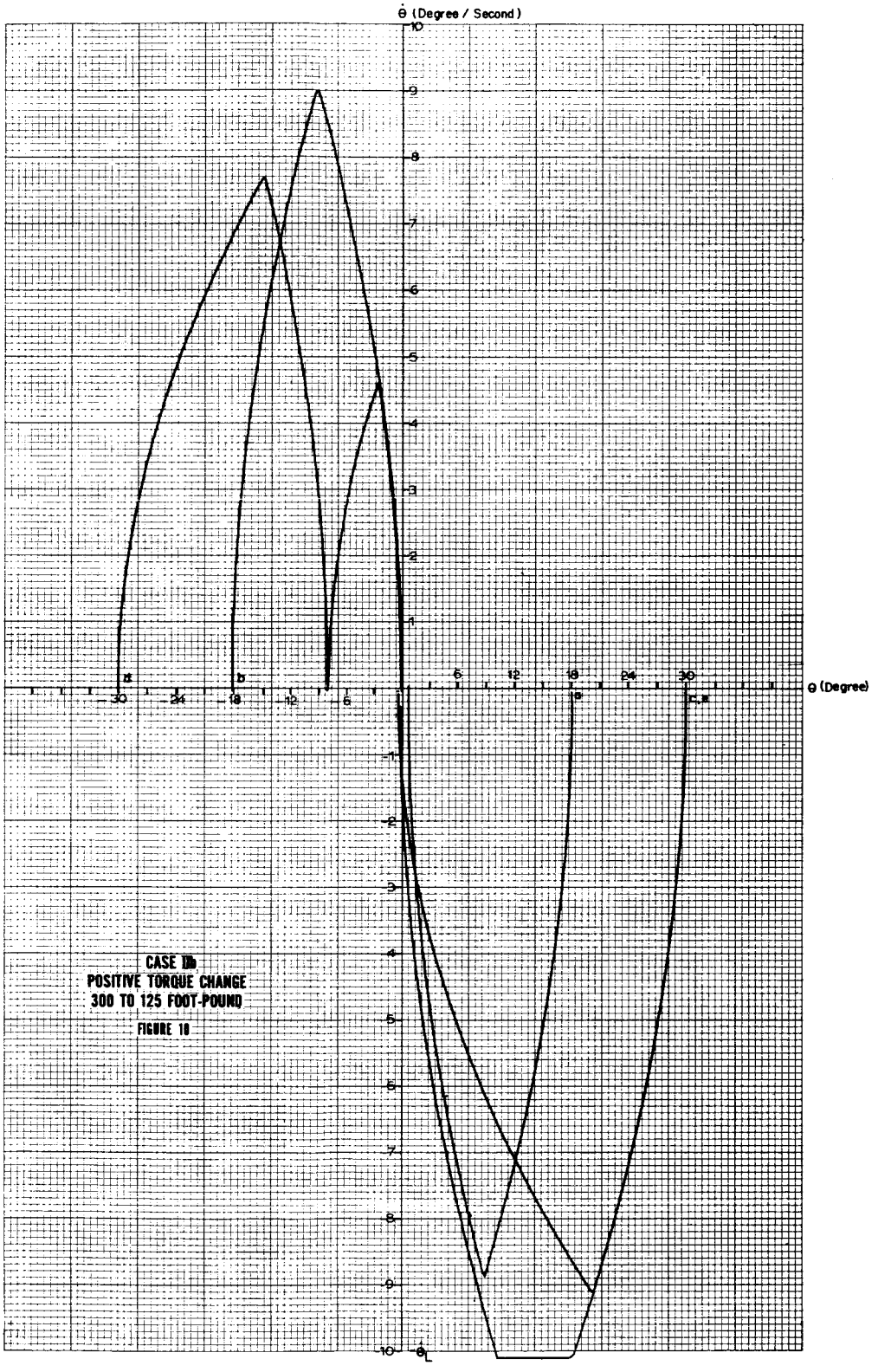

CASE IIb
POSITIVE TORQUE CHANGE
300 TO 125 FOOT-POUND

FIGURE 10

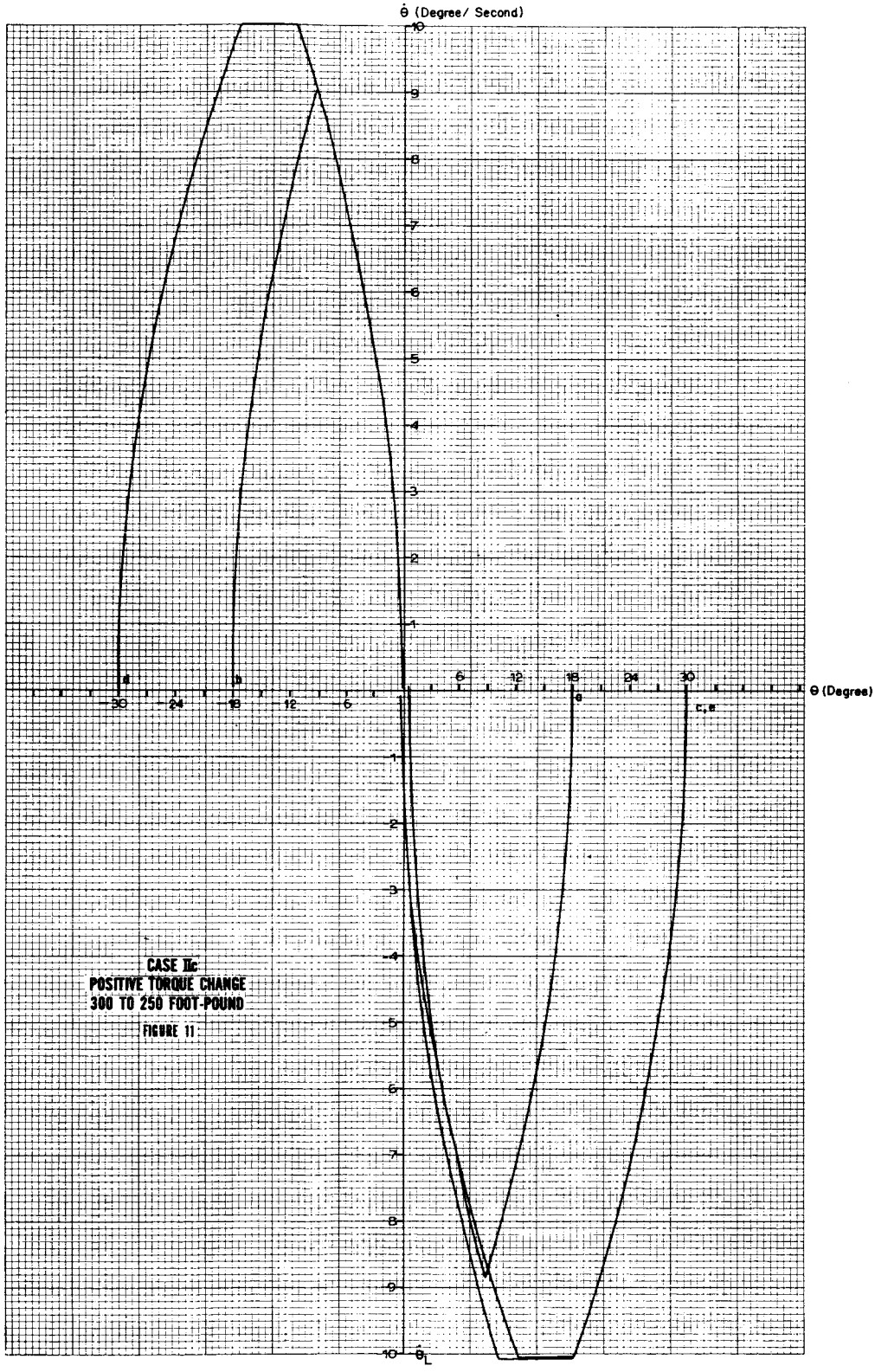

CASE IIc
POSITIVE TORQUE CHANGE
300 TO 250 FOOT-POUND

FIGURE 11

origin. In this test the thrust was actually terminated at an angle and error rate of -0.112 degree and -0.004 degree per second respectively.

(d) Case IId - Figure 12 shows the trajectories resulting from a programmed increase in the positive torque moment arm from 12 to 20 feet which effects a higher positive torque than the previous tests where the change in moment arm caused a lower torque. In this test, the alteration occurring immediately prior to the input at point d did not cause the switching curve to be moved. Switching occurred at the proper point, e, and the limit cycle was immediately acquired, Figure 12b. The torque is shut down at point f which corresponds to point f in Figure 12a. The limit cycle figure illustrates the immediate acquisition of the optimum limit cycle established by the program design. The trajectory in Figure 12a, commencing at point g, shows the relocated positive switching line, switching now taking place at point h.

(e) Case IIe - The trajectories presented in Figure 13 are the result of an increase from 12 to 40 feet in the positive torque moment arm which causes some difficulty in acquiring the limit cycle. Because of the extreme change, the negative switching curve is once again erroneously moved causing switching to occur at point f instead of point e. The limit cycle is not acquired at point g as the switching caused the limit cycle box to be overshot, so another A loop is automatically entered. Switching now occurs on the proper switching line for positive torque at point h but since a rate is derived only every one-tenth degree, turn-off time (t_{NC}) cannot be accurately computed. This results in a hunting condition since the program is attempting to correct. Eventually, the limit cycle is acquired.

The hunting that occurred in this test is not caused by the change in

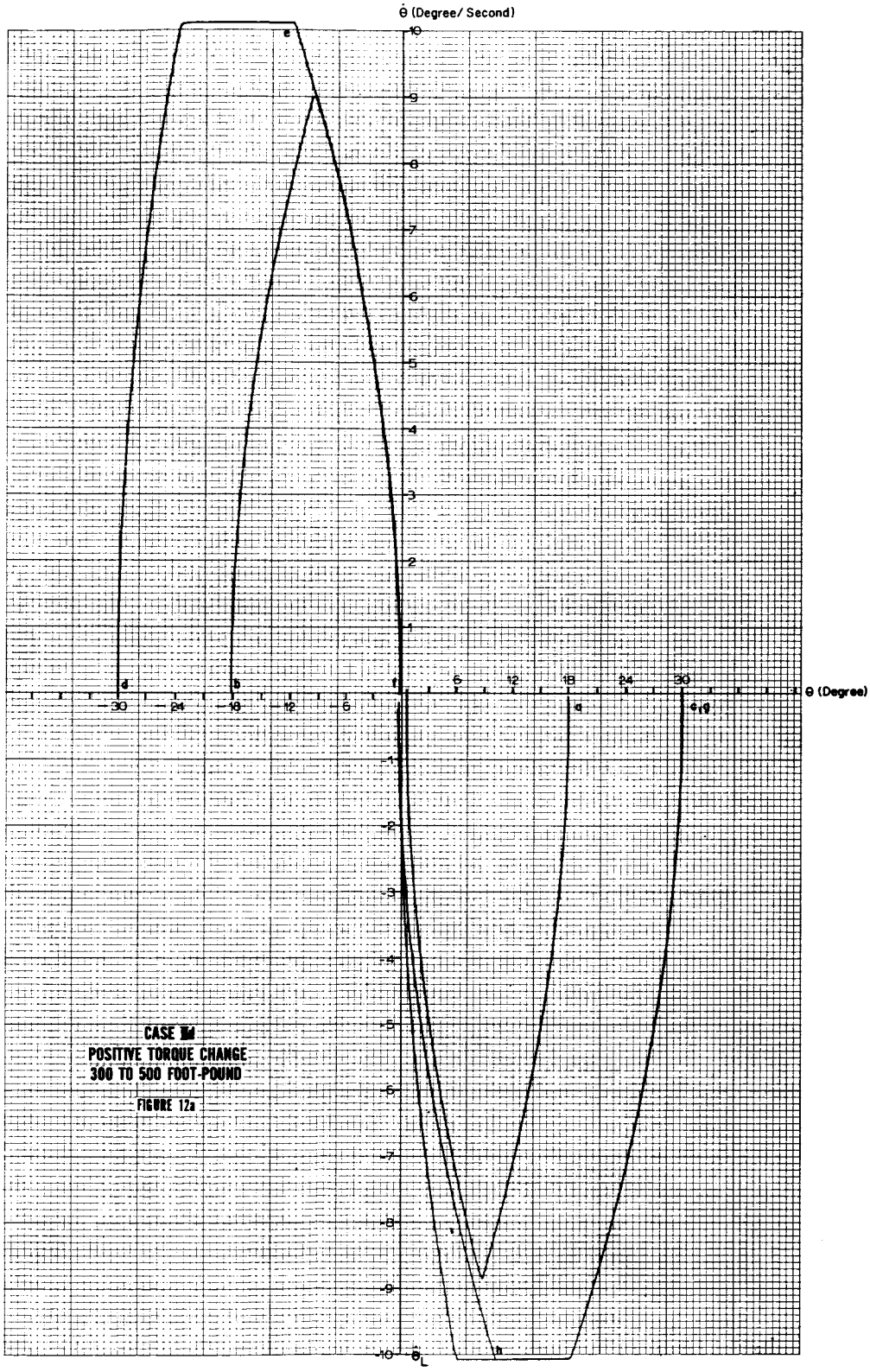

CASE IId
POSITIVE TORQUE CHANGE
300 TO 500 FOOT-POUND

FIGURE 12a

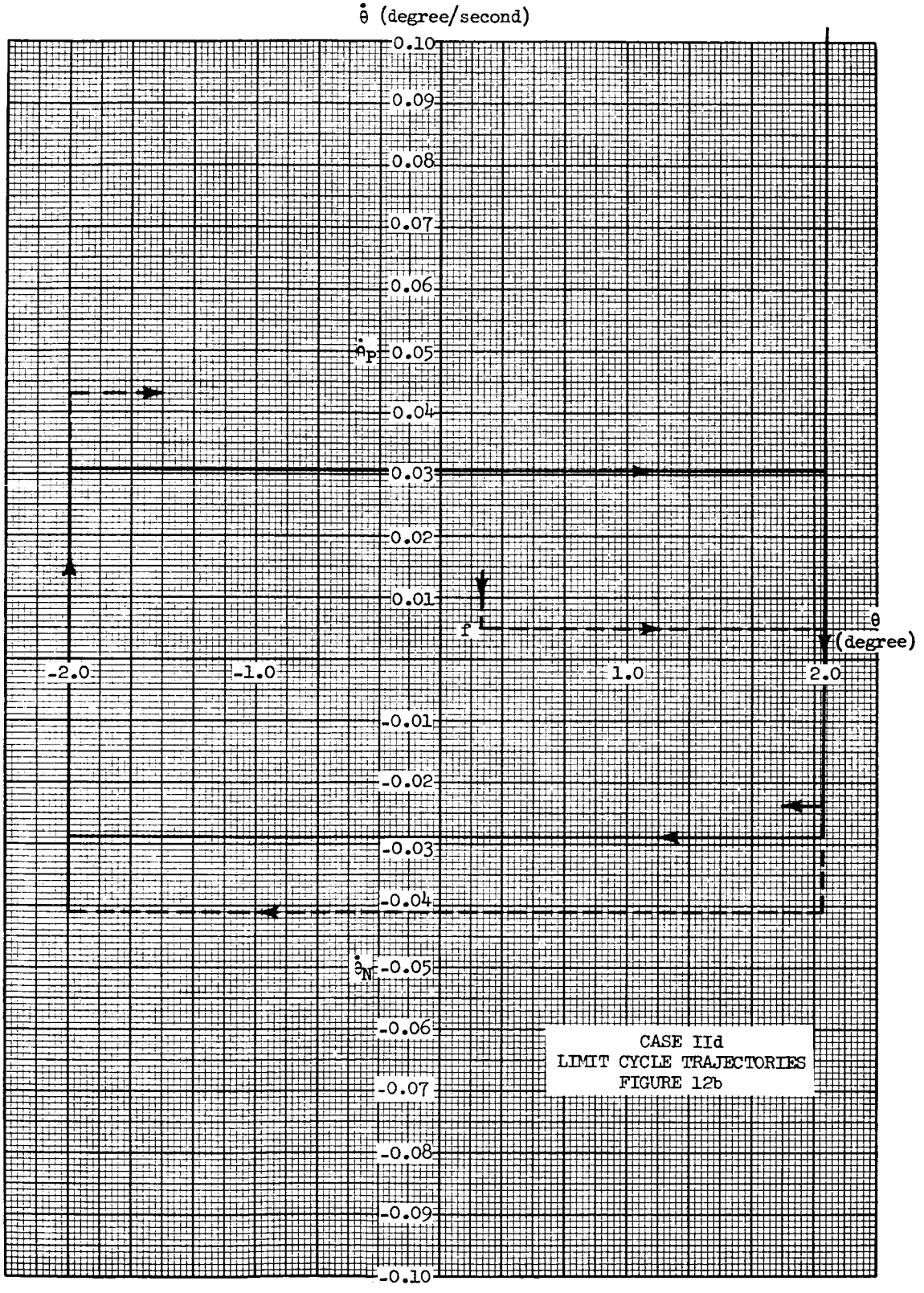

CASE IId
LIMIT CYCLE TRAJECTORIES
FIGURE 12b

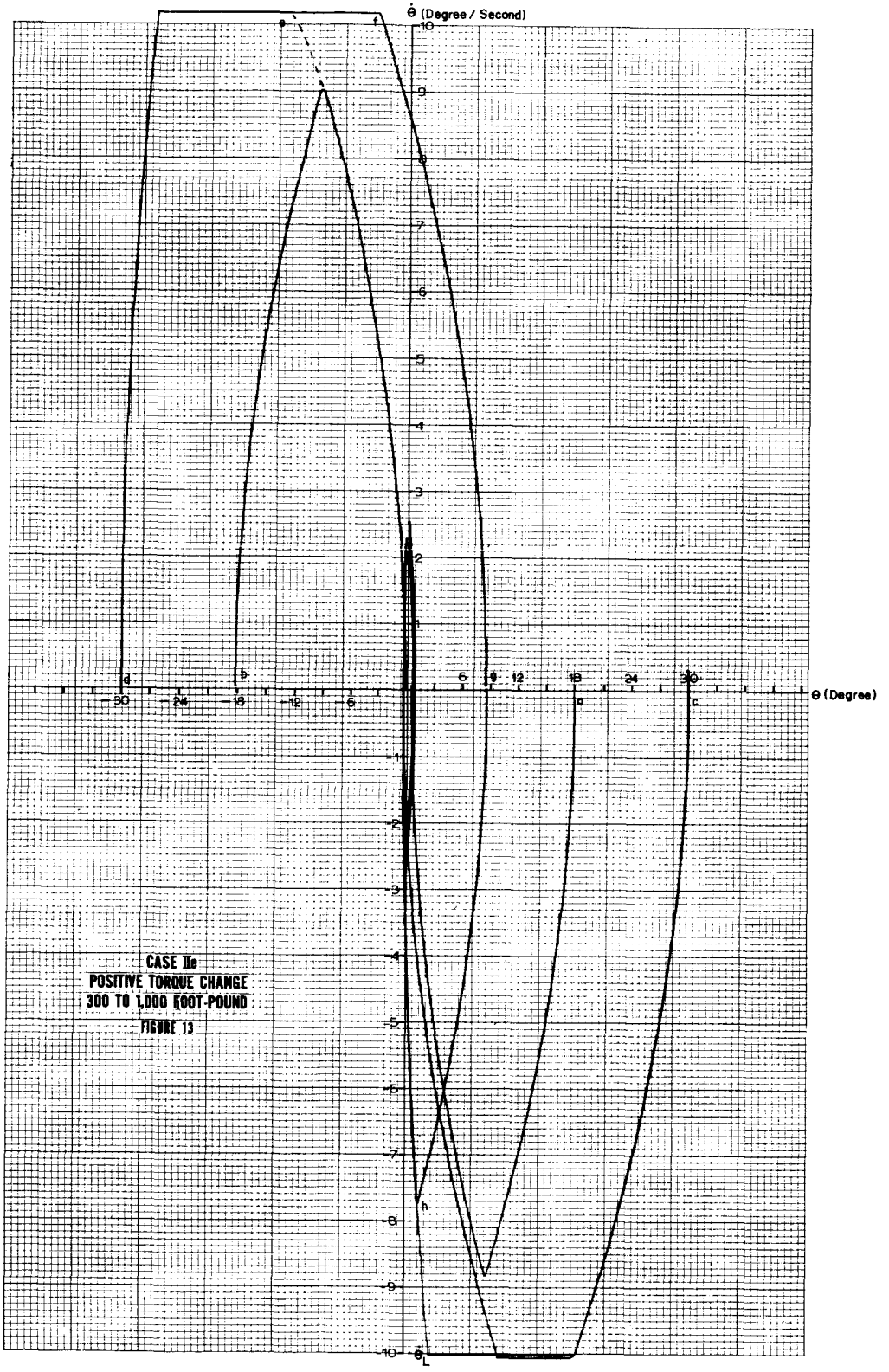

CASE IIe
POSITIVE TORQUE CHANGE
300 TO 1,000 FOOT-POUND
FIGURE 13

moment arm but rather by the resulting high acceleration. Trajectories are so steep in the region of origin that the timing based on derived rates cannot be accurate. To correct this minor deficiency, the top of the limit cycle box ($\dot{\theta}_c$) must be increased to accommodate higher accelerations. It is important to note that the system is not unstable as hunting always results in the acquisition of a stable limit cycle.

Preceding paragraphs discussed the effects of various changes in positive torque that introduce errors to which the system must adapt. More important though, are the conditions under which the changes were made. Positive torque was altered prior to an input causing the application of positive torque, the general result being that the change was picked up by the program prior to switchover. Subsequent paragraphs discuss changes in the negative torque which, when applied at the same place in the input sequence, will not be realized until after switchover has occurred.

(f) Case IIf - This test represents the first in a series to determine the effects of changing the moment arm of the torque not being applied until switchover occurs. In all previous tests the moment arm change is picked up immediately after the input sequence is repeated. However, when the negative torque moment arm is altered, the switching curve remains fixed regardless of the magnitude because the change is not detected until an input of opposite polarity causes the altered acceleration to be derived.

All cases involving the changing of the negative torque moment arm begin with a moment arm of 11 feet. In this test the moment arm is decreased from 11 to 3 feet, with the result that the trajectory from point d, Figure 14, does not switch at the proper place and the limit cycle box is overshot.

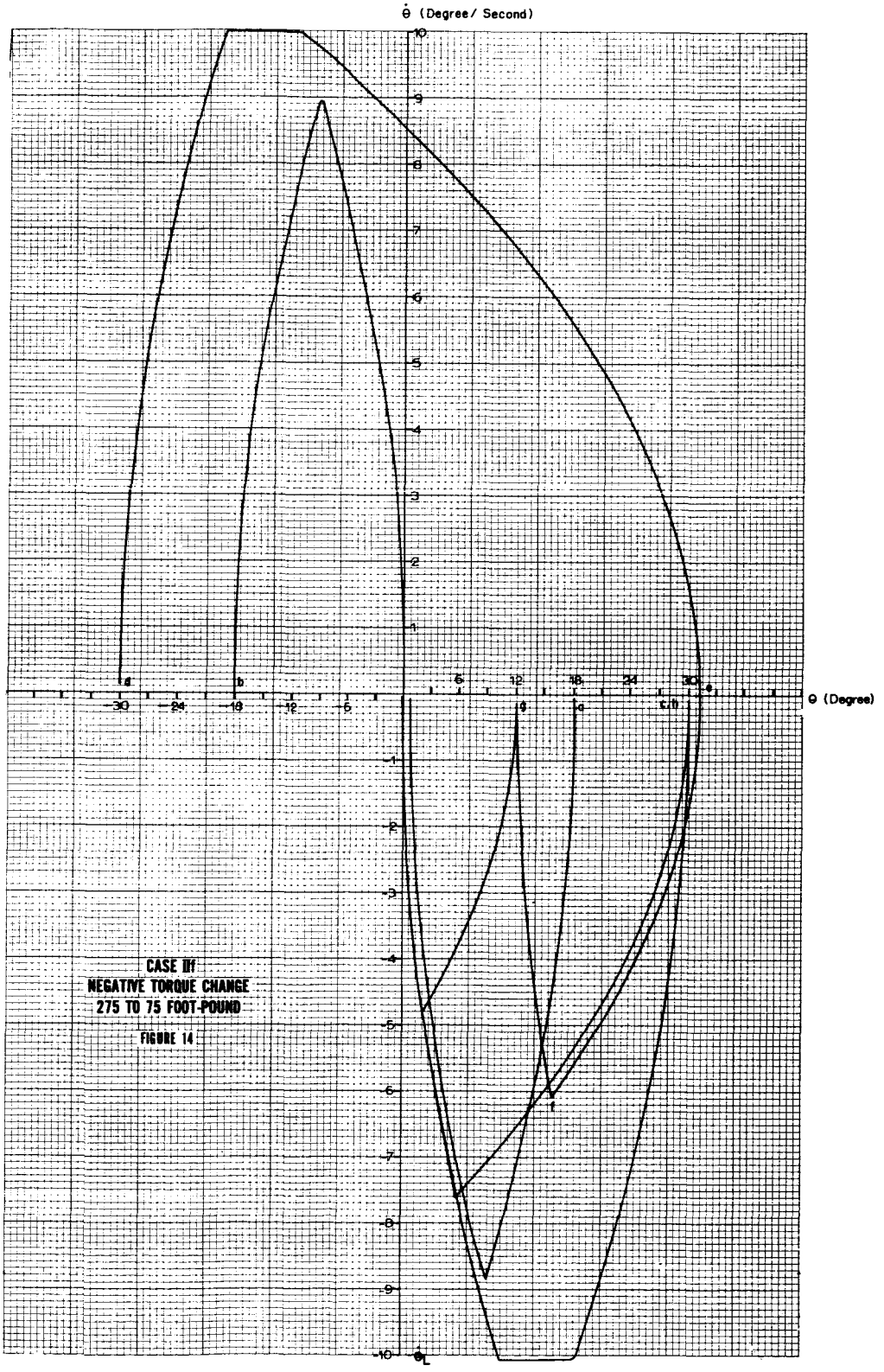

CASE III
NEGATIVE TORQUE CHANGE
275 TO 75 FOOT-POUND

FIGURE 14

Consequently, the control program is returned to an A minus loop at point e where the change in negative torque is detected. From point e the trajectory is the same type as occurred when the positive moment arm was changed. When torque is applied at point e, a large change in acceleration is sensed and the switching line moved. Switching at point f causes the limit cycle box to be undershot as in Case IIa. At point g the logic returns control to an A minus loop which corrects the switching curve and acquires the limit cycle.

On the next input at point h, the limit cycle is acquired after the first switchover, corrected for nonsymmetry in the torques. The effect of a drastic torque reduction applied after switchover is an overshoot which basically establishes the same condition prevailing when the torque applied before switching is reduced.

(g) Case IIg - In this test a small decrease, from 11 to 9 feet, in the negative torque moment arm is investigated. The 25 per cent change in acceleration does not cause an overshoot of the limit cycle box on the first attempt. With the input at point e, Figure 15, the new negative acceleration is derived and both switching curves corrected. Switching occurs at the correct place and the limit cycle is acquired immediately.

3.3.2 Summary of Test Results. Torque changes fall into two general classes: changes sensed by the acceleration derivation prior to switchover and changes not sensed until an A loop of opposite polarity is entered. Torque changes also result in both increased and decreased accelerations.

In general, no difficulties are encountered if the change in torque is smaller than 50 per cent of original value with limit cycle acquired after the first switchover and updating complete before the next input. If torque alteration is greater than 50 per cent, nonsymmetry results in the limit box

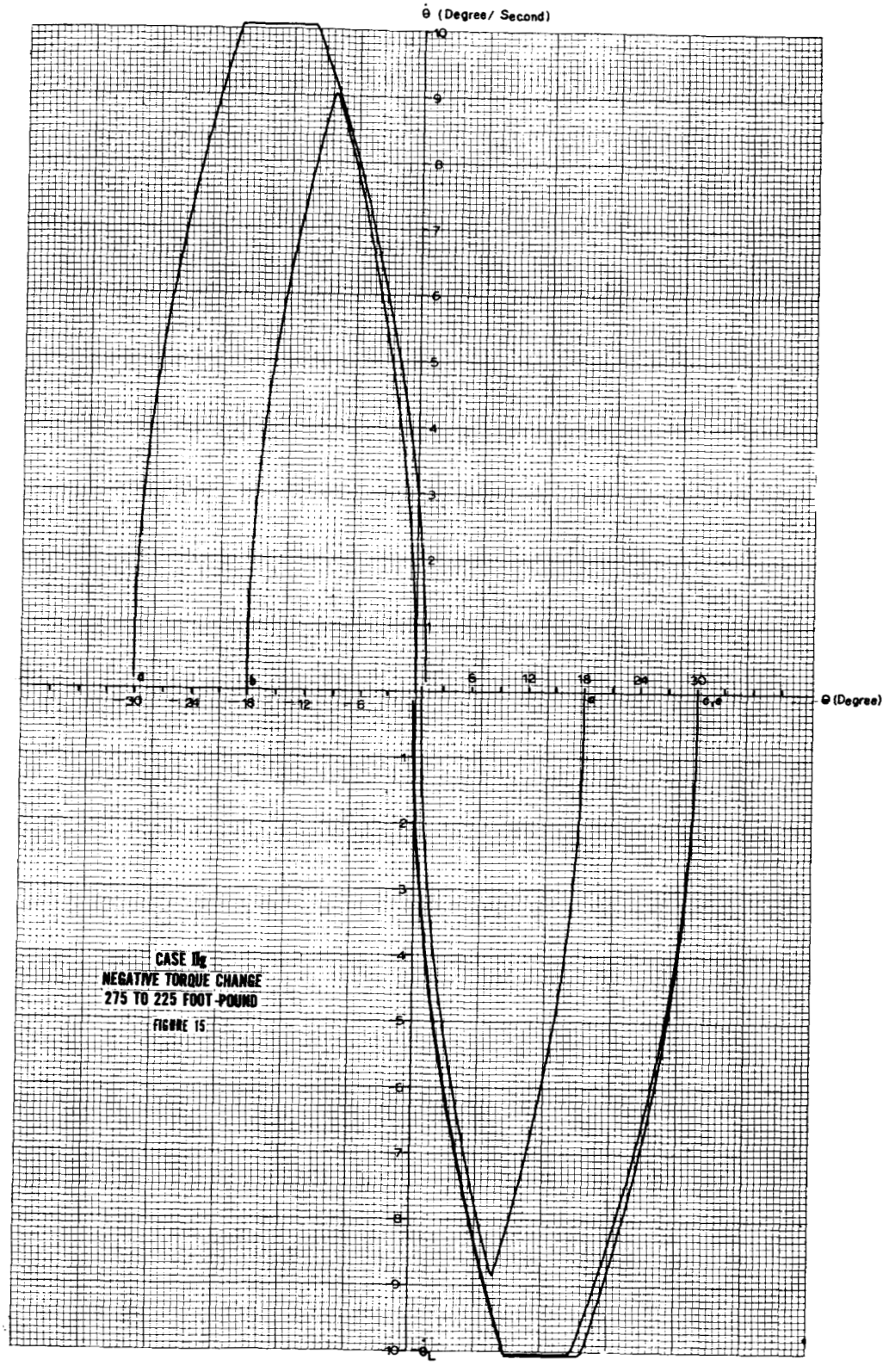
θ̇ (Degree/ Second)
θ (Degree)
CASE IIg
NEGATIVE TORQUE CHANGE
275 TO 225 FOOT-POUND

FIGURE 15

being overshot or undershot. Hunting for the limit cycle box generally completes control parameter updating so that the next inputs acquire the limit cycle without hunting. Nonsymmetries caused by torque or moment arm changes are not likely. If large nonsymmetries occur because of a new system configuration, the ODAACS reestablishes optimum control after the first sequence of positive and negative angular error inputs.

3.4 Limit Cycle Performance. Test cases presented in this Report show the resulting limit cycle. If the optimum switching program terminates thrust inside the limit cycle control box, the final limit cycle is acquired after one traverse of the limit cycle box. The final limit cycle always establishes a rate equal to or less than the design $\dot{\theta}_n$ and $\dot{\theta}_p$.

The limit cycle is maintained in the presence of disturbance torques which reverse the motion of the vehicle or increase the rate of error accumulation. The control program attempts to reestablish the limit cycle no matter what rate results from the disturbance torque.

3.4.1 Bias Torques. A simulation run was made with a steady bias torque applied to the system. The magnitude is typical of the aerodynamic torque experienced by a spacecraft with an inertia of roughly 4,000 slug-feet squared in an orbit having an altitude of 100 miles. The effective constant acceleration caused by this constant torque is 5.31×10^{-4} degrees per second squared. Figure 16 illustrates the phase plane trajectories which result from a torque of this magnitude.

If the required attitude control limits are plus and minus two degrees, the longest limit cycle period which can be established is 280 seconds, corresponding to the path from 5 to 6 in Figure 16. The path corresponds to the

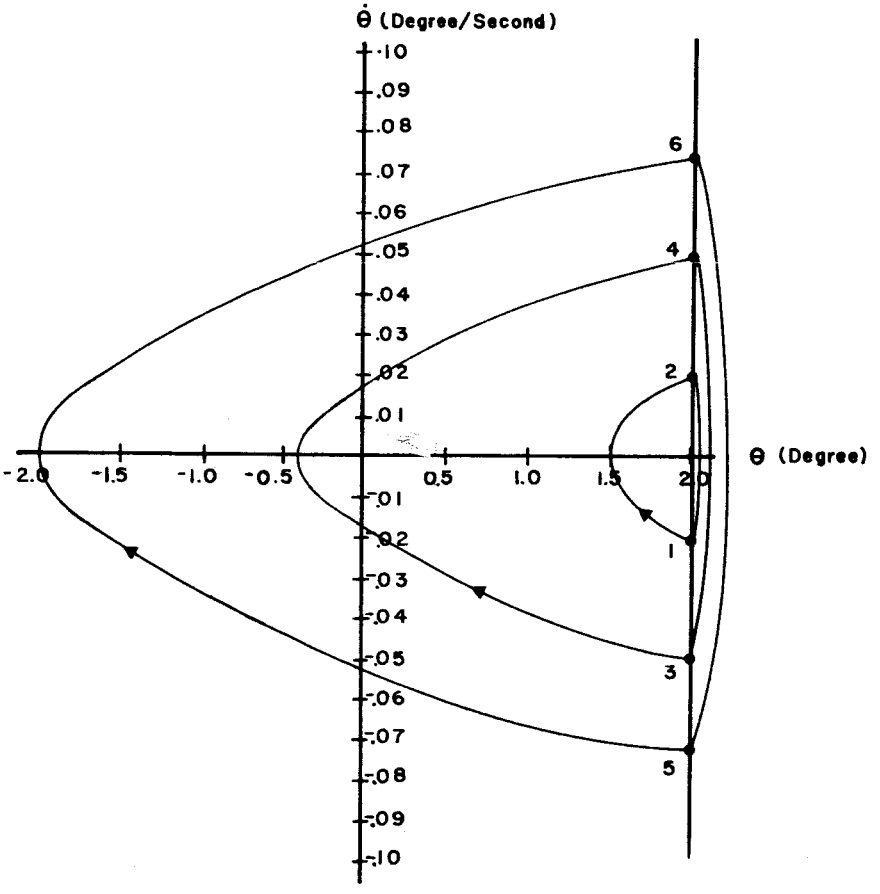

BIAS TORQUE TRAJECTORIES

FIGURE 16

time required for the bias torque to completely reverse the rate, drift to the opposite attitude control limit and return. Thus, only one polarity torque is applied and $\dot{\theta}_n$ or $\dot{\theta}_p$, depending upon the polarity of the bias torque, must be chosen to be that rate which establishes the longest period condition. For the bias torque hypothesized, $\dot{\theta}_n$ should be chosen 0.072 degree per second. However, the value will be different if the resultant bias acceleration alters because of a change in inertia.

It may be possible to program the choice of $\dot{\theta}_n$ or $\dot{\theta}_p$ as a function of the measured torque to inertia ratio. Limit cycle program design is then a function of anticipated bias torque as well as attitude control requirements. $\dot{\theta}_n$ or $\dot{\theta}_p$ are chosen as the initial rates from which bias torque causes the system to drift to the opposite control limit and return without the application of torque.

3.4.2 Disturbance Torques. Disturbance torques are characterized as step changes in plant rate. Figure 17 demonstrates limit cycle control program performance in the presence of disturbance torques. Programmed impulse disturbances increased the rate in the limit cycle at point a and reversed the motion in the limit cycle at point b. Figure 17 shows the limit cycle being maintained throughout the disturbances. The probability of a disturbance torque input during any portion of a control sequence other than the limit cycle is extremely small since the largest amount of time by far is spent in the limit cycle.

3.5 Quantizing Step. The theta subroutine contains a test which compares the difference between two samples of the error with a fixed number (ρ) in the program. If ρ is exceeded by the difference, then a rate is derived

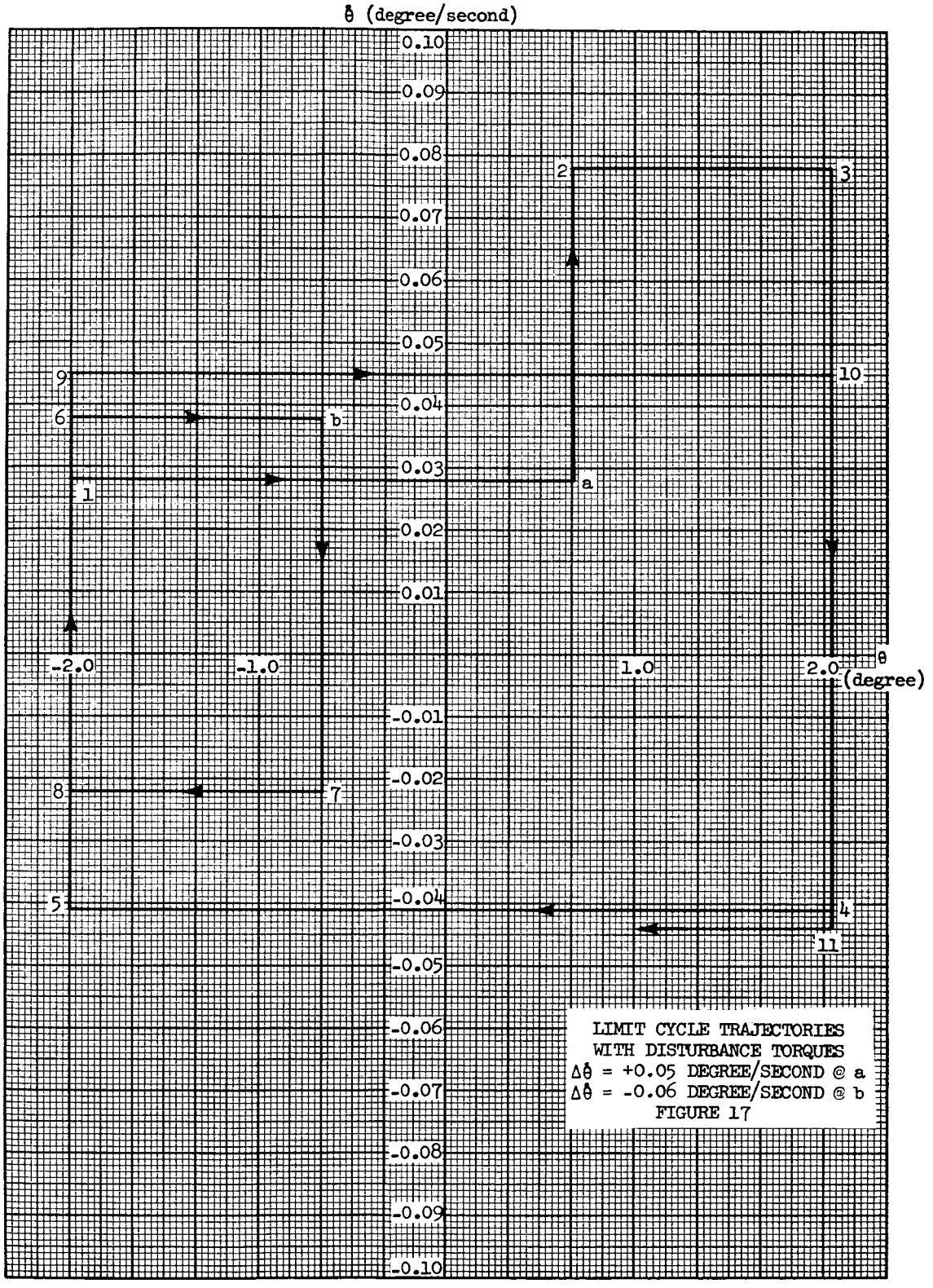

LIMIT CYCLE TRAJECTORIES
WITH DISTURBANCE TORQUES
$\Delta\dot{\theta}$ = +0.05 DEGREE/SECOND @ a
$\Delta\dot{\theta}$ = -0.06 DEGREE/SECOND @ b
FIGURE 17

in the following program step. Thus, ρ is effectively a quantizer since no input samples are accepted until ρ is exceeded. The other immediate result is that a rate effectively is derived every ρ degrees in error and can cause some control difficulties under some combinations of plant parameters.

The basic limitation on the size of the quantizing step can be seen by referring to Figure 18. When θ_c has been chosen, the acceleration of the plant, determined by the torque to inertia ratio, results in a change in θ of $\Delta\theta$ between $\dot{\theta}_c$ and zero rates. If $\Delta\theta$ is smaller than ρ, the rate will never be derived within this interval; consequently the limit cycle will never be acquired in the sense in which the control program attempts to establish the limit cycle portion. The resulting limit cycle oscillation, Figure 19, is the more familiar type generally seen in simple relay servomechanisms.

3.6 Switchover Accuracy. A series of computer runs determined the accuracy with which the positive to negative torque switchover was accomplished. A sequence of negative angular errors was introduced with fixed plant parameters and no trajectory rate limit. Absence of a rate limit allows the rate to build up to a higher value, of more interest in the performance analysis of the switchover prediction equations.

As shown in McDonnell Report A005, the switching point is anticipated through primed switching equation quantities which include the effects of torquer time lags and the rate derivation technique. Switching and prediction equations are repeated here.

$$\theta' = \theta + \dot{\theta} t_{NB} \tag{3}$$

$$\dot{\theta}' = \dot{\theta} - \varphi \frac{n\Delta t}{4 K_p} \tag{4}$$

$$\varphi \left(\theta + K_n \dot{\theta} \left| \dot{\theta} \right| \right) \leq 0 \tag{5}$$

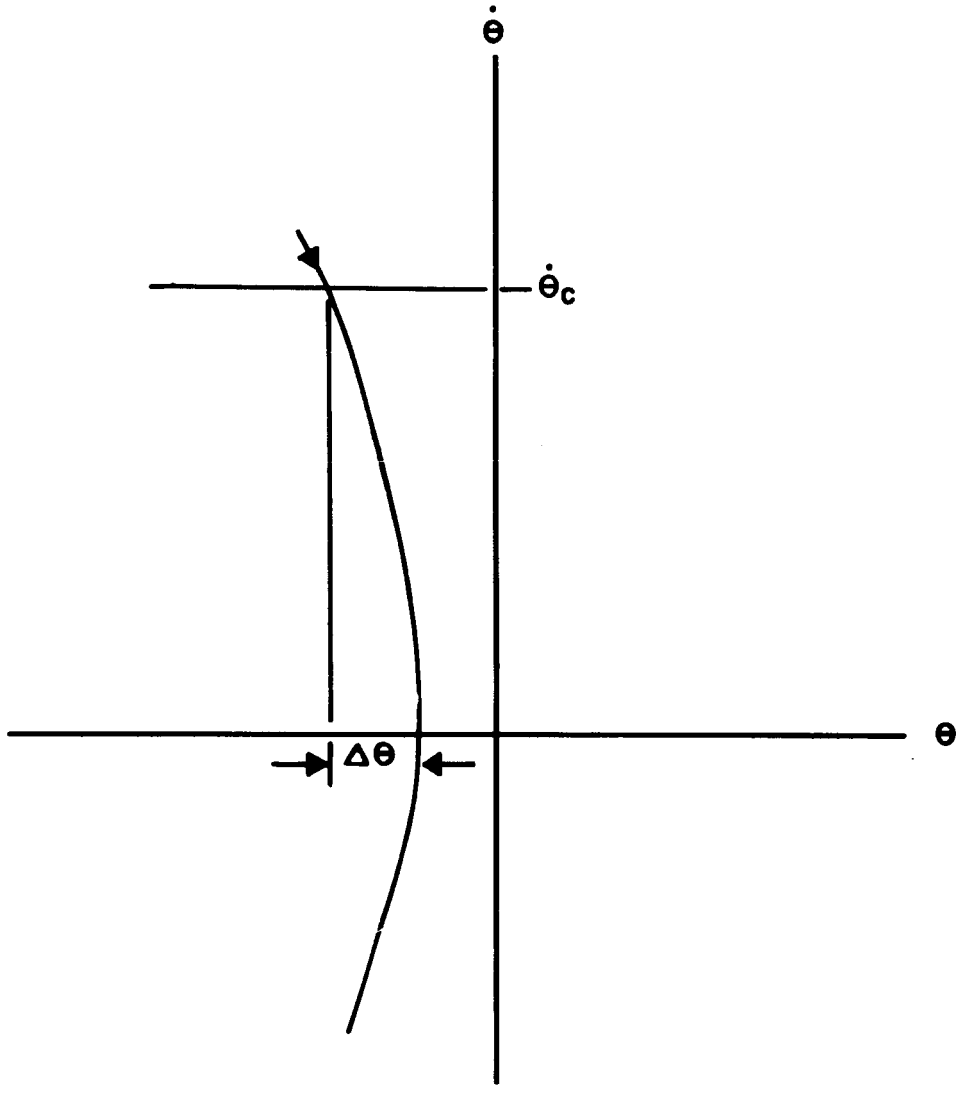

MAXIMUM ALLOWABLE QUANTIZING STEP

FIGURE 18

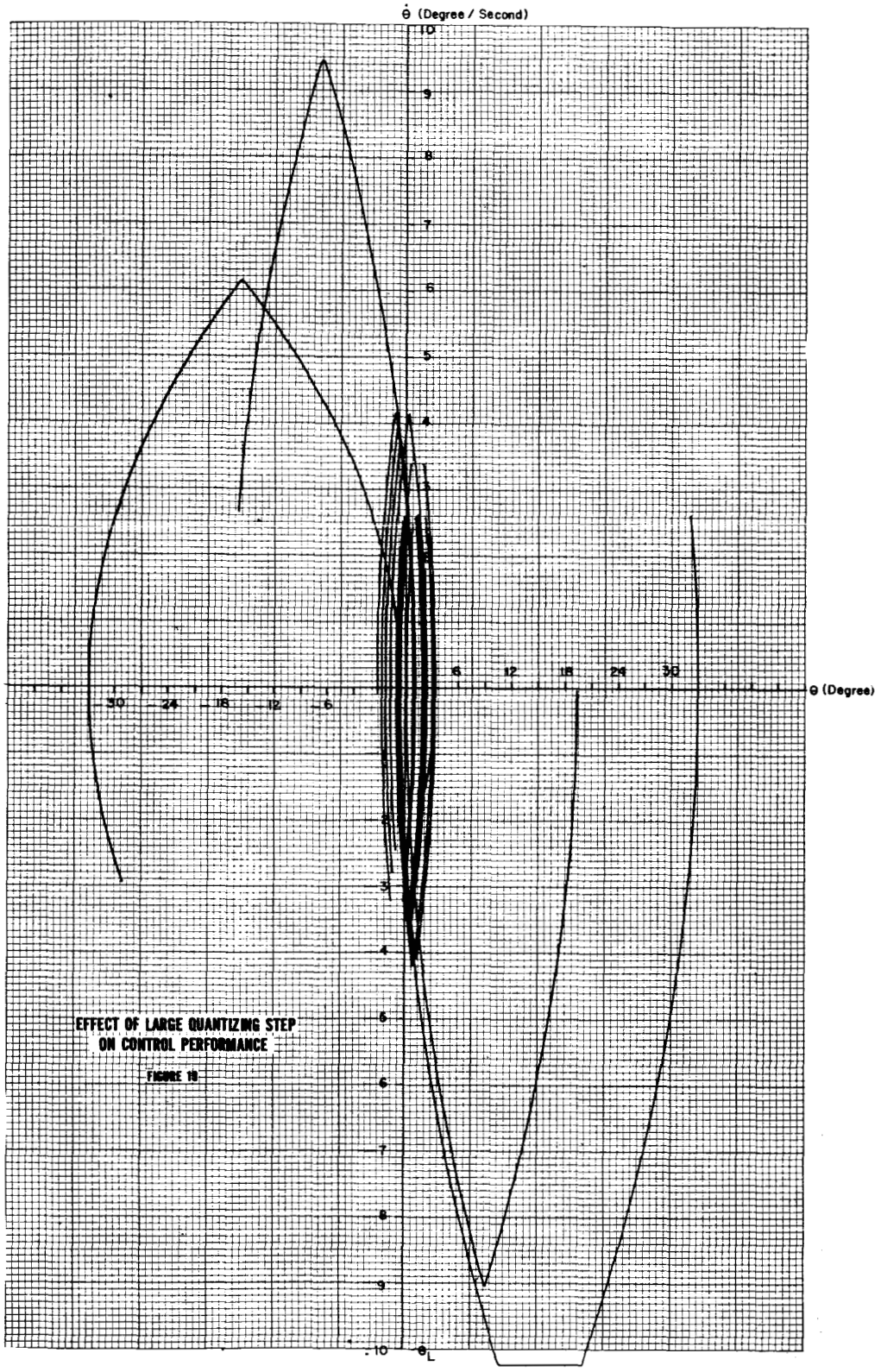

EFFECT OF LARGE QUANTIZING STEP ON CONTROL PERFORMANCE

FIGURE 19

The equations relate to the positive to negative torque switchover, the case investigated in the computer runs. The data generated and conclusions drawn are equally valid for negative to positive thrust reversal.

It is seen from Equation 3 that θ is adjusted by the time required to turn on the negative thrust (t_{NB}). The rate ($\dot{\theta}$) is adjusted by extrapolation to the end point of the sampling interval during which the last value of $\dot{\theta}$ was derived. It is recalled that the output of the theta subroutine gives the average value of $\dot{\theta}$ at the mid-point of the sampling interval.

Errors in θ and $\dot{\theta}$ from the theoretical switching point are given in Table I, the errors in θ being larger than anticipated. The program receives a

TABLE I
SWITCHOVER ERRORS

I (slug-feet^2) x 10^4	θ Error (degree) RMS	$\dot{\theta}$ Error (degree/second) RMS
0.3916	0.385	0.047
0.7832	0.291	0.257
1.5664	0.197	0.168
3.1325	0.192	0.100
6.2658	0.187	0.087
12.5318	0.180	0.101

sample of θ every one-tenth degree as established in the theta subroutine; therefore, the error should not exceed one-tenth degree. Further examination reveals that the major portion of the error is not contributed by θ measuring inaccuracies but by inaccuracies in the switching equation. The switching point theoretically occurs at the switching equation solution point.

$$\theta + K\dot{\theta} \mid \dot{\theta} \mid = 0 \tag{6}$$

Rewriting Equation (6) in functional notation

$$f(\theta, \dot{\theta}, K) = \theta + K\dot{\theta}^2 \tag{7}$$

where $\dot{\theta} \mid \dot{\theta} \mid$ is replaced by $\dot{\theta}^2$ for the purpose of differentiating the function in the succeeding error analysis. The total differential error in $f(\theta, \dot{\theta}, K)$ is expressed in terms of the partial derivative

$$df = \frac{\partial f}{\partial \theta} d\theta + \frac{\partial f}{\partial \dot{\theta}} d\dot{\theta} + \frac{\partial f}{\partial K} dK, \tag{8}$$

the partial derivatives defining the error coefficients related to each source. From Equation (7) the partial derivatives are:

$$\frac{\partial f}{\partial \theta} = 1 \tag{9}$$

$$\frac{\partial f}{\partial \dot{\theta}} = 2K\dot{\theta} \tag{10}$$

$$\frac{\partial f}{\partial K} = \dot{\theta}^2 \tag{11}$$

Figure 20 presents the error coefficients plotted as functions of the rate at which switchover is occurring. It is seen that the error in switchover is considerably more sensitive to errors in K than either of the other two error sources. Switching errors caused by $\dot{\theta}$ and K errors increase with increasing $\dot{\theta}$ which correlates well with the measured switching errors plotted in Figure 21 from Table I. As the inertia of the plant increases, switchover occurs at lower rates, accuracy thus improving. A further contribution to increased accuracy is an improvement in the accuracy of derived acceleration. Increased accuracy is effected by longer time averaging, a direct result of the lower acceleration which prevents the rate from building up as fast as at higher accelerations.

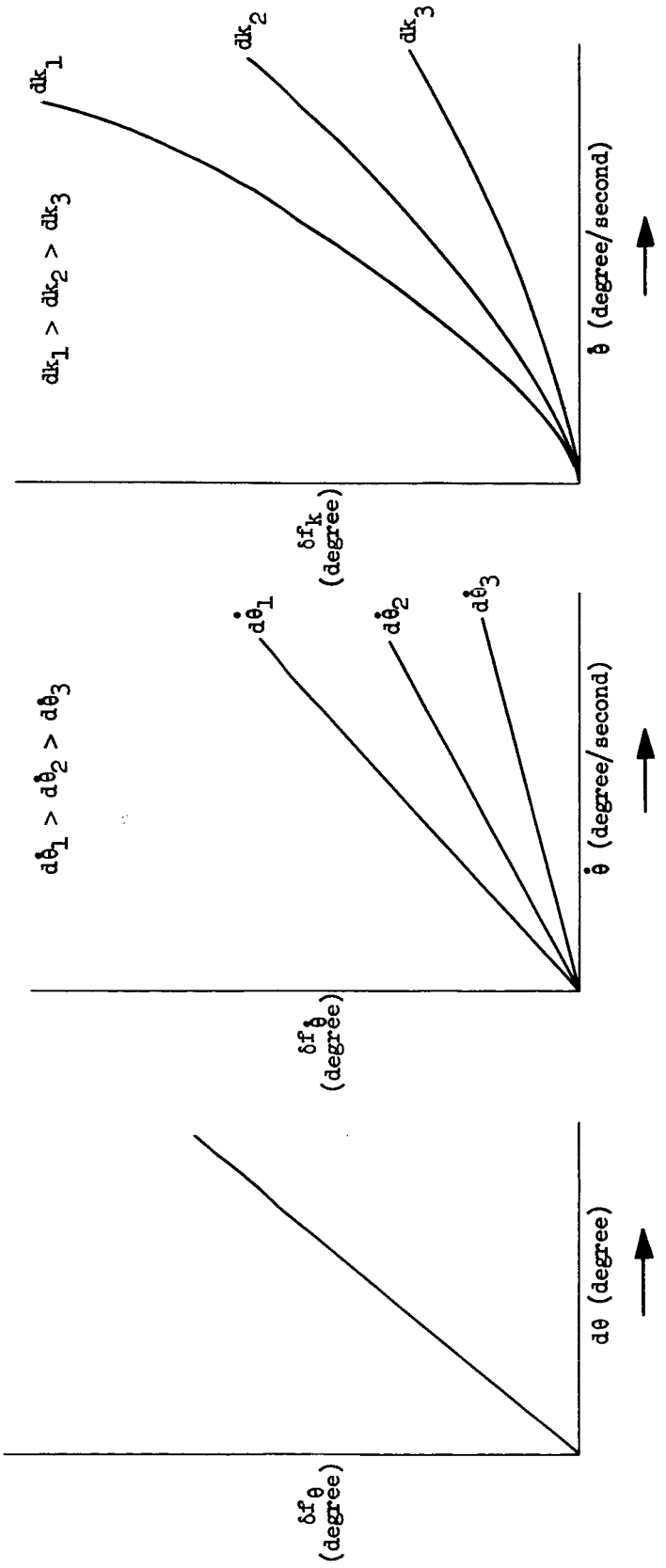

SWITCHING ERROR SENSITIVITIES

FIGURE 20

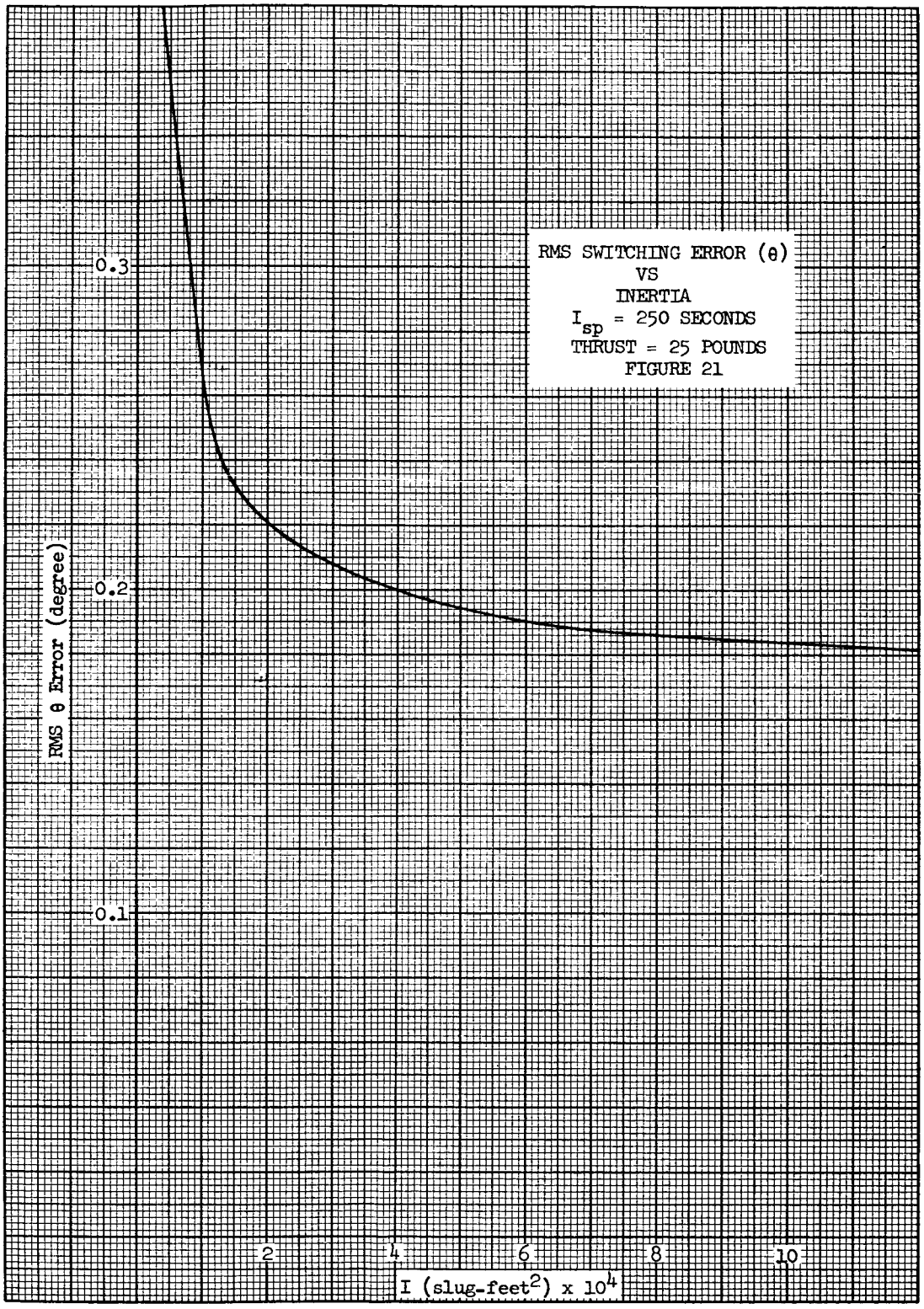
RMS SWITCHING ERROR (θ)
VS
INERTIA
I_{sp} = 250 SECONDS
THRUST = 25 POUNDS
FIGURE 21
RMS θ Error (degree)
0.3
0.2
0.1
2
4
6
8
10
I (slug-feet^2) x 10^4

4. PARAMETRIC STUDY

4.1 Speed of Response. The performance parameters which describe the System in terms of speed of response are derived below as functions of system parameters I, I_{sp}, L and $\dot{\theta}_L$. Recalling from McDonnell Report A005

$$\ddot{\theta} = \frac{L}{I} \text{ and} \tag{12}$$

$$\dot{\theta} = \ddot{\theta}t \tag{13}$$

From Equation (13), the time required to accumulate a change in rate ($\Delta\dot{\theta}$) is

$$t = \frac{\Delta\dot{\theta}}{\ddot{\theta}} \tag{14}$$

Substituting Equation (12) into Equation (14) gives

$$t = \frac{I\Delta\dot{\theta}}{L} \tag{15}$$

The angular change after time (t) is

$$\Delta\theta = \frac{\ddot{\theta}t^2}{2} \tag{16}$$

Substituting Equations (12) and (15) into Equation (16) yields

$$\Delta\theta = \frac{\frac{I}{L}(\Delta\dot{\theta})^2}{2} \tag{17}$$

From the symmetry of the phase plane trajectory

$$\theta_o = \left\{ \begin{array}{l} 2\Delta\theta, \ \Delta\dot{\theta} < \dot{\theta}_L \\ 2\Delta\theta + \theta_{RL}, \ \Delta\dot{\theta} = \dot{\theta}_L \end{array} \right\} \tag{18}$$

The time the system is drifting at the rate limit ($\dot{\theta}_L$) is

$$t_{RL} = \frac{\theta_{RL}}{\dot{\theta}_L} \tag{19}$$

and from Equation (18)

$$t_{RL} = \frac{\theta_o - 2\Delta\theta}{\dot{\theta}_L} \tag{20}$$

Substituting for $\Delta\theta$ from Equation (17)

$$t_{RL} = \frac{\theta_o}{\dot{\theta}_L} - \frac{I}{L}\left(\frac{\Delta\dot{\theta}^2}{\dot{\theta}_L}\right) \tag{21}$$

except in the rate limiting case where $\Delta\dot{\theta} = \dot{\theta}_L$; therefore,

$$t_{RL} = \left(\frac{\theta_o}{\dot{\theta}_L} - \frac{I}{L}\dot{\theta}_L\right), \quad t_{RL} \geq 0 \tag{22}$$

A restriction is placed on Equation (22) since negative time has no meaning. The second term on the right hand side of Equation (22) is a positive constant for any system configuration, thereby establishing the point at which this expression gives a positive result. Interpreted physically, this is the θ_o input which causes rate limiting for the particular combination of parameters $\dot{\theta}_L$, I and L.

The total time to correct the initial error input (θ_o) is the time spent accelerating and accumulating $\Delta\theta$, Equation (17), plus the time spent at the rate limit. From Equation (18)

$$\theta_o = 2\Delta\theta, \text{ when } \Delta\dot{\theta} < \dot{\theta}_L \tag{23}$$

Substituting Equation (23) into Equation (17) yields

$$\theta_o = \frac{I}{L}(\Delta\dot{\theta})^2 \text{ and} \tag{24}$$

$$\Delta\dot{\theta} = \left(\frac{L}{I}\theta_o\right)^{\frac{1}{2}} \tag{25}$$

Since $\Delta\dot{\theta}$ is the change in $\dot{\theta}$ while the System is accelerating and the initial rate ($\dot{\theta}_o$) is generally near zero, $\Delta\dot{\theta}$ is redefined $\dot{\theta}_M$, the maximum value of $\dot{\theta}$ during application of a control torque. Equation (25) now becomes

$$\dot{\theta}_M = \left(\frac{L}{I}\theta_o\right)^{\frac{1}{2}} \tag{26}$$

where $\dot{\theta}_M \leq \dot{\theta}_L$ since the rate can never exceed $\dot{\theta}_L$. The total time accelerating is simply the time to $\dot{\theta}_M$ and return to zero with alternating polarity

torques or twice the time to accelerate to $\dot{\theta}_M$. From Equation (15)

$$t_A = \frac{2I}{L}\dot{\theta}_M \tag{27}$$

and the total response time is

$$t_T = t_A + t_{RL} \tag{28}$$

or from Equation (27)

$$t_T = \frac{2I}{L}\dot{\theta}_M + t_{RL} \tag{29}$$

Equations (22) and (29) give the response time as a function of $\dot{\theta}_L$, I, L and θ_o.

4.2 Fuel Consumption. The expression for fuel consumption as a function of various system parameters is derived below. The weight of fuel consumed in time (t) is

$$W = \frac{T}{I_{sp}}t \tag{30}$$

where I_{sp} = the specific thruster impulse in units of seconds and T = the thruster output in pounds. From Equation (27), the time which the thruster is on during any maneuver

$$t_A = \frac{2I}{L}\dot{\theta}_M \tag{31}$$

Therefore, from Equation (30) the weight of the fuel consumed on each attitude maneuver is

$$W = \frac{2IT}{LI_{sp}}\dot{\theta}_M \tag{32}$$

The torque (L) is

$$L = TR \tag{33}$$

where T is the thrust and L the moment arm. Substituting Equation (33) into Equation (32)

$$W = \frac{2I}{RI_{sp}}\dot{\theta}_M \qquad (34)$$

4.3 System Configuration Studies. Equations (22), (26), (29) and (34) were used to study the fuel consumption and speed of response for various system configurations. System parameters $\dot{\theta}_L$ and I, varied during the study, were chosen because of their significant effect on performance characteristics. One of the study parameters is incorporated into the ODAACS design ($\dot{\theta}_L$) and the other is a parameter of the controlled plant (I). Other plant parameters remain fixed throughout a typical mission and, in any event, have little effect on the speed of response and fuel consumption. Control program design parameters other than $\dot{\theta}_L$ primarily affect the accuracy and stability of the control process and have little influence on fuel consumption and response time. Therefore, $\dot{\theta}_L$ was selected as the control parameter to be examined.

A series of computations was performed with the equations previously described. The value of $\dot{\theta}_L$ was varied from 3 to 10 degrees per second and inertia from 1,000 to 64,000 slug-feet squared. The response time and fuel consumption were computed for each combination of $\dot{\theta}_L$ and I for angular error inputs (θ_o) of 5 to 90 degrees.

4.4 Results and Conclusions. Figures (22) through (29) are curves showing total response time as a function of $\dot{\theta}_L$ for values of θ_o. Each figure has a corresponding inertia (I). If rate limiting occurs at some point (θ_o, $\dot{\theta}_L$), the curve for t_T is flat for all higher values of $\dot{\theta}_L$ at the same θ_o, meaning that since rate limiting does not occur at the higher $\dot{\theta}_L$, response time is the same for all higher values of $\dot{\theta}_L$. The asymptotes which each of the individual

θ_o curves approach are the minimum response times for particular θ_o and I combinations. It is noted that the response time for a particular input error increases exponentially as the rate at which limiting occurs lessens.

When the selected $\dot{\theta}_L$ is low (e.g., three degrees per second), there is not much spread in the response time over the range of inertias, Figures 22 through 29. The effects of chosen $\dot{\theta}_L$'s on speed of response are illustrated by Figures 30 through 33, curves of the total response time (t_T) as a function of inertia (I) with ($\dot{\theta}_L$), the rate limit value, as the parameter. The curves demonstrate that the choice of rate limit values has the greatest response time effect at lower inertias since rate limiting occurs for smaller values of θ_o at the lower inertias.

At higher inertias a larger error (θ_o) is required for rate limiting. Convergence of the curves for all values of $\dot{\theta}_L$ indicates that system response time becomes increasingly independent of $\dot{\theta}_L$ and more dependent upon inertia. If response time requirements and maximum and minimum anticipated inertia are known, a set of curves similar to Figures 30 through 33 can be used for choosing a best value for the rate limit based upon speed of response.

Figures 34 through 41 are plots of the time spent at the rate limit (t_{RL}) as a function of the initial error (θ_o) with inertia the parameter. There is one set of curves for each rate limit value to illustrate the linear relationship between θ_o and the time spent drifting at the rate limit. The point at which the curves break away from the θ_o axis is the value of θ_o at which rate limiting occurs for any choice of $\dot{\theta}_L$.

Figures 42 through 49 present the fuel consumed as a function of $\dot{\theta}_L$ for various initial errors (θ_o). Fuel consumption is a linear function of the rate limit for any input (θ_o) as long as rate limiting occurs. When the rate

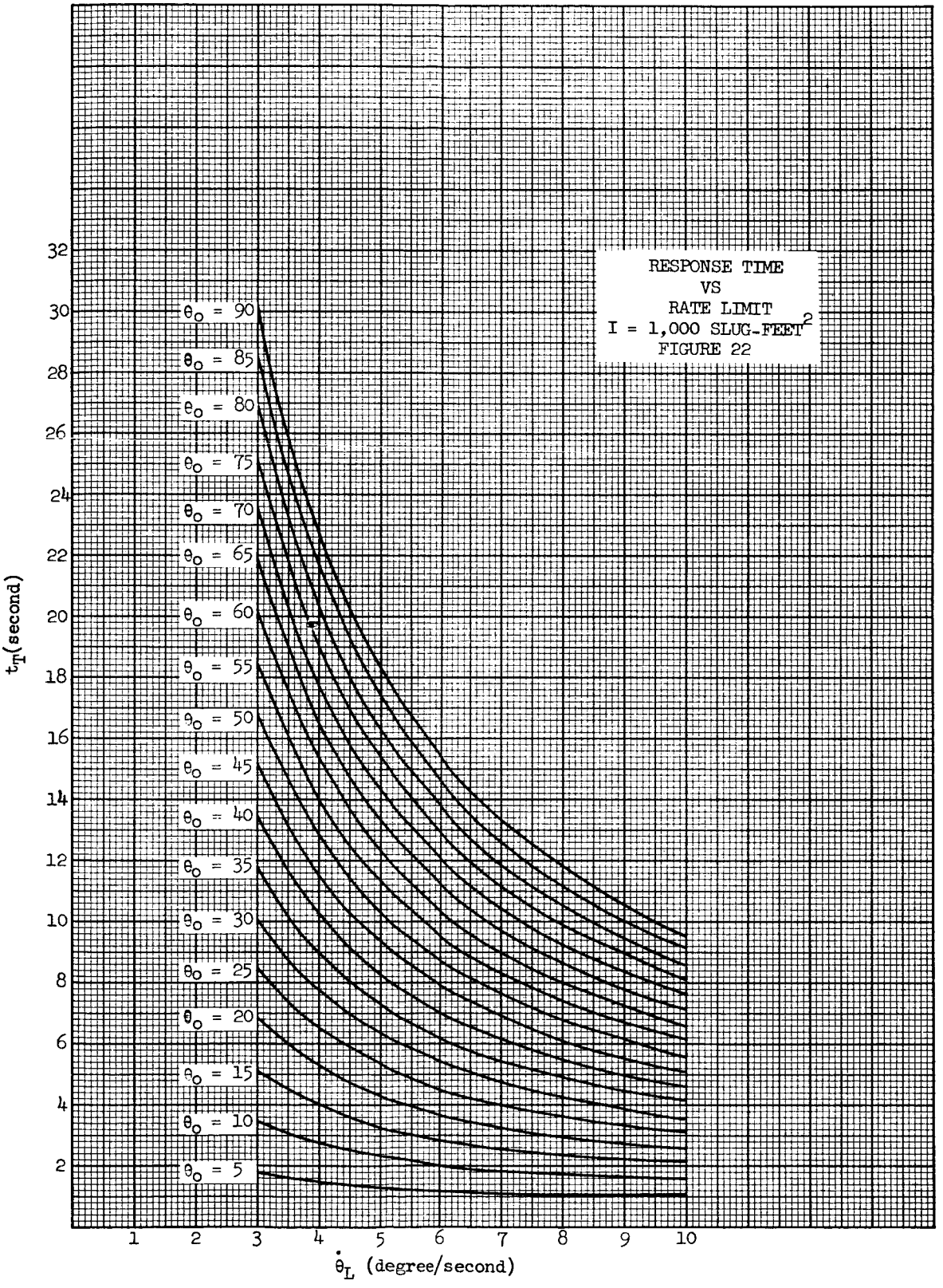
RESPONSE TIME
VS
RATE LIMIT
I = 1,000 SLUG-FEET²
FIGURE 22
θ_o = 90
θ_o = 85
θ_o = 80
θ_o = 75
θ_o = 70
θ_o = 65
θ_o = 60
θ_o = 55
θ_o = 50
θ_o = 45
θ_o = 40
θ_o = 35
θ_o = 30
θ_o = 25
θ_o = 20
θ_o = 15
θ_o = 10
θ_o = 5
t_T (second)
2
4
6
8
10
12
14
16
18
20
22
24
26
28
30
32
1
2
3
4
5
6
7
8
9
10
$\dot{\theta}_L$ (degree/second)

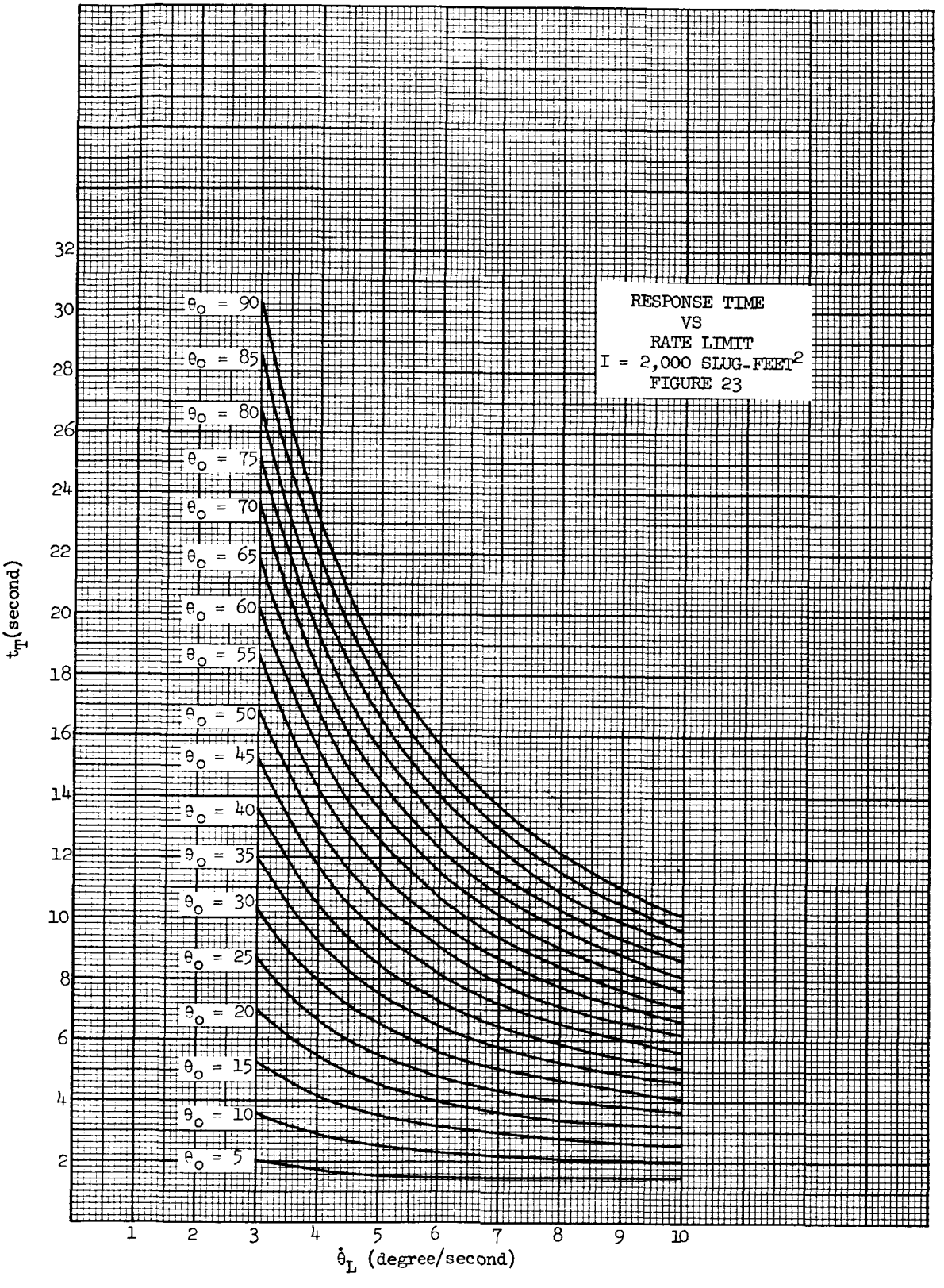
RESPONSE TIME
VS
RATE LIMIT
I = 2,000 SLUG-FEET²
FIGURE 23
t_T (second)
$\dot{\theta}_L$ (degree/second)
θ_o = 90
θ_o = 85
θ_o = 80
θ_o = 75
θ_o = 70
θ_o = 65
θ_o = 60
θ_o = 55
θ_o = 50
θ_o = 45
θ_o = 40
θ_o = 35
θ_o = 30
θ_o = 25
θ_o = 20
θ_o = 15
θ_o = 10
θ_o = 5
32
30
28
26
24
22
20
18
16
14
12
10
8
6
4
2
1
2
3
4
5
6
7
8
9
10

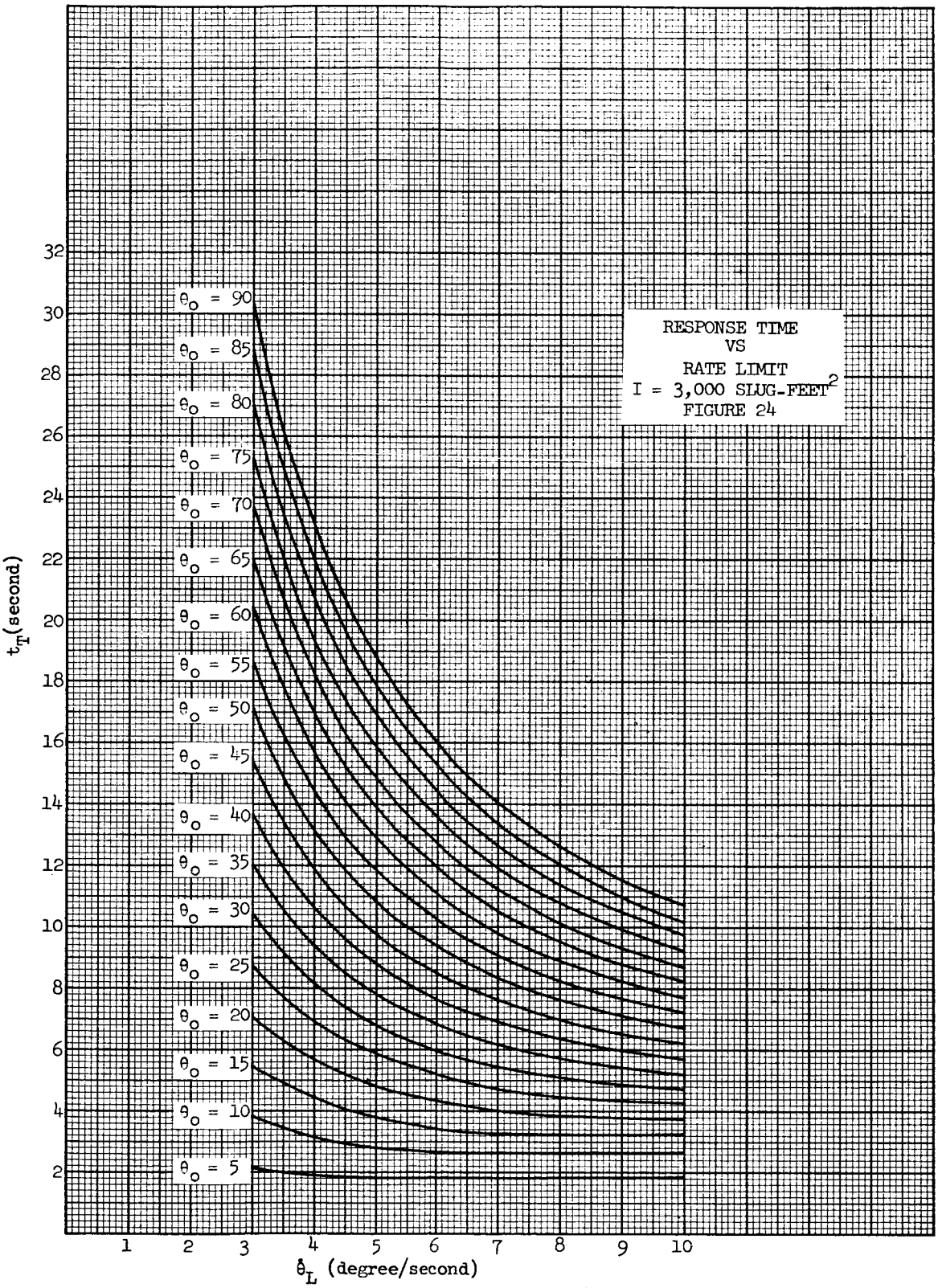
RESPONSE TIME
VS
RATE LIMIT
I = 3,000 SLUG-FEET^2
FIGURE 24
θ_o = 90
θ_o = 85
θ_o = 80
θ_o = 75
θ_o = 70
θ_o = 65
θ_o = 60
θ_o = 55
θ_o = 50
θ_o = 45
θ_o = 40
θ_o = 35
θ_o = 30
θ_o = 25
θ_o = 20
θ_o = 15
θ_o = 10
θ_o = 5
t_T (second)
32
30
28
26
24
22
20
18
16
14
12
10
8
6
4
2
1
2
3
4
5
6
7
8
9
10
$\dot{\theta}_L$ (degree/second)

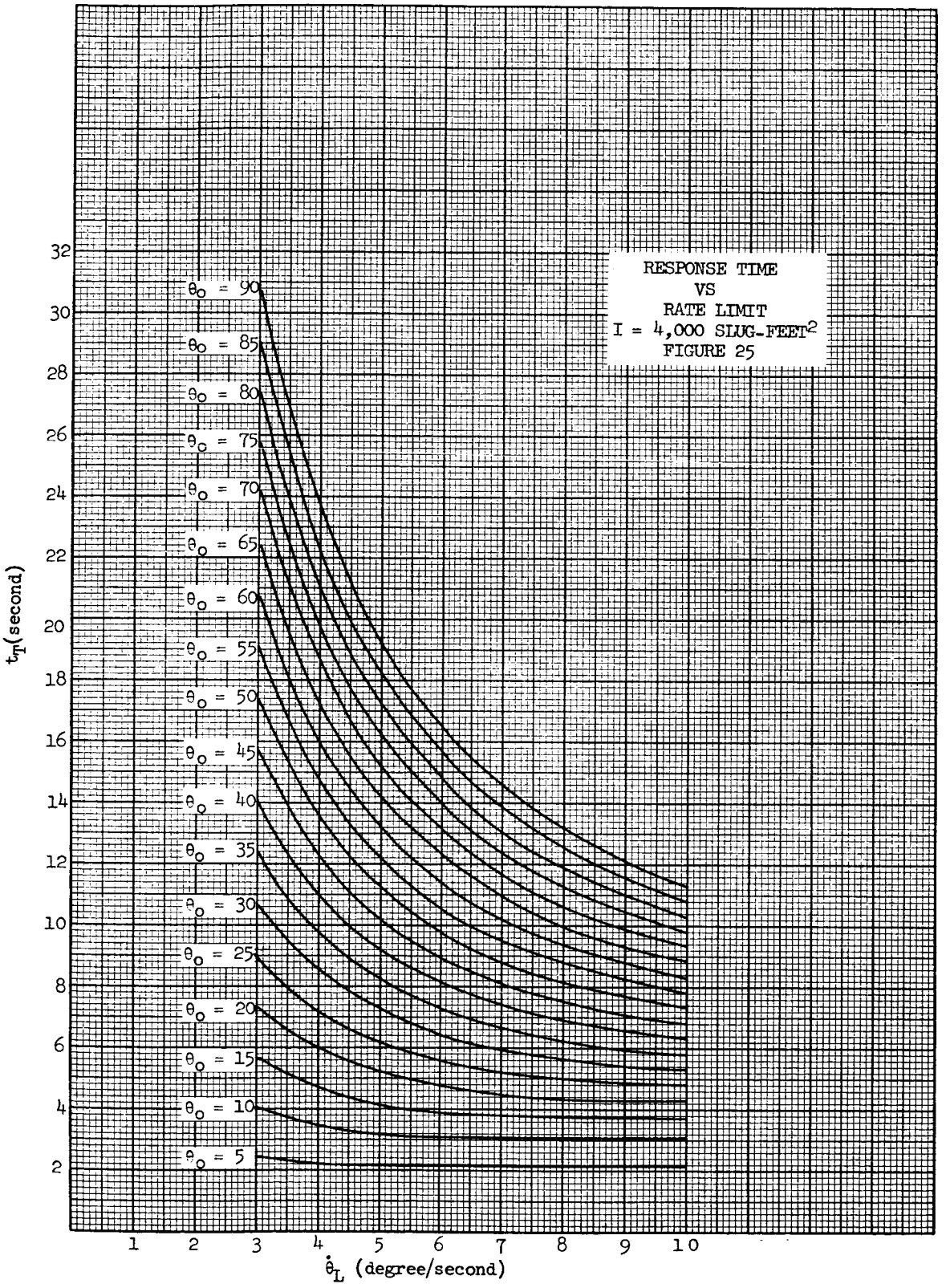
RESPONSE TIME
VS
RATE LIMIT
I = 4,000 SLUG-FEET²
FIGURE 25
t_T(second)
$\dot{\theta}_L$ (degree/second)
θ_o = 90
θ_o = 85
θ_o = 80
θ_o = 75
θ_o = 70
θ_o = 65
θ_o = 60
θ_o = 55
θ_o = 50
θ_o = 45
θ_o = 40
θ_o = 35
θ_o = 30
θ_o = 25
θ_o = 20
θ_o = 15
θ_o = 10
θ_o = 5
32
30
28
26
24
22
20
18
16
14
12
10
8
6
4
2
1
2
3
4
5
6
7
8
9
10

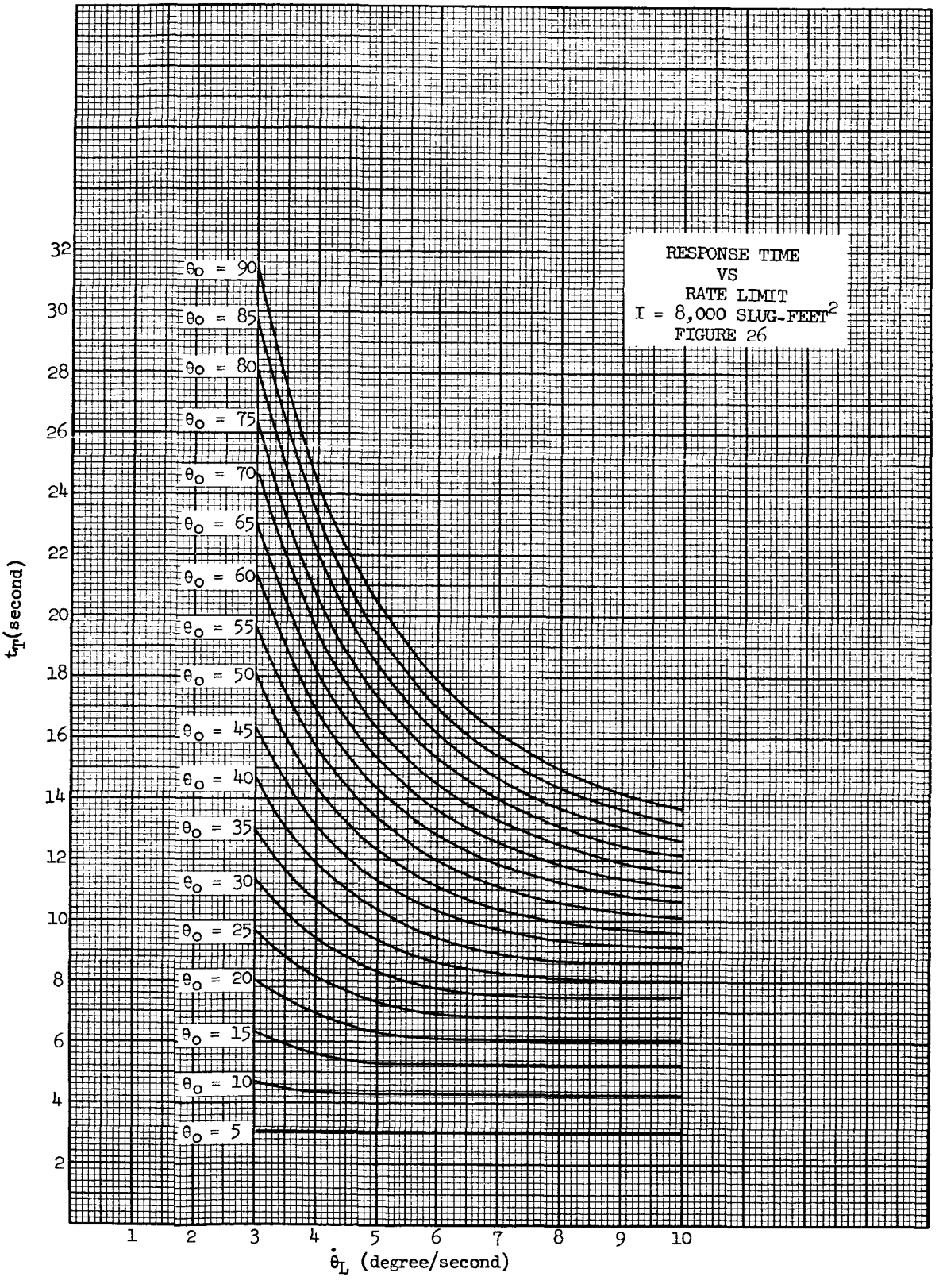
RESPONSE TIME
VS
RATE LIMIT
I = 8,000 SLUG-FEET^2
FIGURE 26
θ_o = 90
θ_o = 85
θ_o = 80
θ_o = 75
θ_o = 70
θ_o = 65
θ_o = 60
θ_o = 55
θ_o = 50
θ_o = 45
θ_o = 40
θ_o = 35
θ_o = 30
θ_o = 25
θ_o = 20
θ_o = 15
θ_o = 10
θ_o = 5
t_T (second)
32
30
28
26
24
22
20
18
16
14
12
10
8
6
4
2
1
2
3
4
5
6
7
8
9
10
$\dot{\theta}_L$ (degree/second)

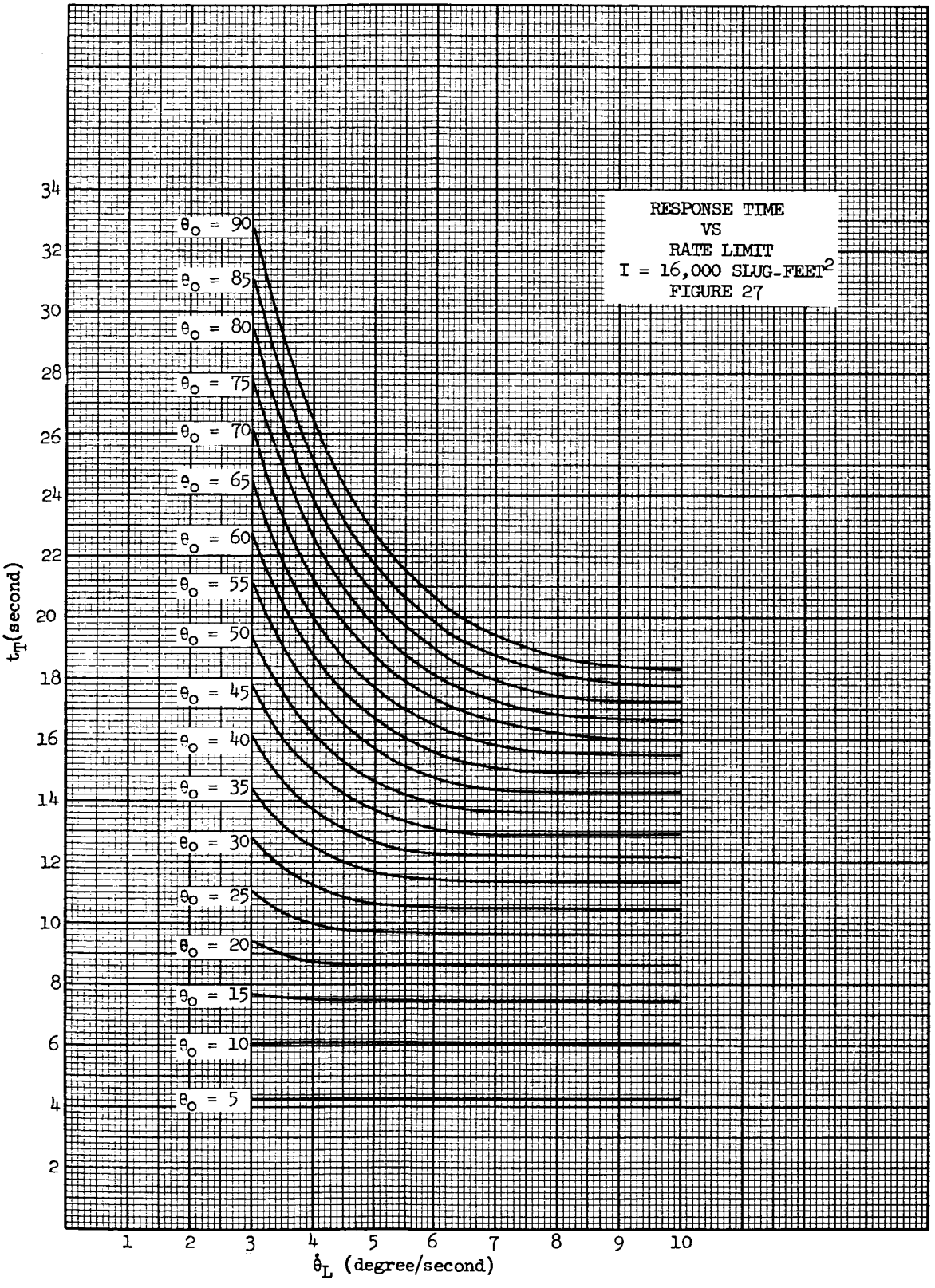
RESPONSE TIME
VS
RATE LIMIT
I = 16,000 SLUG-FEET²
FIGURE 27
θo = 90
θo = 85
θo = 80
θo = 75
θo = 70
θo = 65
θo = 60
θo = 55
θo = 50
θo = 45
θo = 40
θo = 35
θo = 30
θo = 25
θo = 20
θo = 15
θo = 10
θo = 5
tT (second)
2
4
6
8
10
12
14
16
18
20
22
24
26
28
30
32
34
1
2
3
4
5
6
7
8
9
10
θ̇L (degree/second)

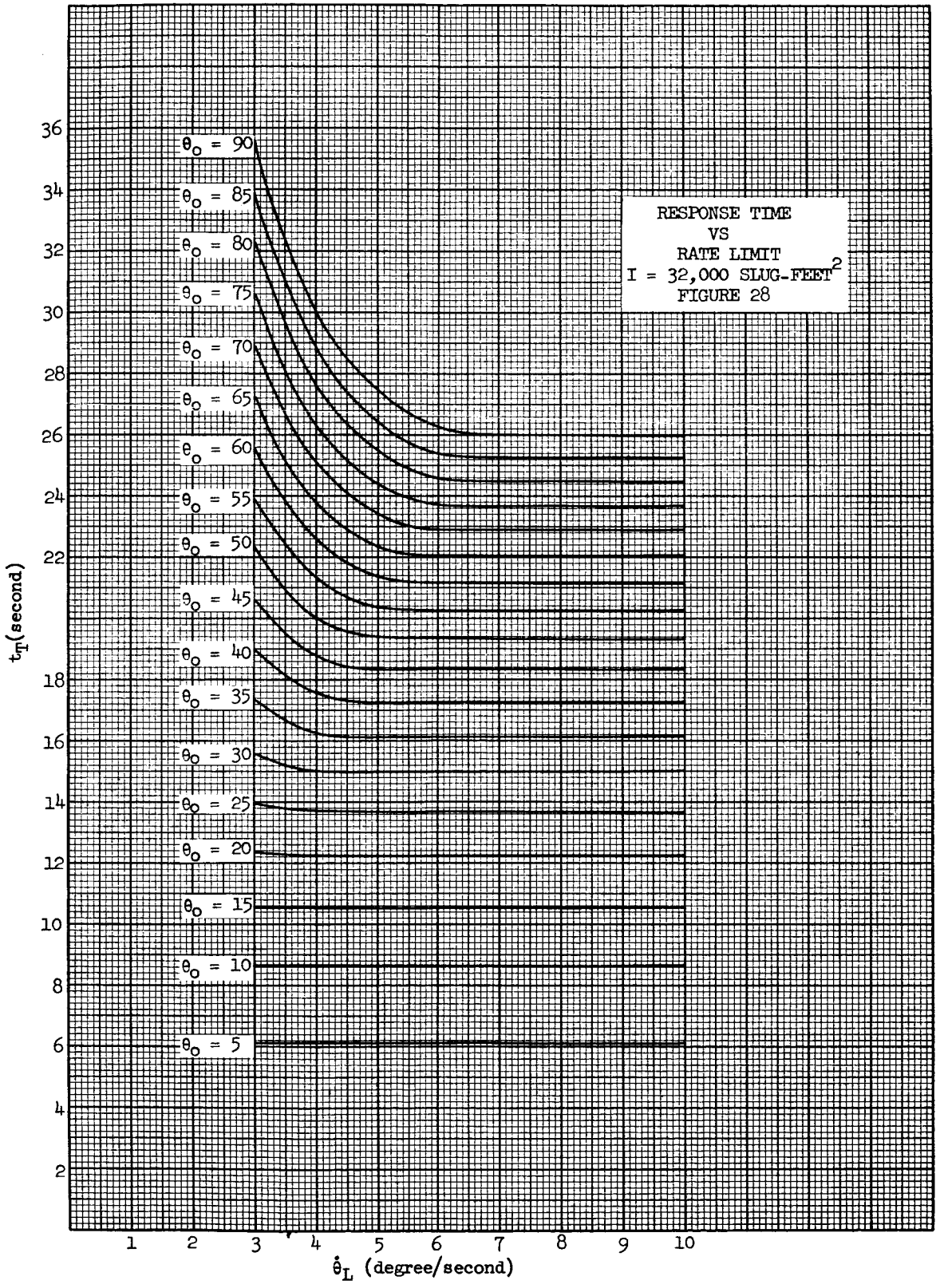
RESPONSE TIME
VS
RATE LIMIT
I = 32,000 SLUG-FEET²
FIGURE 28
θo = 90
θo = 85
θo = 80
θo = 75
θo = 70
θo = 65
θo = 60
θo = 55
θo = 50
θo = 45
θo = 40
θo = 35
θo = 30
θo = 25
θo = 20
θo = 15
θo = 10
θo = 5
tT (second)
θ̇L (degree/second)
2
4
6
8
10
12
14
16
18
22
24
26
28
30
32
34
36
1
2
3
4
5
6
7
8
9
10

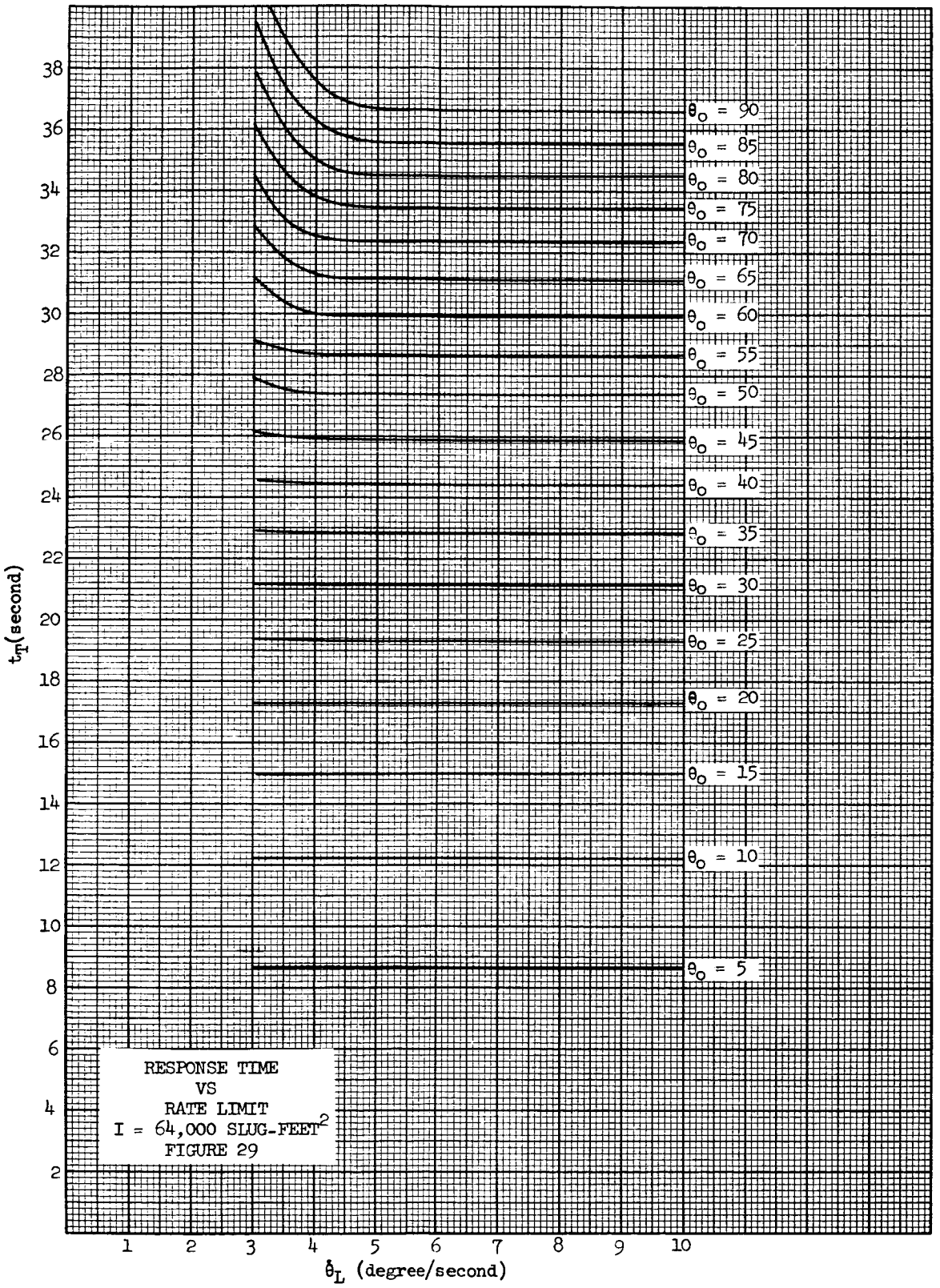
t_T(second)
38
36
34
32
30
28
26
24
22
20
18
16
14
12
10
8
6
4
2
θ_o = 90
θ_o = 85
θ_o = 80
θ_o = 75
θ_o = 70
θ_o = 65
θ_o = 60
θ_o = 55
θ_o = 50
θ_o = 45
θ_o = 40
θ_o = 35
θ_o = 30
θ_o = 25
θ_o = 20
θ_o = 15
θ_o = 10
θ_o = 5
RESPONSE TIME
VS
RATE LIMIT
I = 64,000 SLUG-FEET^2
FIGURE 29
1
2
3
4
5
6
7
8
9
10
$\dot{\theta}_L$ (degree/second)

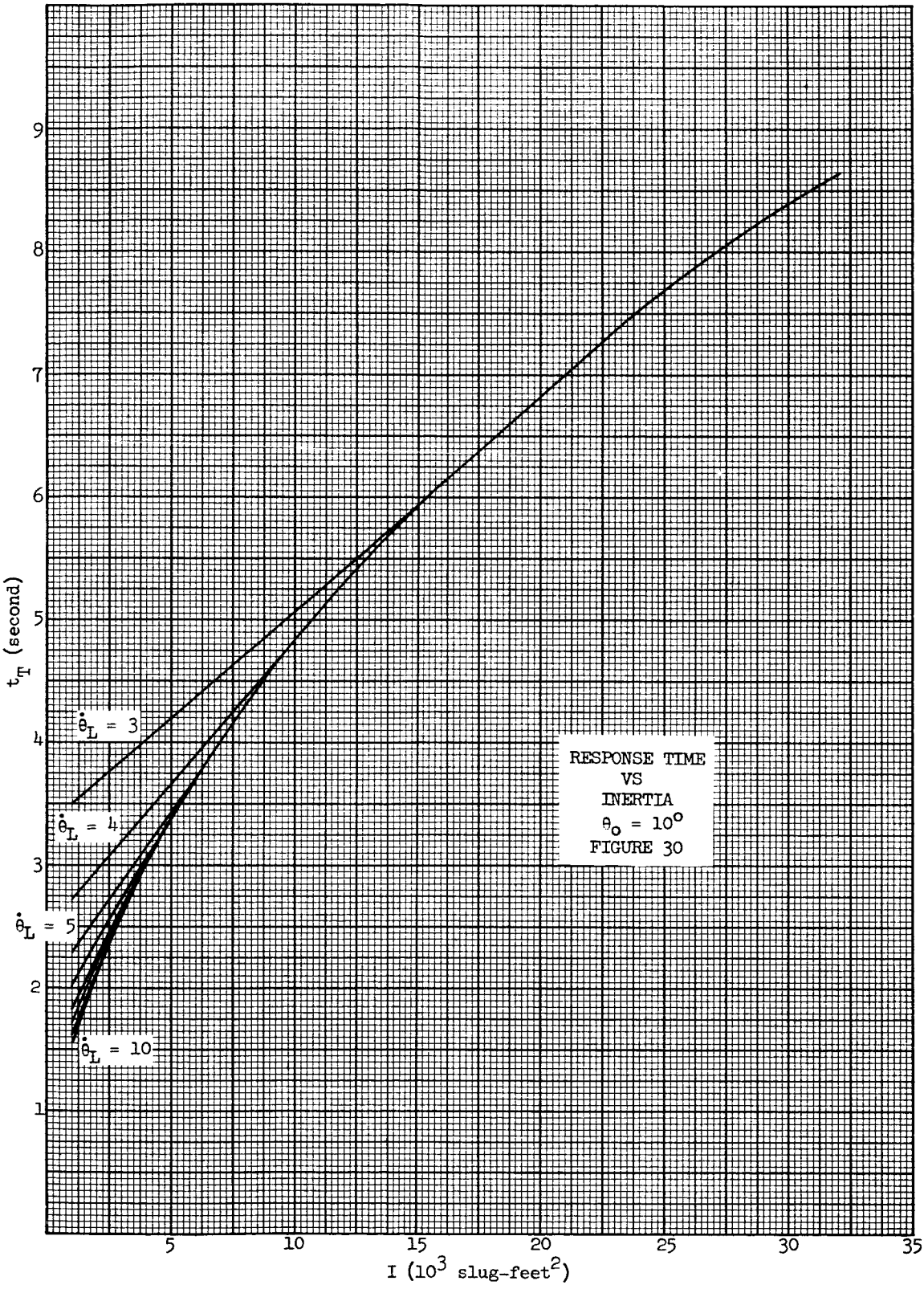
9
8
7
6
5
4
3
2
1
t_T (second)
$\dot{\theta}_L$ = 3
$\dot{\theta}_L$ = 4
$\dot{\theta}_L$ = 5
$\dot{\theta}_L$ = 10
RESPONSE TIME
VS
INERTIA
θ_o = 10°
FIGURE 30
5
10
15
20
25
30
35
I (10^3 slug-feet^2)

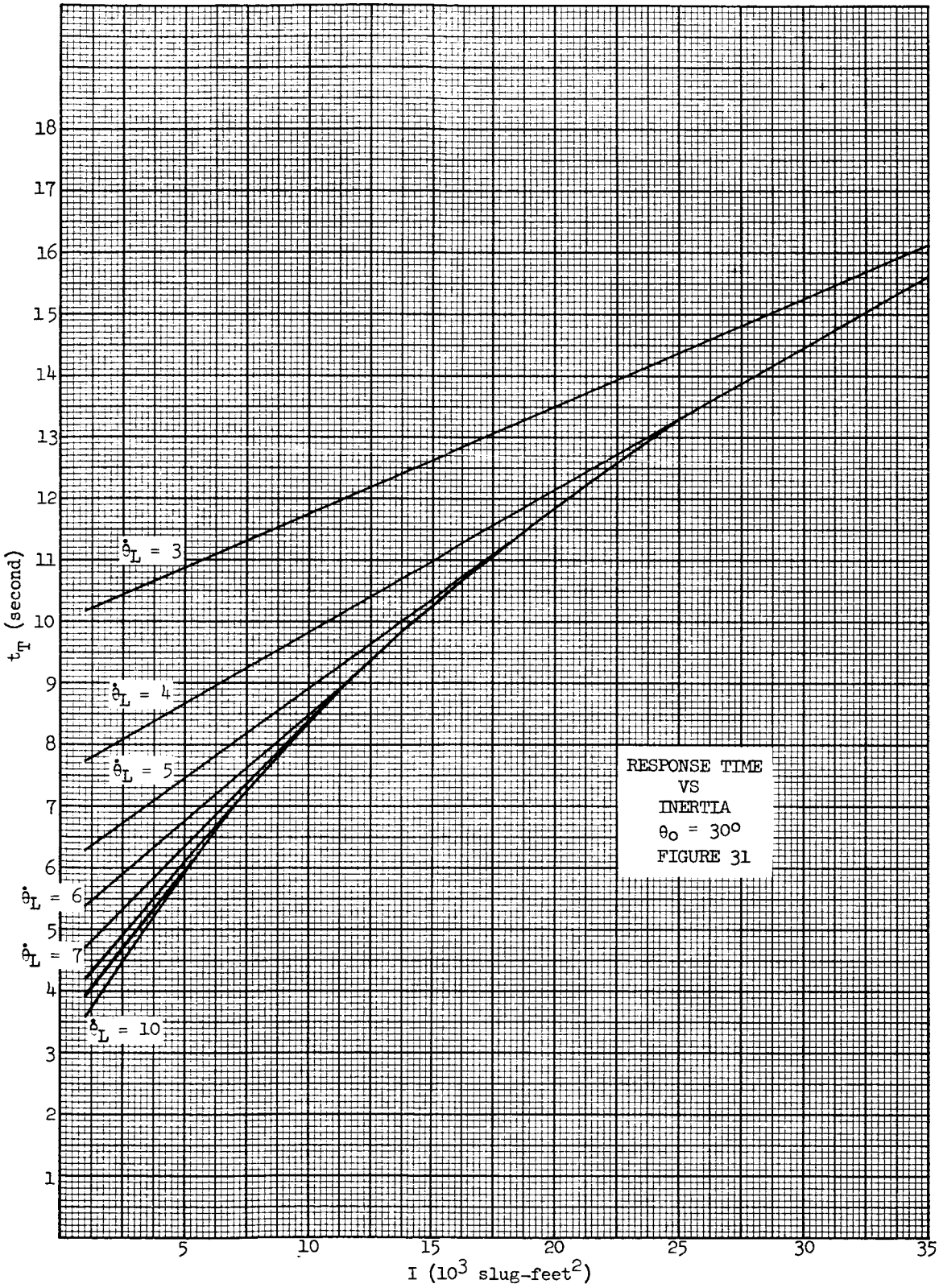
t_T (second)
I (10^3 slug-feet^2)
$\dot{\theta}_L$ = 3
$\dot{\theta}_L$ = 4
$\dot{\theta}_L$ = 5
$\dot{\theta}_L$ = 6
$\dot{\theta}_L$ = 7
$\dot{\theta}_L$ = 10
RESPONSE TIME
VS
INERTIA
θ_o = 30°
FIGURE 31

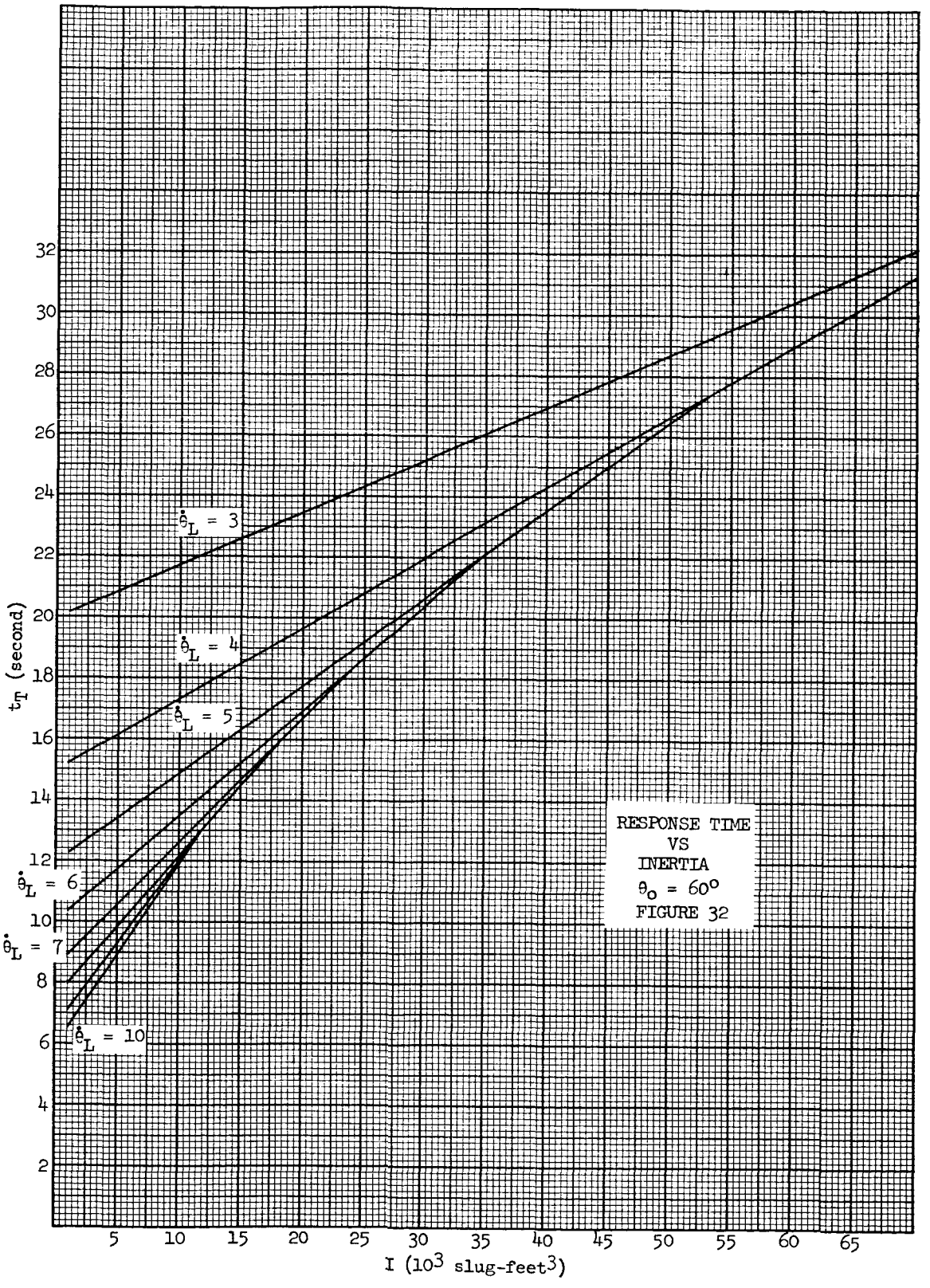
32
30
28
26
24
22
20
18
16
14
12
10
8
6
4
2
t_T (second)
$\dot{\theta}_L$ = 3
$\dot{\theta}_L$ = 4
$\dot{\theta}_L$ = 5
$\dot{\theta}_L$ = 6
$\dot{\theta}_L$ = 7
$\dot{\theta}_L$ = 10
5 10 15 20 25 30 35 40 45 50 55 60 65
I (10^3 slug-feet^3)
RESPONSE TIME
VS
INERTIA
θ_o = 60°
FIGURE 32

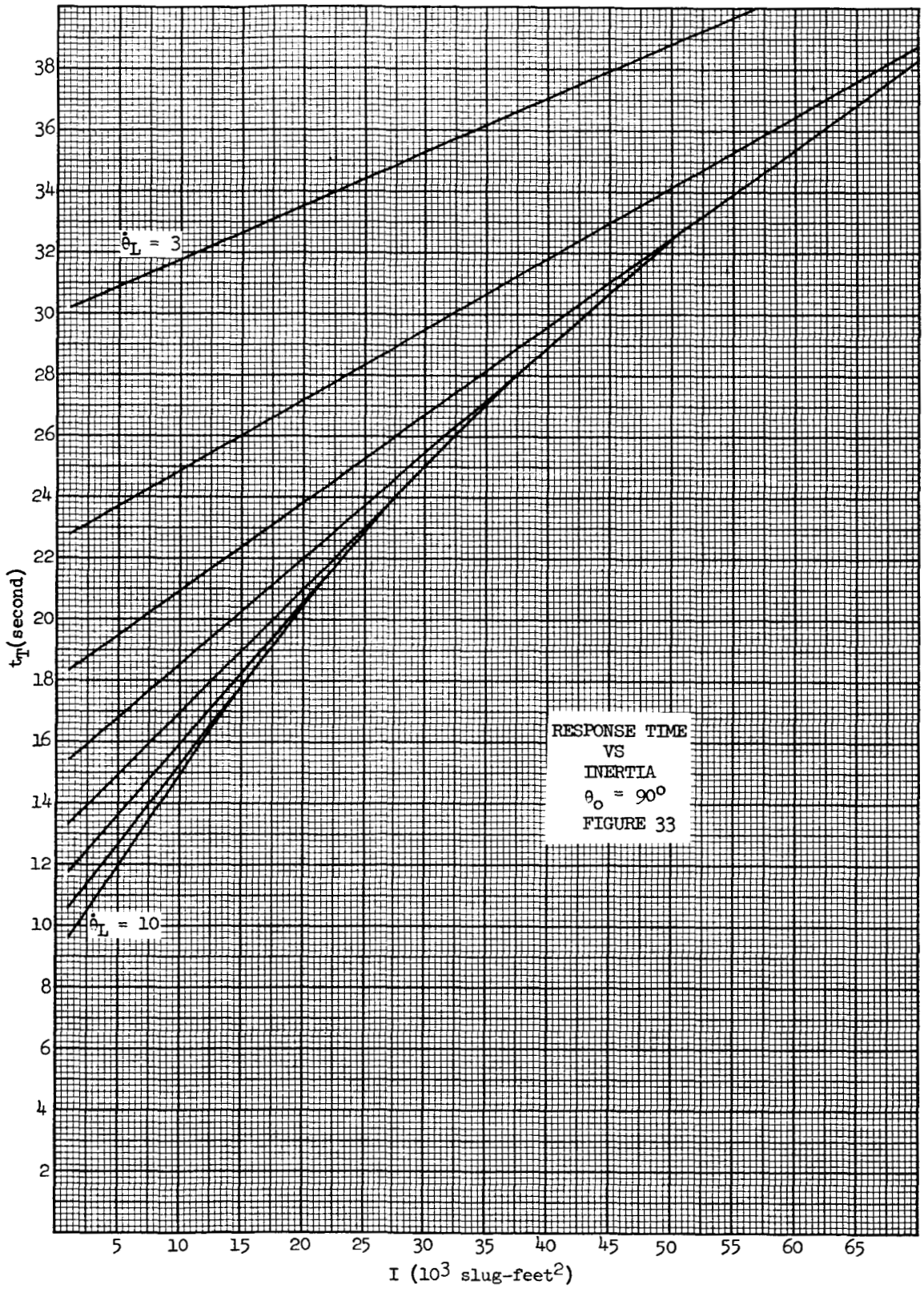
$\dot{\theta}_L$ = 3
$\dot{\theta}_L$ = 10
t_T(second)
38
36
34
32
30
28
26
24
22
20
18
16
14
12
10
8
6
4
2
5
10
15
20
25
30
35
40
45
50
55
60
65
I (10^3 slug-feet^2)
RESPONSE TIME
VS
INERTIA
θ_o = 90°
FIGURE 33

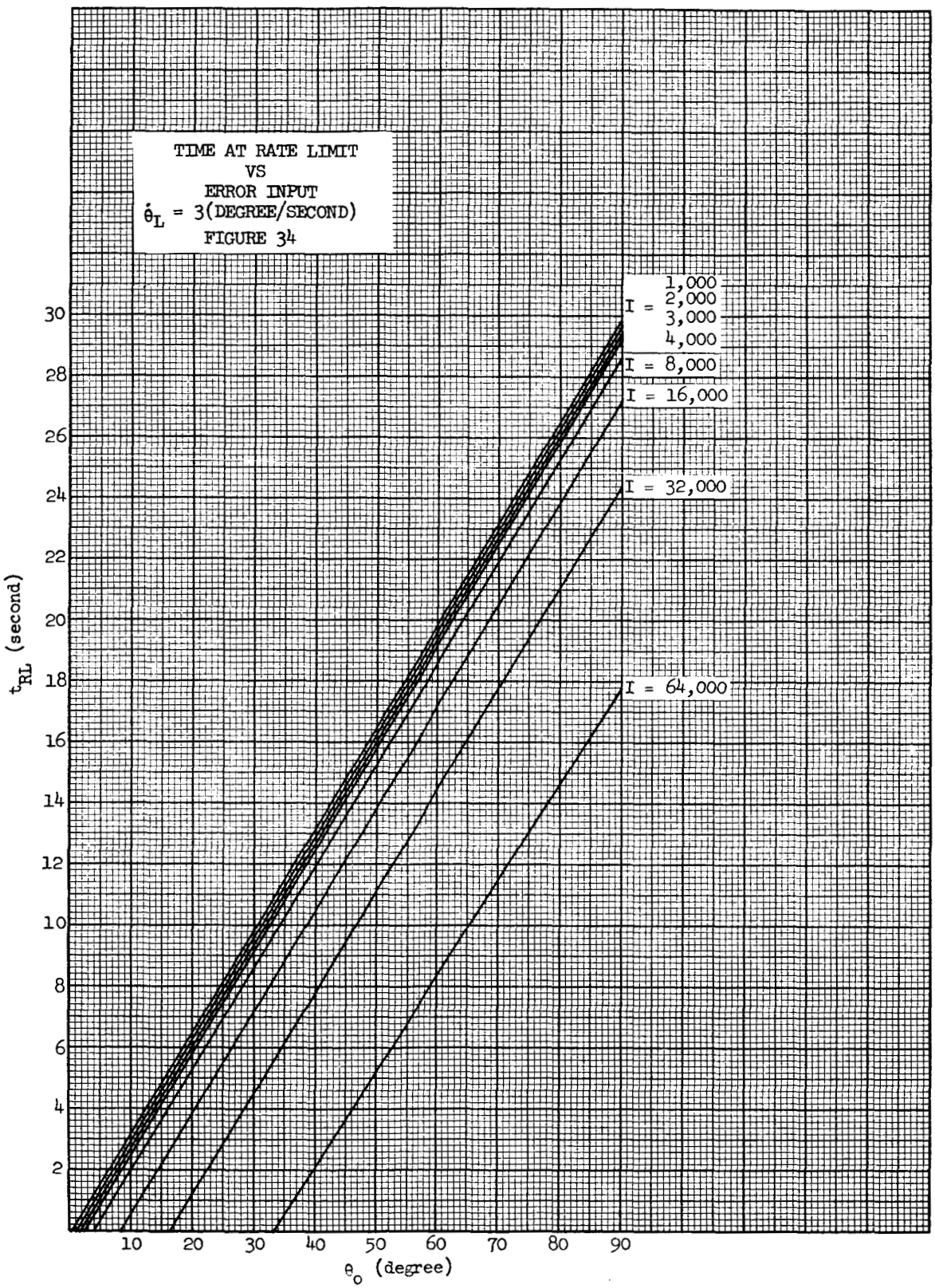
TIME AT RATE LIMIT
VS
ERROR INPUT
$\dot{\theta}_L$ = 3(DEGREE/SECOND)
FIGURE 34
I = 1,000
2,000
3,000
4,000
I = 8,000
I = 16,000
I = 32,000
I = 64,000
t_{RL} (second)
θ_o (degree)
2
4
6
8
10
12
14
16
18
20
22
24
26
28
30
10
20
30
40
50
60
70
80
90

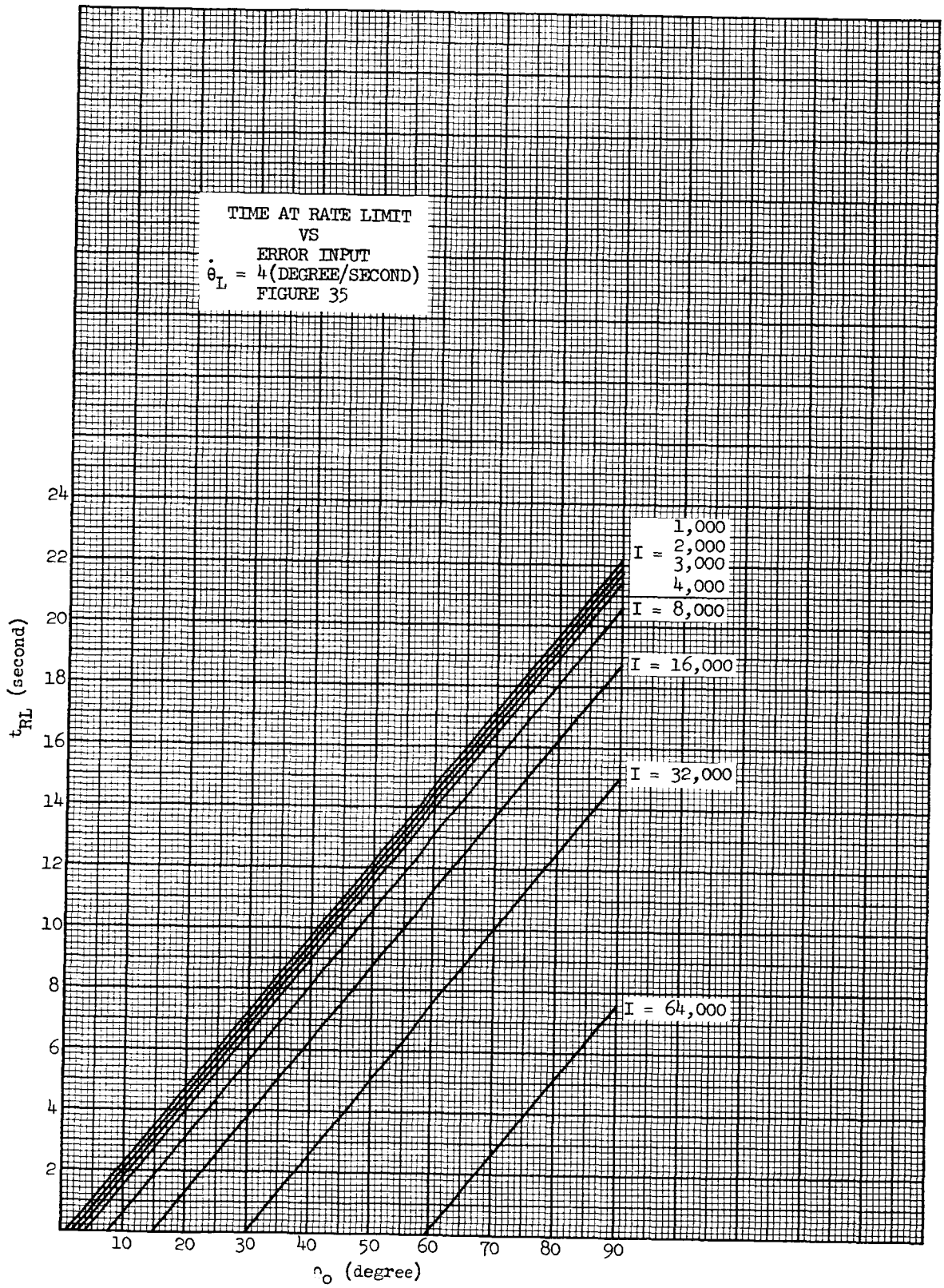
TIME AT RATE LIMIT
VS
ERROR INPUT
$\dot{\theta}_L$ = 4(DEGREE/SECOND)
FIGURE 35
t_{RL} (second)
θ_o (degree)
I = 1,000
2,000
3,000
4,000
I = 8,000
I = 16,000
I = 32,000
I = 64,000
2
4
6
8
10
12
14
16
18
20
22
24
10
20
30
40
50
60
70
80
90

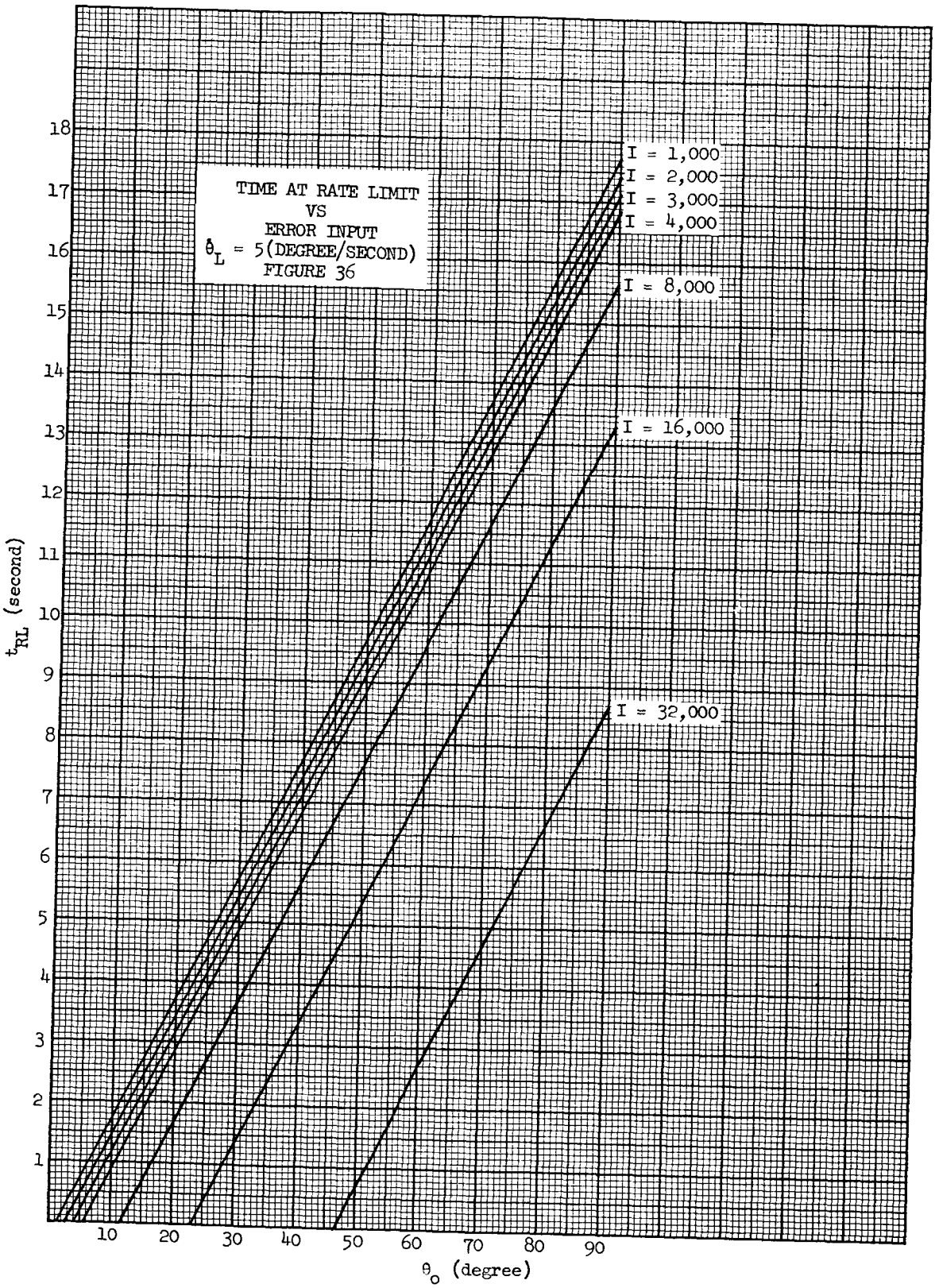
TIME AT RATE LIMIT
VS
ERROR INPUT
$\dot{\theta}_L$ = 5(DEGREE/SECOND)
FIGURE 36
I = 1,000
I = 2,000
I = 3,000
I = 4,000
I = 8,000
I = 16,000
I = 32,000
t_{RL} (second)
θ_o (degree)
1
2
3
4
5
6
7
8
9
10
11
12
13
14
15
16
17
18
10
20
30
40
50
60
70
80
90

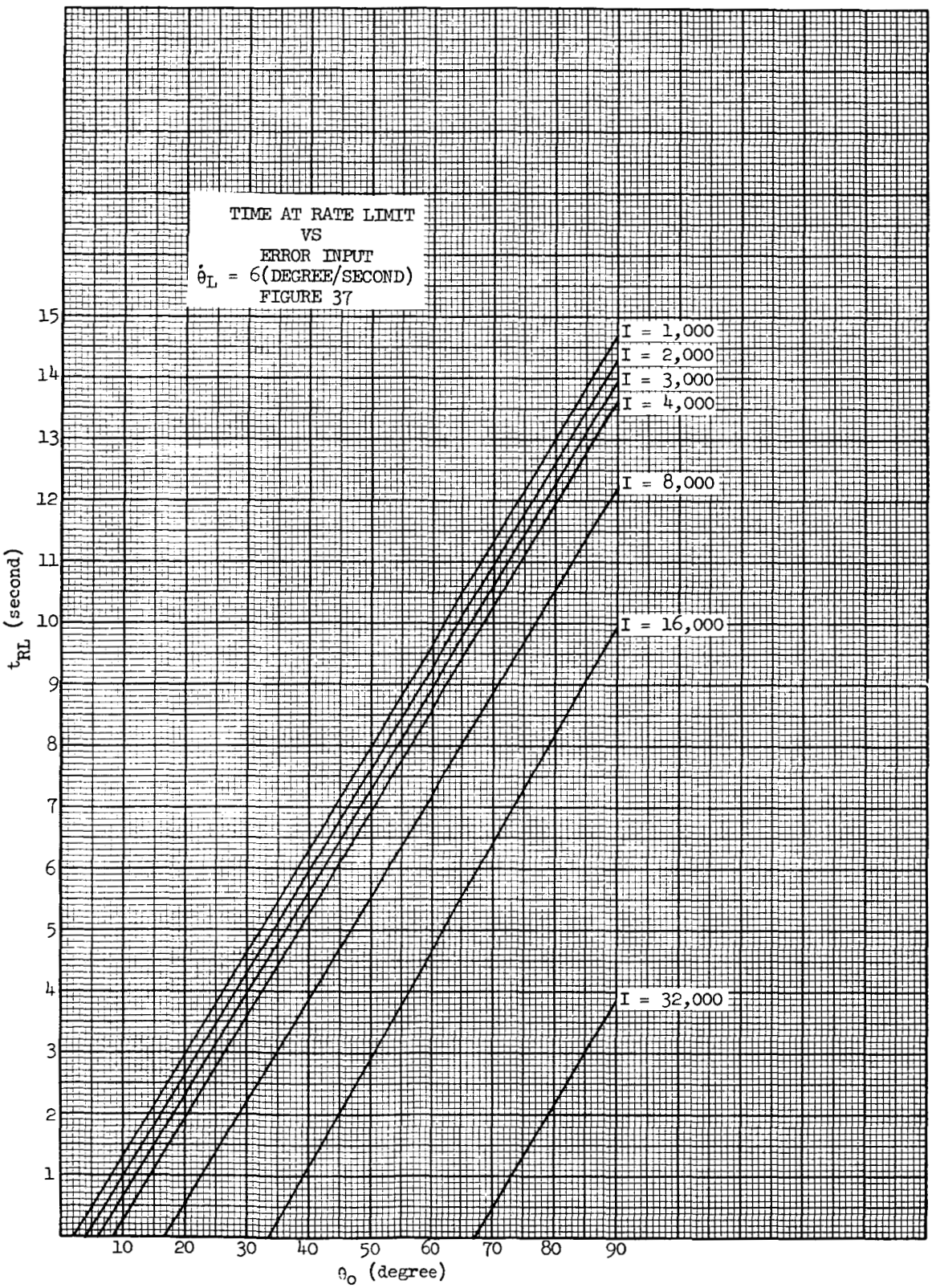
TIME AT RATE LIMIT
VS
ERROR INPUT
$\dot{\theta}_L$ = 6(DEGREE/SECOND)
FIGURE 37
I = 1,000
I = 2,000
I = 3,000
I = 4,000
I = 8,000
I = 16,000
I = 32,000
t_{RL} (second)
θ_o (degree)
1
2
3
4
5
6
7
8
9
10
11
12
13
14
15
10
20
30
40
50
60
70
80
90

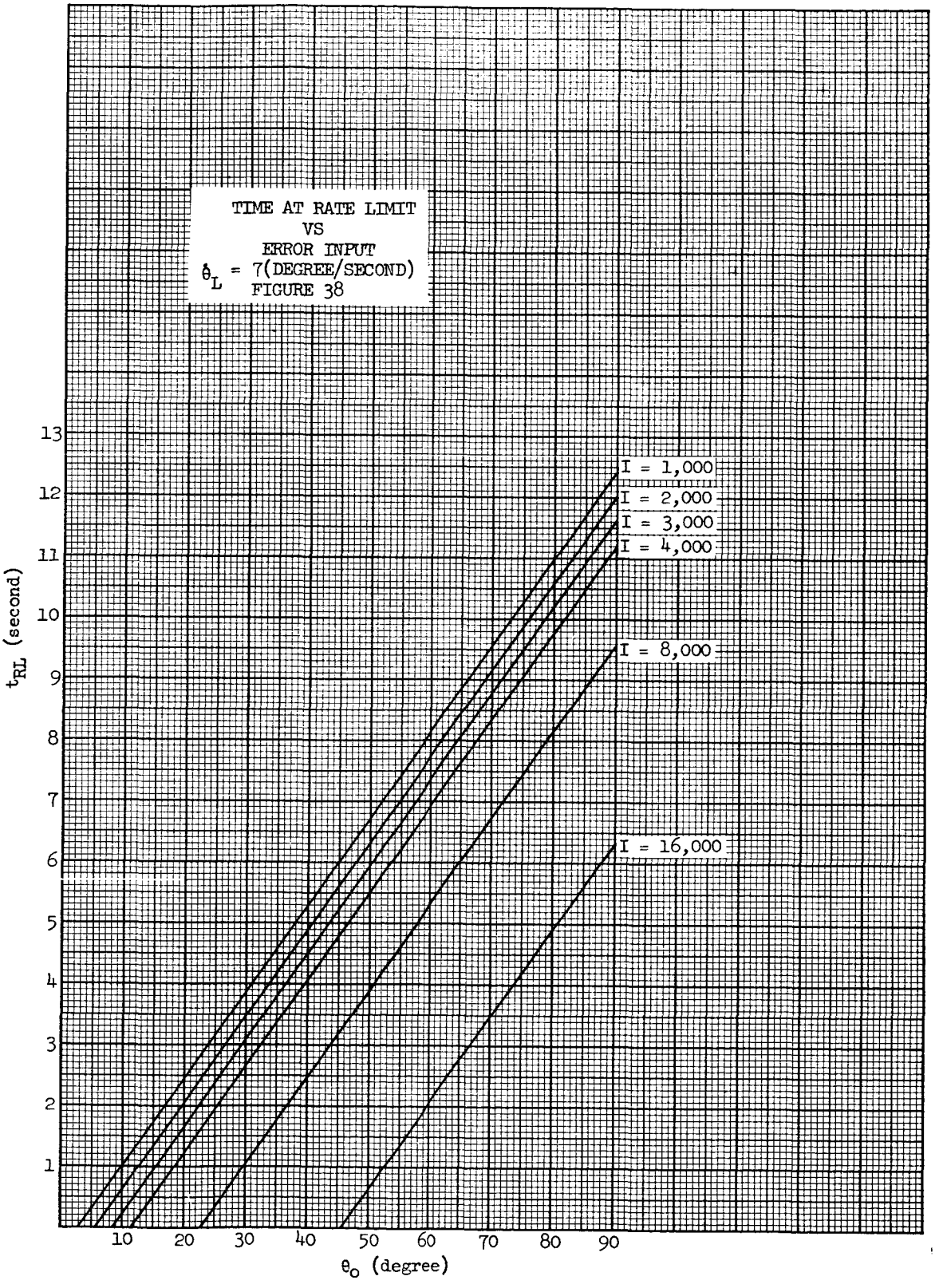
TIME AT RATE LIMIT
VS
ERROR INPUT
$\dot{\theta}_L$ = 7(DEGREE/SECOND)
FIGURE 38
I = 1,000
I = 2,000
I = 3,000
I = 4,000
I = 8,000
I = 16,000
t_{RL} (second)
θ_o (degree)
1
2
3
4
5
6
7
8
9
10
11
12
13
10
20
30
40
50
60
70
80
90

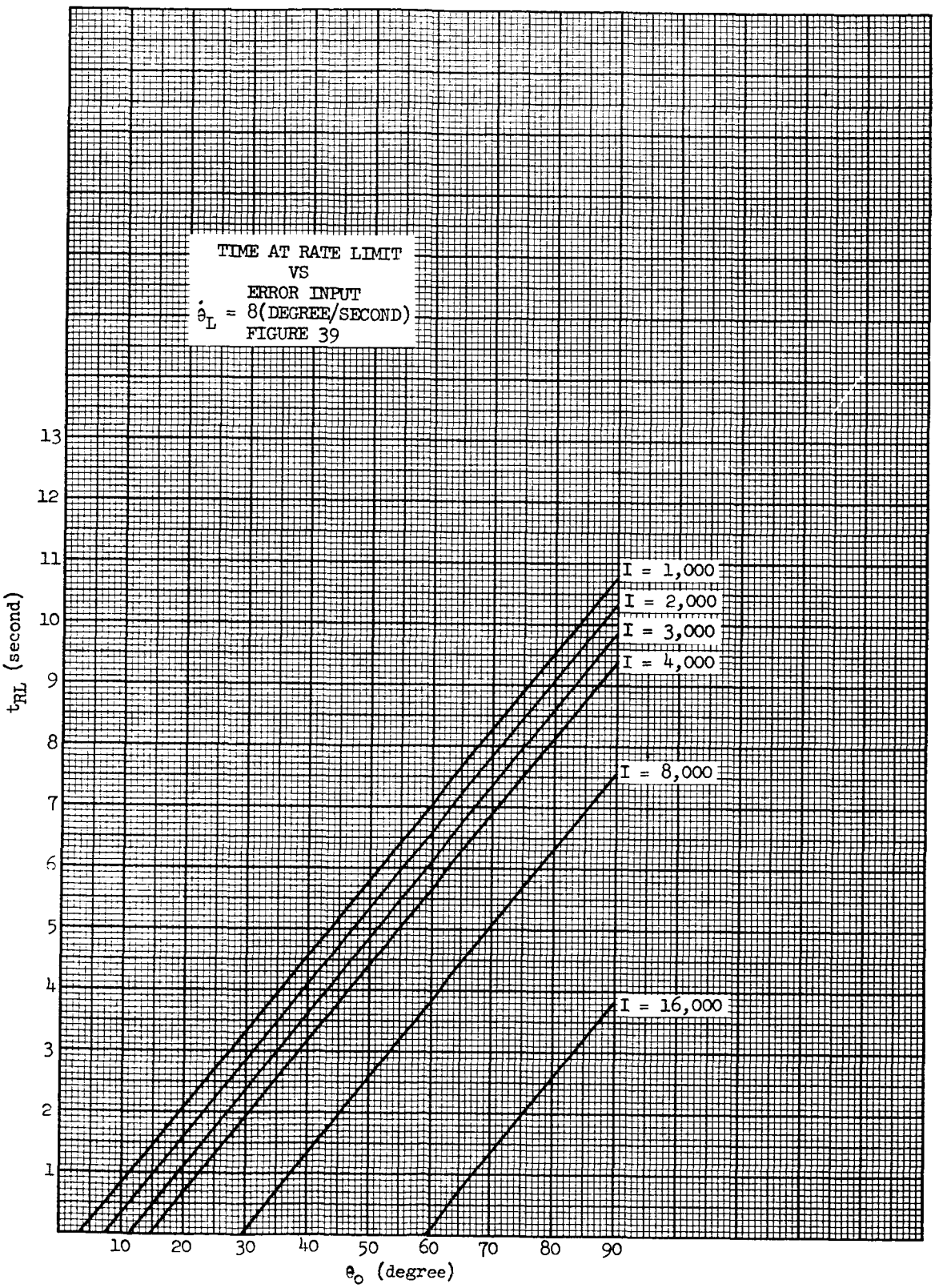
TIME AT RATE LIMIT
VS
ERROR INPUT
$\dot{\theta}_L$ = 8(DEGREE/SECOND)
FIGURE 39
t_{RL} (second)
13
12
11
10
9
8
7
6
5
4
3
2
1
I = 1,000
I = 2,000
I = 3,000
I = 4,000
I = 8,000
I = 16,000
10
20
30
40
50
60
70
80
90
θ_o (degree)

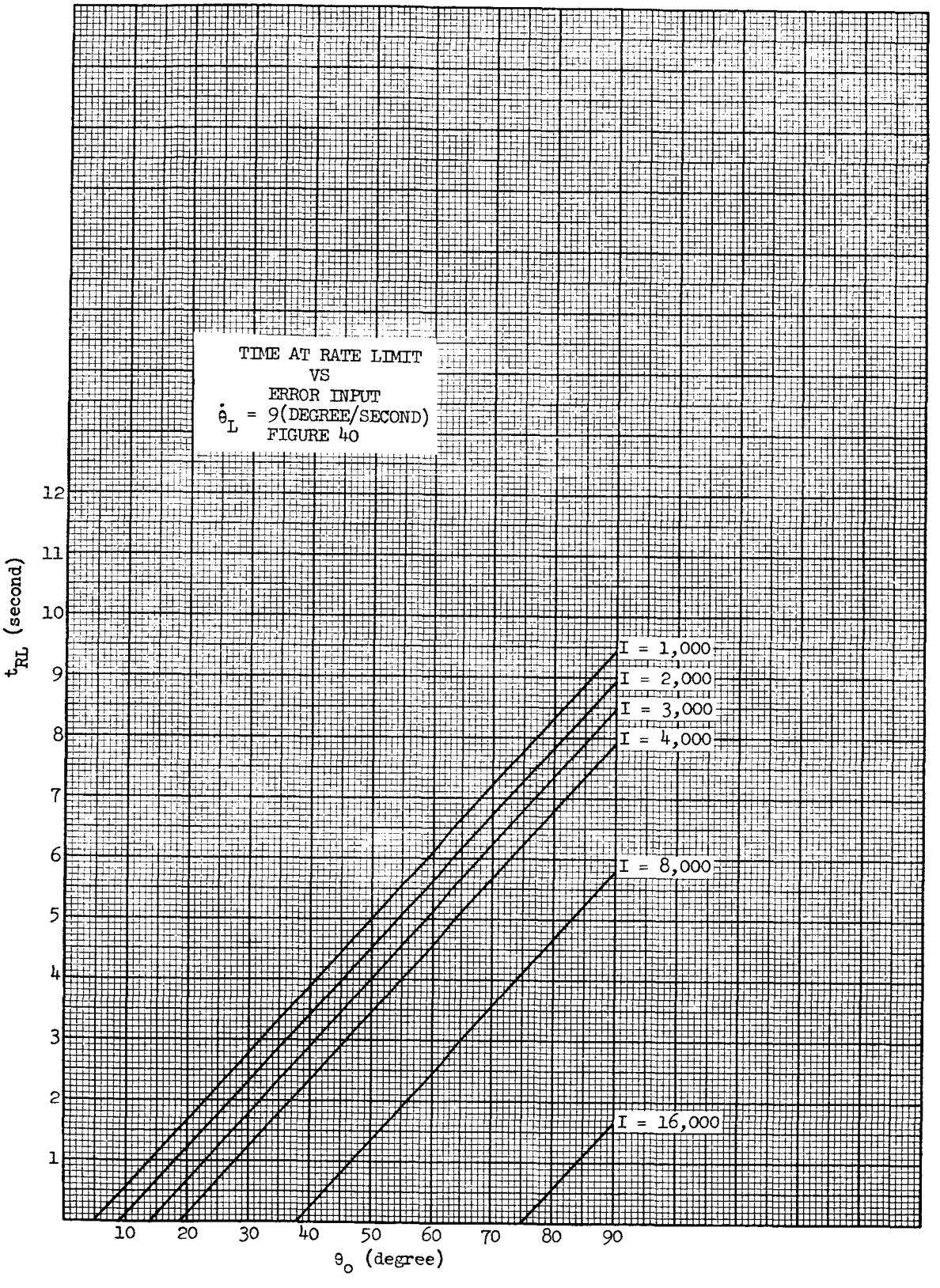
TIME AT RATE LIMIT
VS
ERROR INPUT
$\dot{\theta}_L$ = 9(DEGREE/SECOND)
FIGURE 40
t_{RL} (second)
12
11
10
9
8
7
6
5
4
3
2
1
I = 1,000
I = 2,000
I = 3,000
I = 4,000
I = 8,000
I = 16,000
10
20
30
40
50
60
70
80
90
θ_o (degree)

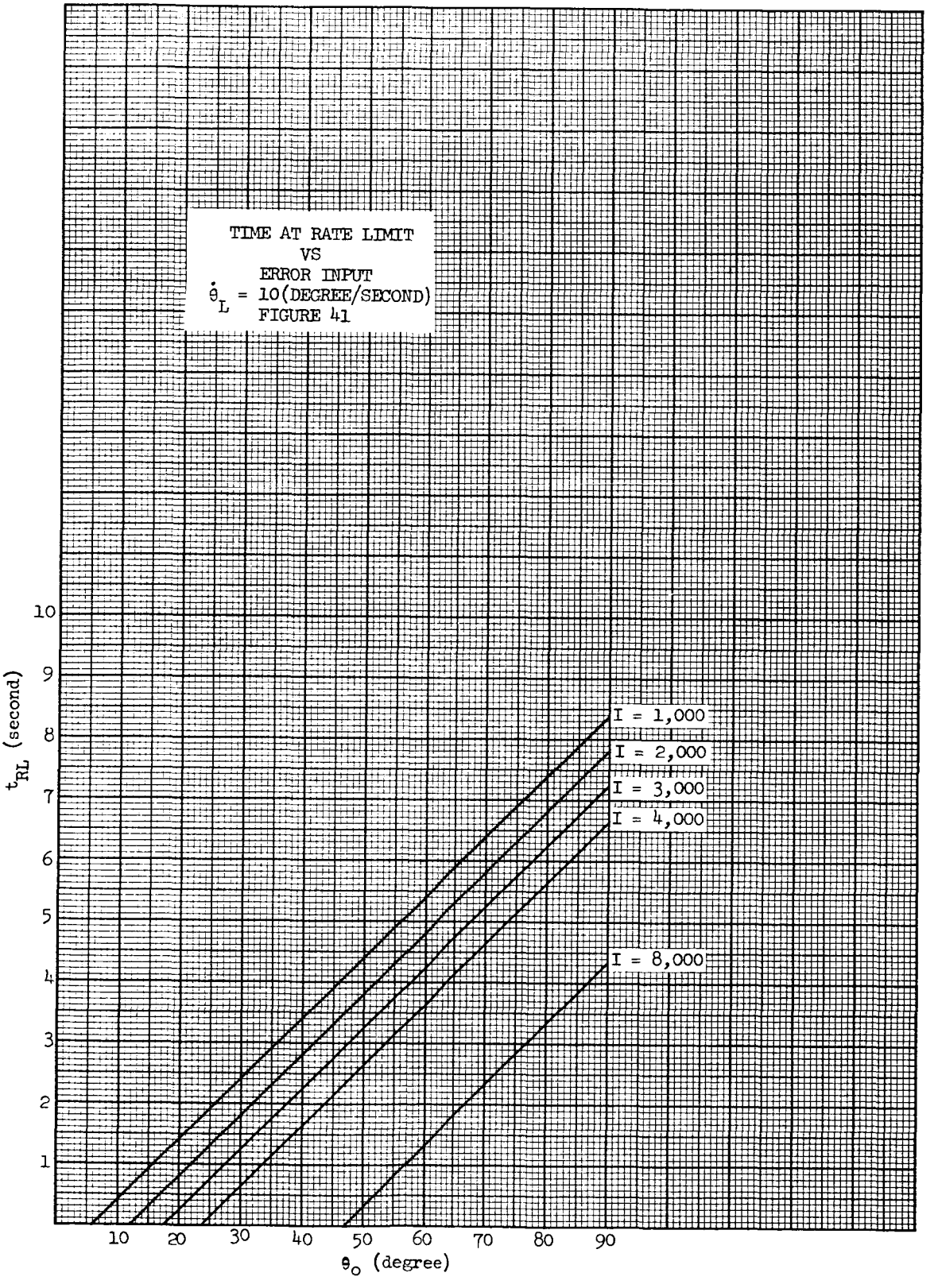
TIME AT RATE LIMIT
VS
ERROR INPUT
$\dot{\theta}_L$ = 10(DEGREE/SECOND)
FIGURE 41
t_{RL} (second)
10
9
8
7
6
5
4
3
2
1
I = 1,000
I = 2,000
I = 3,000
I = 4,000
I = 8,000
10
20
30
40
50
60
70
80
90
θ_o (degree)

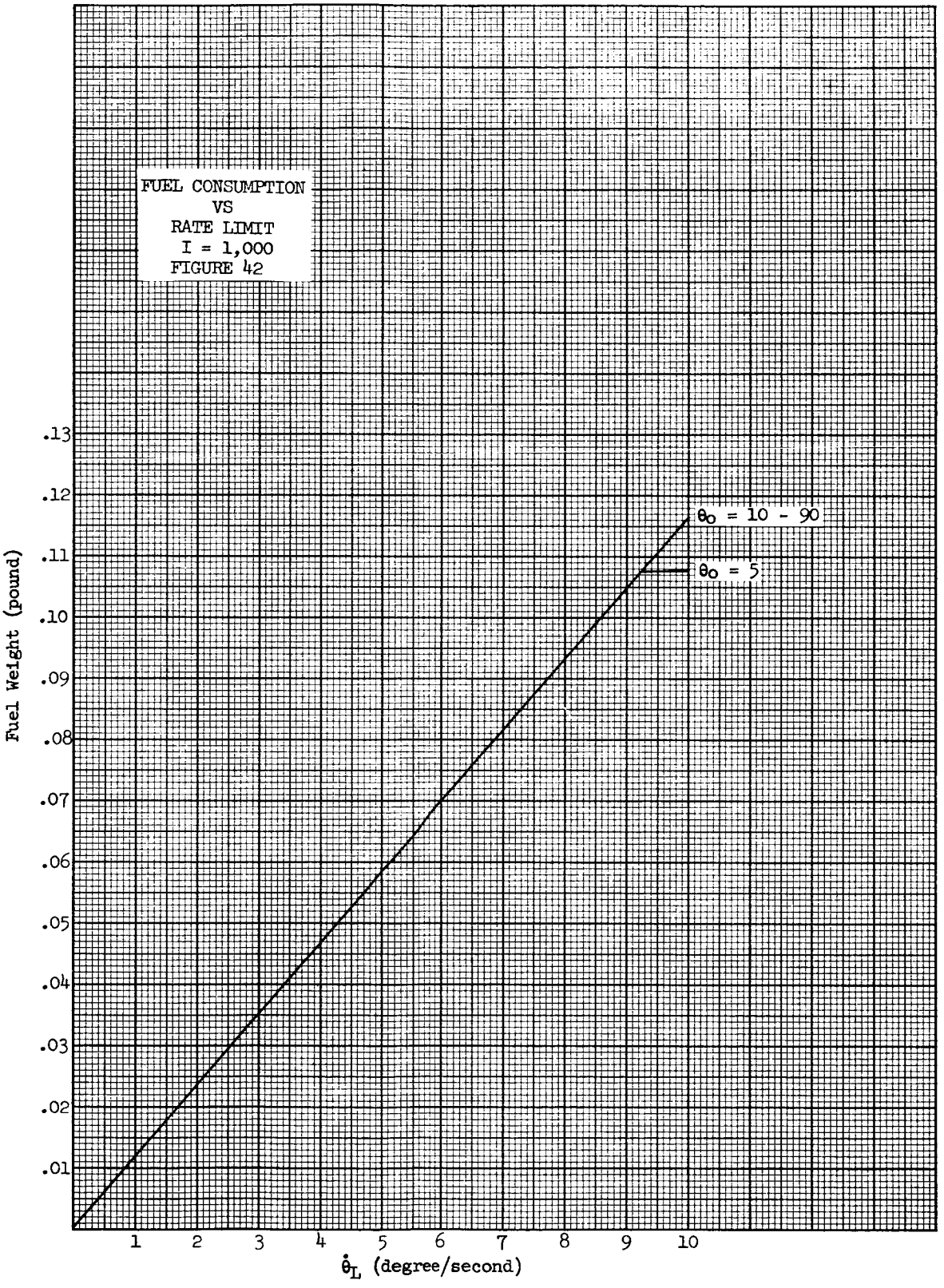
FUEL CONSUMPTION
VS
RATE LIMIT
I = 1,000
FIGURE 42
Fuel Weight (pound)
.13
.12
.11
.10
.09
.08
.07
.06
.05
.04
.03
.02
.01
θo = 10 - 90
θo = 5
1
2
3
4
5
6
7
8
9
10
θ̇L (degree/second)

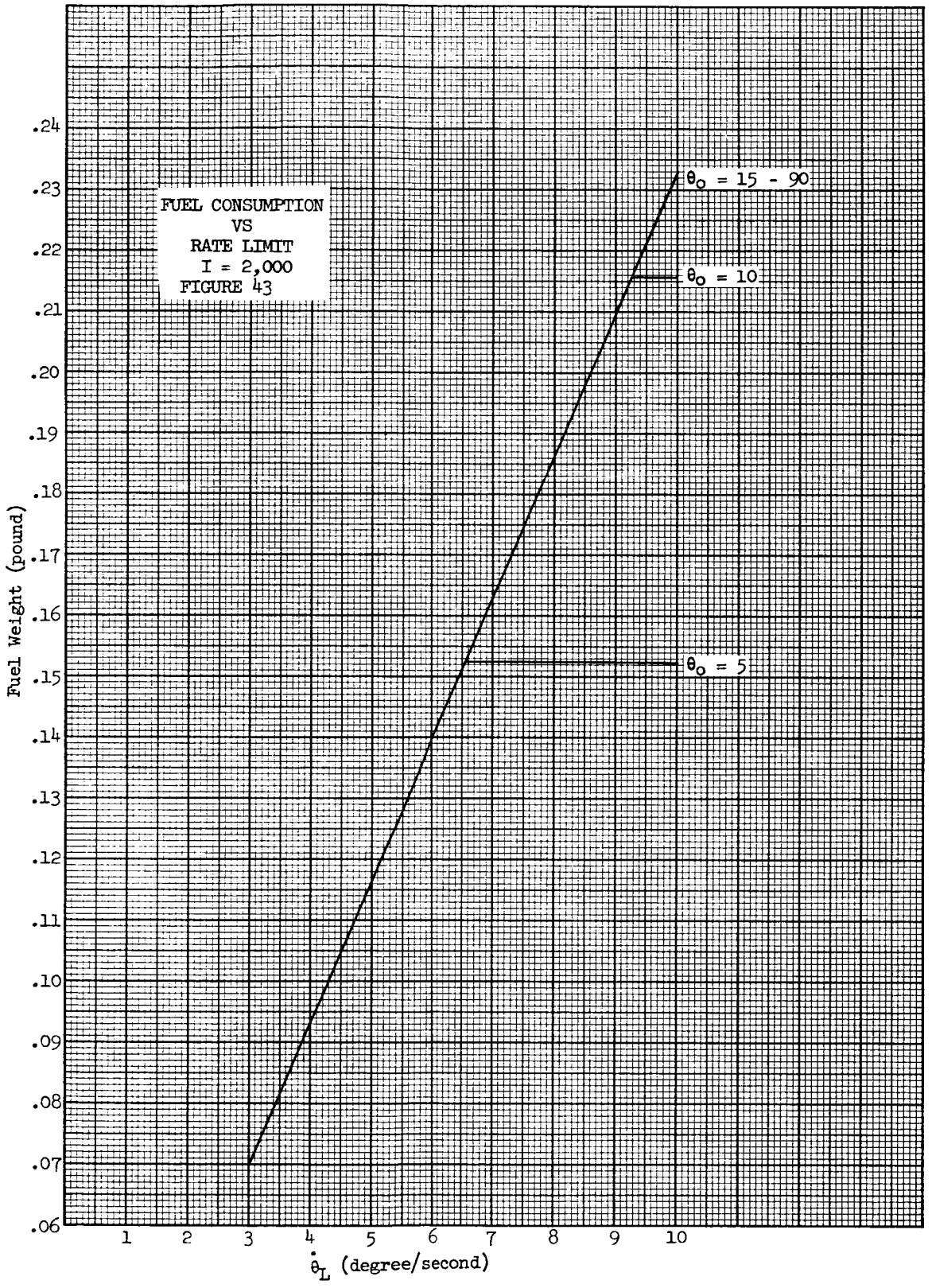
FUEL CONSUMPTION
VS
RATE LIMIT
I = 2,000
FIGURE 43
θ_o = 15 - 90
θ_o = 10
θ_o = 5
Fuel Weight (pound)
.24
.23
.22
.21
.20
.19
.18
.17
.16
.15
.14
.13
.12
.11
.10
.09
.08
.07
.06
1
2
3
4
5
6
7
8
9
10
$\dot{\theta}_L$ (degree/second)

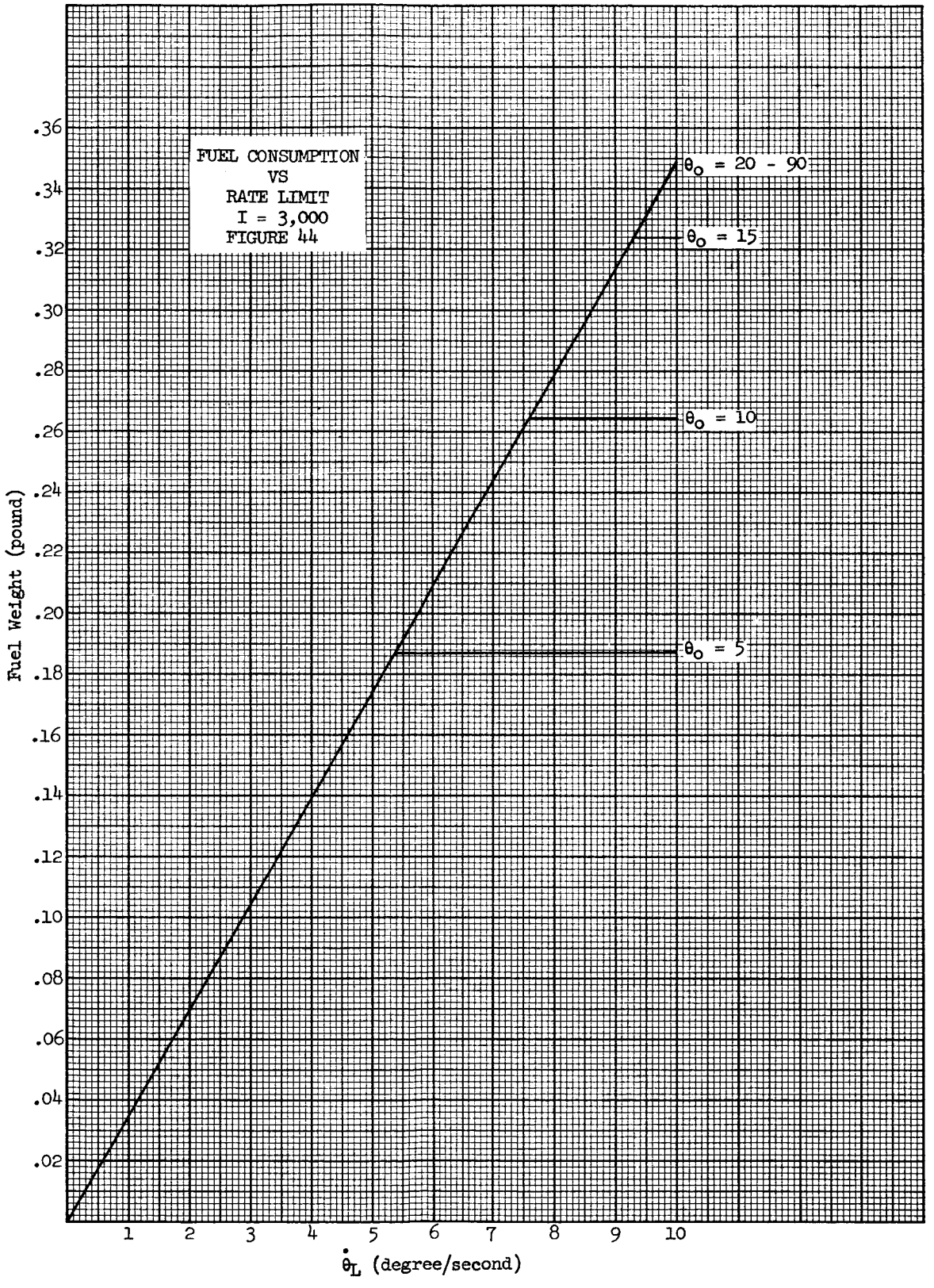
FUEL CONSUMPTION
VS
RATE LIMIT
I = 3,000
FIGURE 44
θ_o = 20 - 90
θ_o = 15
θ_o = 10
θ_o = 5
Fuel Weight (pound)
.36
.34
.32
.30
.28
.26
.24
.22
.20
.18
.16
.14
.12
.10
.08
.06
.04
.02
1
2
3
4
5
6
7
8
9
10
$\dot{\theta}_L$ (degree/second)

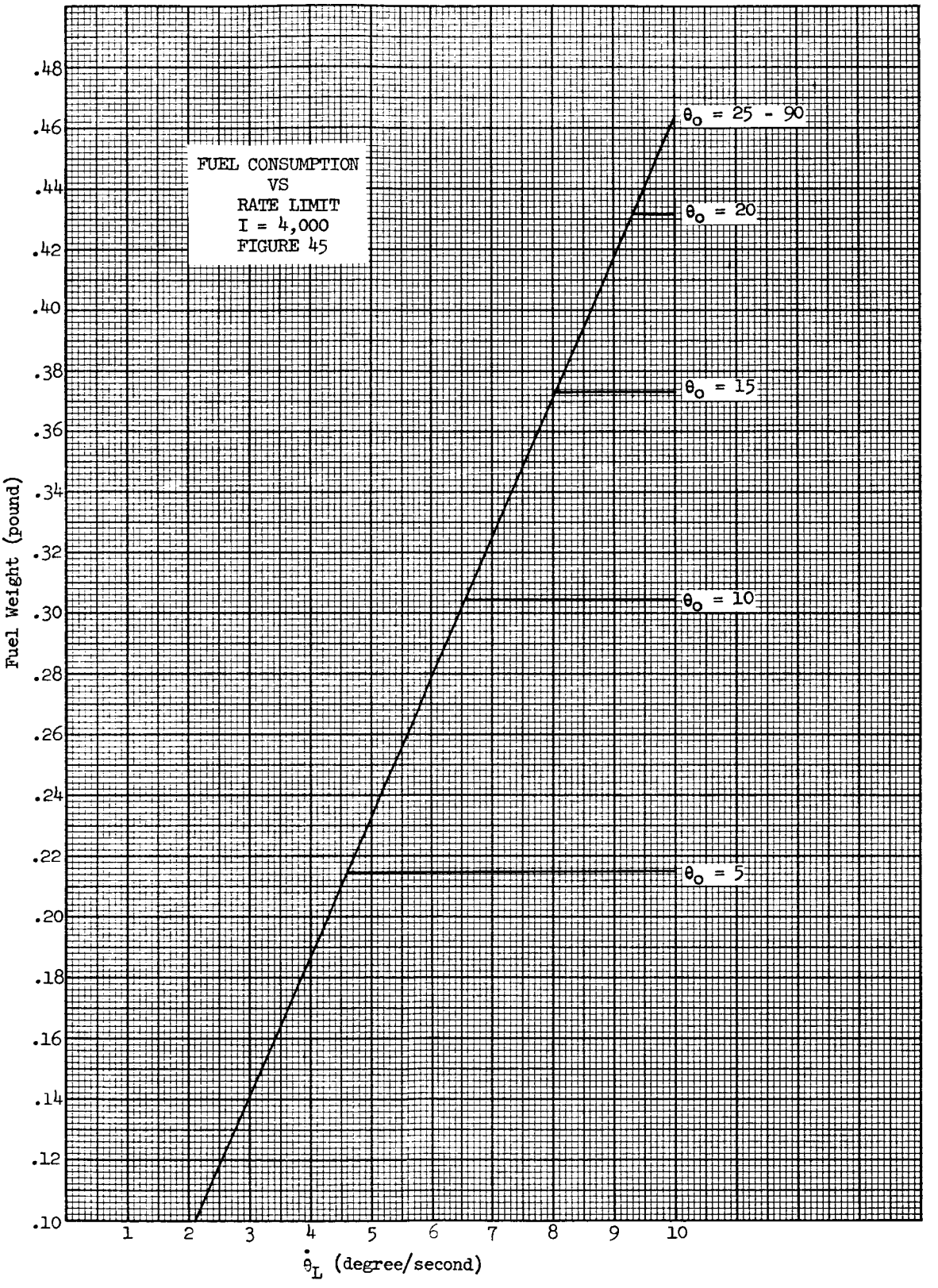
FUEL CONSUMPTION
VS
RATE LIMIT
I = 4,000
FIGURE 45
Fuel Weight (pound)
.48
.46
.44
.42
.40
.38
.36
.34
.32
.30
.28
.26
.24
.22
.20
.18
.16
.14
.12
.10
1
2
3
4
5
6
7
8
9
10
$\dot{\theta}_L$ (degree/second)
θ_o = 25 - 90
θ_o = 20
θ_o = 15
θ_o = 10
θ_o = 5

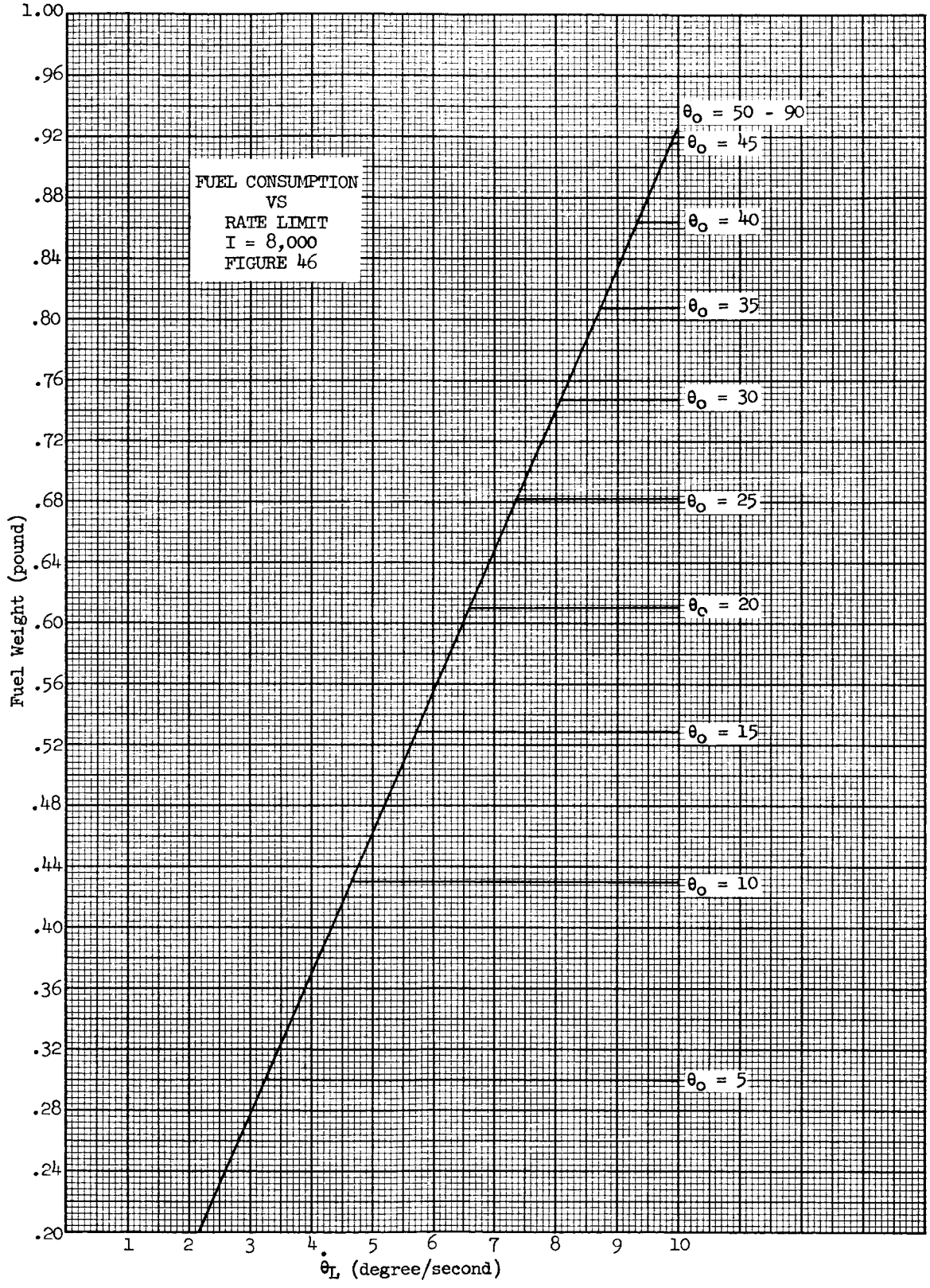
FUEL CONSUMPTION
VS
RATE LIMIT
I = 8,000
FIGURE 46
Fuel Weight (pound)
1.00
.96
.92
.88
.84
.80
.76
.72
.68
.64
.60
.56
.52
.48
.44
.40
.36
.32
.28
.24
.20
1
2
3
4
5
6
7
8
9
10
$\dot{\theta}_L$ (degree/second)
θ_o = 50 - 90
θ_o = 45
θ_o = 40
θ_o = 35
θ_o = 30
θ_o = 25
θ_o = 20
θ_o = 15
θ_o = 10
θ_o = 5

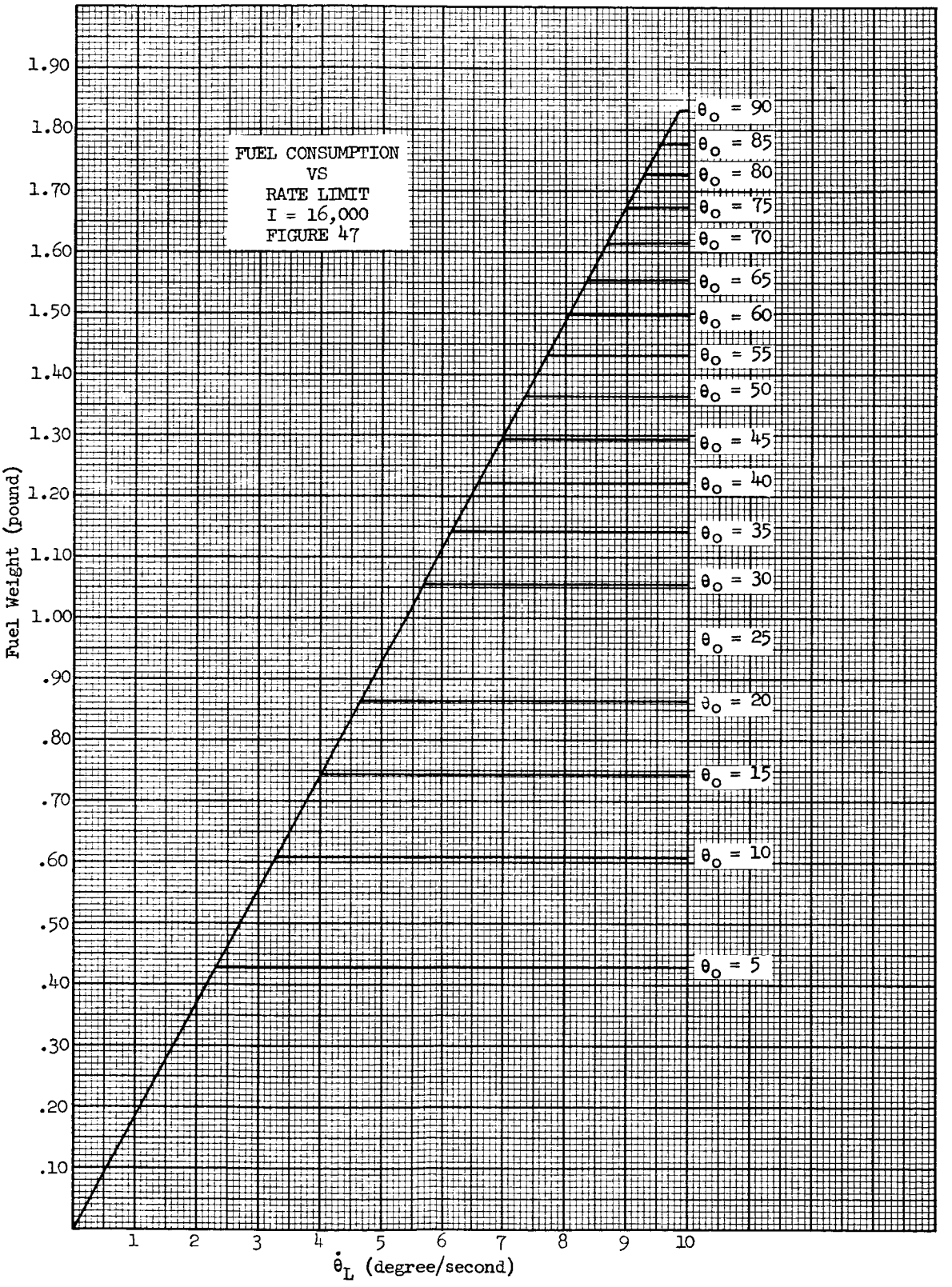
FUEL CONSUMPTION
VS
RATE LIMIT
I = 16,000
FIGURE 47
Fuel Weight (pound)
1.90
1.80
1.70
1.60
1.50
1.40
1.30
1.20
1.10
1.00
.90
.80
.70
.60
.50
.40
.30
.20
.10
θo = 90
θo = 85
θo = 80
θo = 75
θo = 70
θo = 65
θo = 60
θo = 55
θo = 50
θo = 45
θo = 40
θo = 35
θo = 30
θo = 25
θo = 20
θo = 15
θo = 10
θo = 5
1
2
3
4
5
6
7
8
9
10
θ̇L (degree/second)

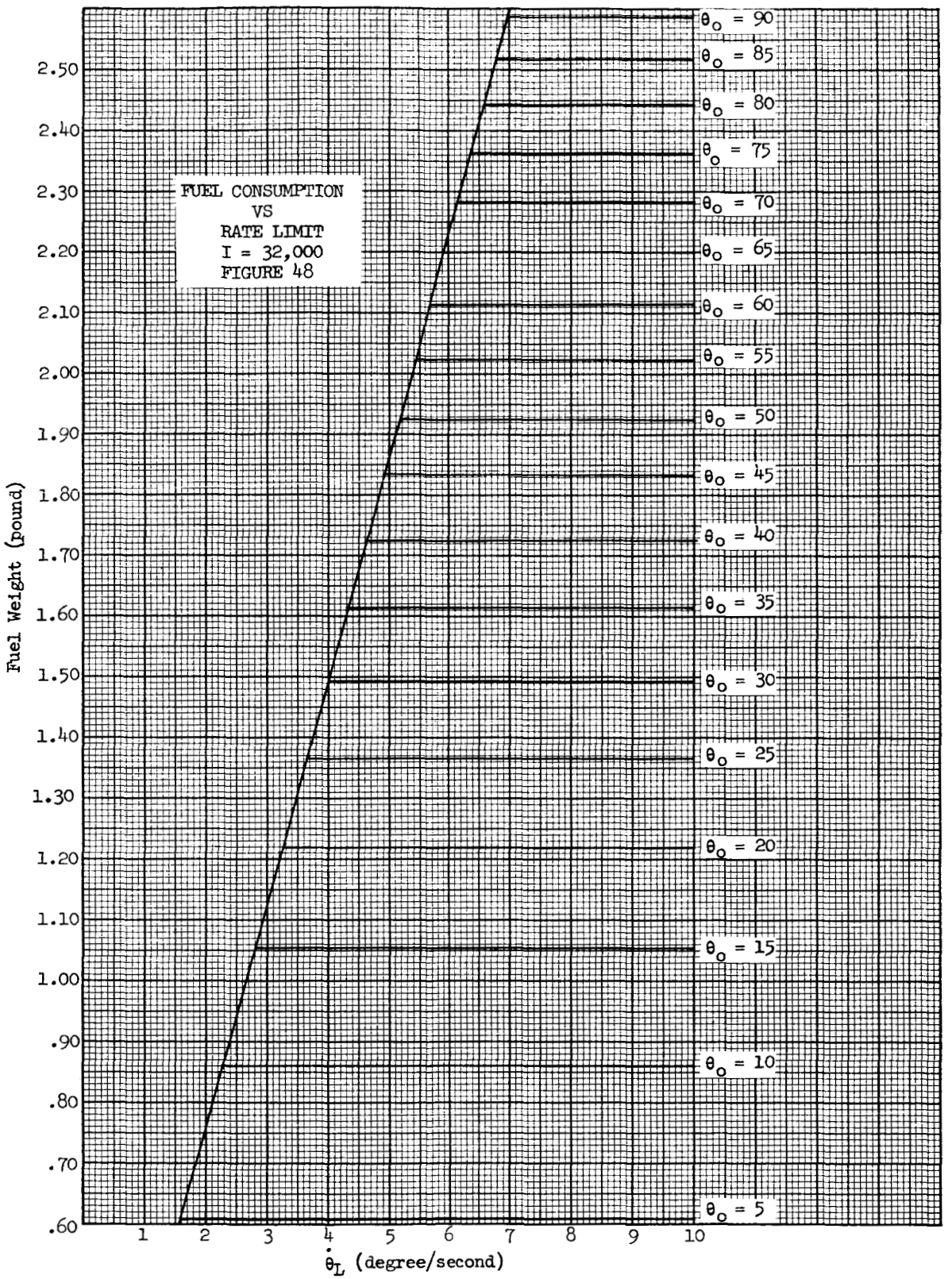
FUEL CONSUMPTION
VS
RATE LIMIT
I = 32,000
FIGURE 48
Fuel Weight (pound)
2.50
2.40
2.30
2.20
2.10
2.00
1.90
1.80
1.70
1.60
1.50
1.40
1.30
1.20
1.10
1.00
.90
.80
.70
.60
1
2
3
4
5
6
7
8
9
10
$\dot{\theta}_L$ (degree/second)
θ_o = 90
θ_o = 85
θ_o = 80
θ_o = 75
θ_o = 70
θ_o = 65
θ_o = 60
θ_o = 55
θ_o = 50
θ_o = 45
θ_o = 40
θ_o = 35
θ_o = 30
θ_o = 25
θ_o = 20
θ_o = 15
θ_o = 10
θ_o = 5

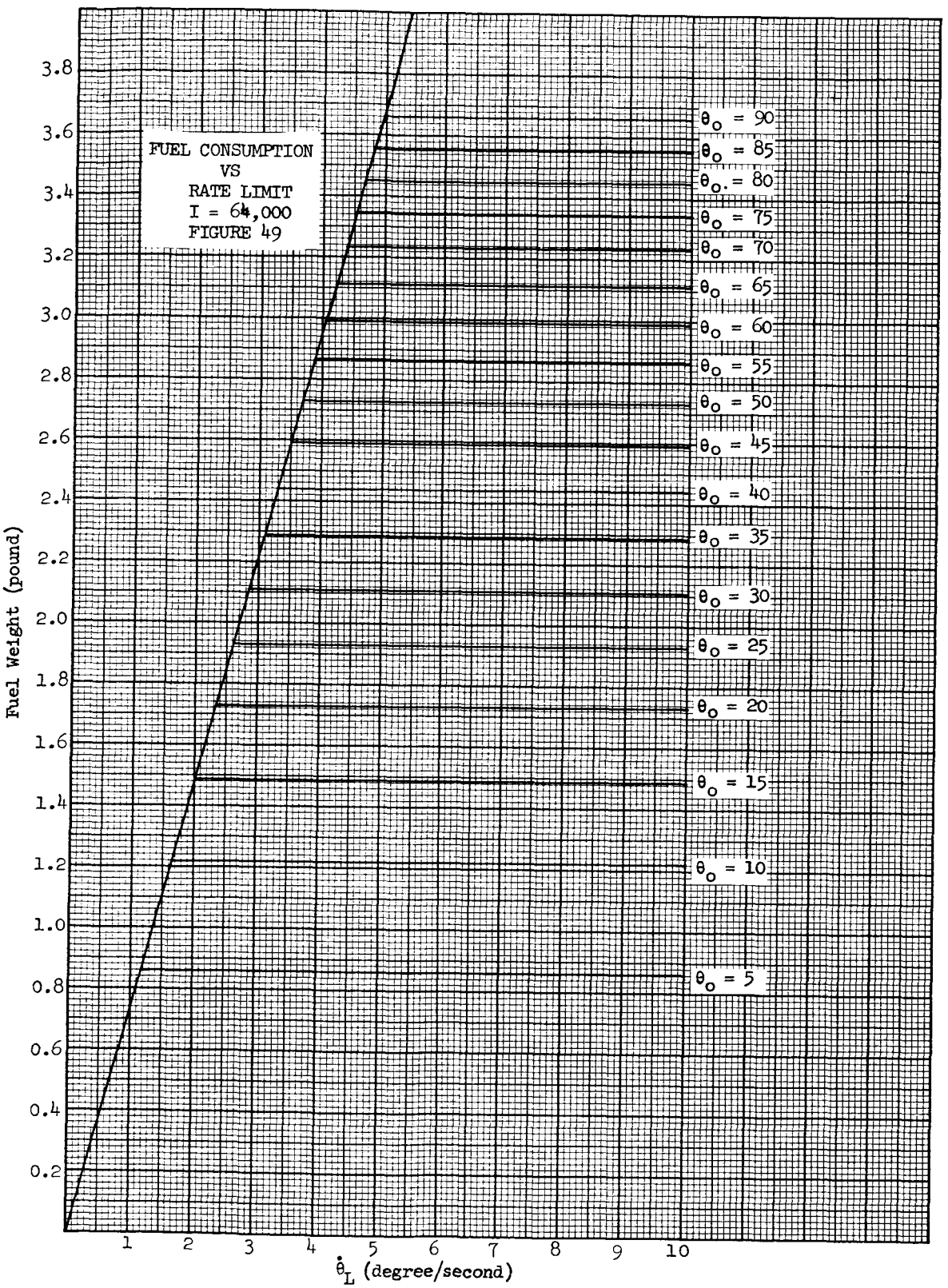
FUEL CONSUMPTION
VS
RATE LIMIT
I = 64,000
FIGURE 49
Fuel Weight (pound)
3.8
3.6
3.4
3.2
3.0
2.8
2.6
2.4
2.2
2.0
1.8
1.6
1.4
1.2
1.0
0.8
0.6
0.4
0.2
1
2
3
4
5
6
7
8
9
10
$\dot{\theta}_L$ (degree/second)
θ_o = 90
θ_o = 85
θ_o = 80
θ_o = 75
θ_o = 70
θ_o = 65
θ_o = 60
θ_o = 55
θ_o = 50
θ_o = 45
θ_o = 40
θ_o = 35
θ_o = 30
θ_o = 25
θ_o = 20
θ_o = 15
θ_o = 10
θ_o = 5

limit is set high enough to prohibit rate limiting for a particular θ_o, fuel consumption becomes a constant or independent of $\dot{\theta}_L$. The amount of fuel consumed is then only a function of θ_o and inertia. In Figure 43, plotted for an inertia of 2,000 slug-feet squared, rate limiting for an initial error of five degrees occurs until the rate limit is above 6.57 degrees per second. Beyond 6.57, fuel consumption is the same, 0.1525 pounds per five degree attitude maneuver. Rate limiting ceases for a 10 degree θ_o at 9.3 degrees per second. For larger inputs, rate limit and fuel consumption in any of the attitude changes are directly proportional to the choice of $\dot{\theta}_L$.

5. SENSOR ACCURACY

5.1 Test Description. To establish accuracy requirements for sensors to be utilized with the ODAACS control program, a series of simulation runs were made in which angular data generated by the simulation of the controlled plant was rounded off to successively fewer binary bits. Thus, resolution became increasingly poorer. The process was continued until unsatisfactory performance resulted from the poor angular resolution of the input data. At this point, necessary data resolution was determined.

5.2 Test Results. Accurate input data is required for accurate rate and acceleration derivation. It was demonstrated in Paragraph 3.6 and Figure 20 that switchover accuracy is most sensitive to errors in the switching constant K_n or K_p, simple functions of derived acceleration. Therefore, it can be anticipated that performance will deteriorate to an unacceptable point when accuracy in the computation of K_n or K_p becomes too poor as occurred during the tests when angular data was rounded to the binary equivalent of 11 bits. At this point an error of 0.053 second in the computed value of K_n caused the limit cycle region to be missed on the first attempt. The error did not result in instability, only hunting for the limit cycle. Figure 50 illustrates the error in the computation of K_n as a function of the number of binary bits of input data resolution. The most severe drop in computational accuracy comes at an input resolution of 11 bits. The resolution required of input data sensors is therefore 12 bits for design performance of the ODAACS Program.

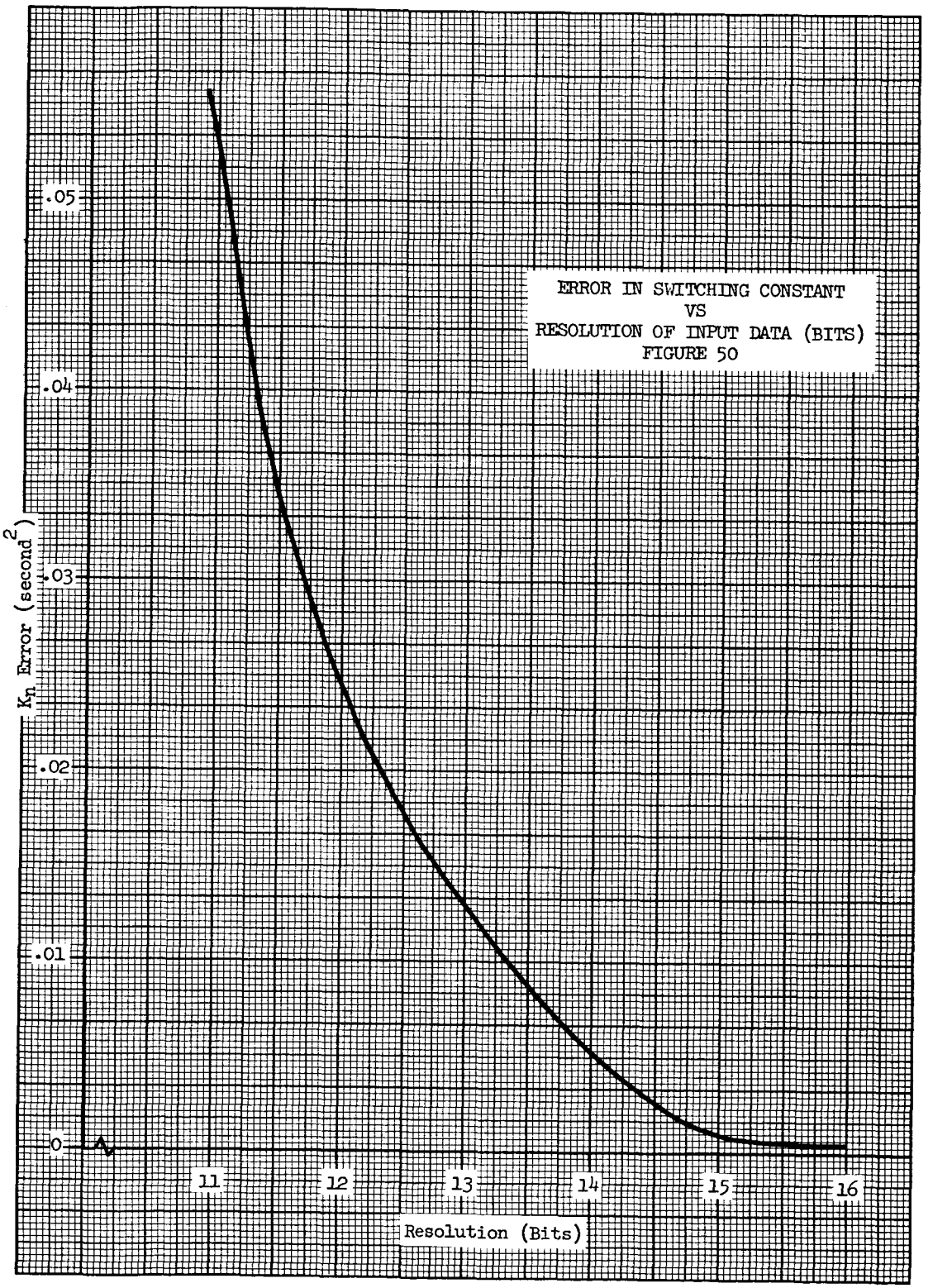
ERROR IN SWITCHING CONSTANT
VS
RESOLUTION OF INPUT DATA (BITS)
FIGURE 50
.05
.04
.03
.02
.01
0
K_n Error (second^2)
11
12
13
14
15
16
Resolution (Bits)

6. COMPUTER REQUIREMENTS

The ODAACS control technique, implemented for the complete three axis case, requires 689 words of memory if a single address, serial machine with a simple set of instruction codes and no indexing or address modification capabilities is employed. Table II gives the breakdown of memory requirements by subprogram.

TABLE II
ODAACS MEMORY REQUIREMENTS

Subprogram	Program Storage	Data and Working Storage	Total
A	208	84	292
B	74	54	128
Theta	81	51	132
Main	77	60	137
Totals	440	249	689

Inputs - Three analog or 12-bit digital channels

Outputs - Six discrete level outputs (ON-OFF)

Input/output requirements are small, only three 12-bit digital input channels and six discrete ON-OFF output channels required.

There is no stringent computational speed requirement since the program operates on the basis of real time inputs. Computations are simple and may be interrupted for other data processing requirements without loss of control capability. It is necessary, however, to provide the three inputs periodically. A sample time of one millisecond per channel is sufficient.

If the computer possesses any indexing or address modification capability,

the program can be condensed considerably from previously stated memory requirements.

7. RESULTS AND FUTURE WORK

7.1 Results. The feasibility of the ODAACS concept has been demonstrated by the results obtained from the simulation performed in this Study. The most extreme changes in system parameters did not cause control instability because the control program is designed to make the optimum decision based upon the measured state of the plant and correct for any errors in the previous decision. The converging decision process always establishes the best trial system state that the physical control system (i.e. thrusters) can accomplish.

The accommodated torque to inertia ratio range is a function of the ODAACS design. Acceleration on the lower end is limited by the values selected for θ_{L2} and $\dot{\theta}_c$. The limit cycle box should be entered from the top; that is, the error should be less than θ_{L2} before the error rate is less than $\dot{\theta}_c$ to assure acquisition of the limit cycle after termination of torque. Since higher acceleration is characterized by a steeper phase plane parabola in the vicinity of the origin, the highest acceleration which can be controlled is one allowing a change of ρ between $\dot{\theta}_c$ and the zero rate. Thus, the upper limit on acceleration is established by the choice of $\dot{\theta}_c$ and ρ in the theta subroutine.

The design of the ODAACS control program for a particular application, then, is simply the choice of θ_{L2}, $\dot{\theta}_c$ and ρ for the particular maximum and minimum acceleration anticipated. The selection of $\dot{\theta}_L$ is predicated on the trade-off between fuel consumption and speed of response. With the freedom to make design choices, there is theoretically no limit to either the range of accelerations or torque to inertia ratio that the ODAACS can control.

Limit cycle control parameters are determined by the required attitude limits (θ_{L2}) and minimum impulse available ($\dot{\theta}_n$ and $\dot{\theta}_p$). The selection of $\dot{\theta}_n$ and $\dot{\theta}_p$ is influenced also by the anticipated bias torque.

Input data must have a basic resolution of 12 bits to maintain accurate control. This resolution is within the state of the art for angular transducers.

7.2 Additional Capabilities. An additional capability for fuel management, based on a variety of management criteria, can be incorporated into the ODAACS Program if desired. Fuel management is dependent upon the ability to compute the amount of fuel consumed during an attitude maneuver, a quantity directly proportional to the change in rate.

If the system accelerates for a length of time (t), the change in rate is

$$\Delta\dot{\theta} = \ddot{\theta}t \tag{35}$$

and since

$$\ddot{\theta} = \frac{1}{2K},\ K = K_n,\ K_p \tag{36}$$

$$\Delta\dot{\theta} = \frac{t}{2K} \tag{37}$$

The weight of fuel consumed in t is

$$W = \frac{T}{I_{sp}}t \tag{38}$$

where T = thrust in pounds, t = time in seconds and I_{sp} = rocket specific impulse $\left(\frac{\text{pounds per second}}{\text{pounds}}\right)$. Solving Equation (38) for t

$$t = \frac{I_{sp}}{T}W, \tag{39}$$

the time to consume W pounds of fuel. Substituting Equation (39) into Equation (37)

$$\Delta\dot{\theta} = \frac{I_{sp}}{2KT} W \text{ and} \tag{40}$$

$$W = \left(\frac{2KT}{I_{sp}}\right) \Delta\dot{\theta} \tag{41}$$

In any attitude maneuver employing the ODAACS, the total change in rate will be

$$\Delta\dot{\theta} = 2\dot{\theta}_{max}, \quad \dot{\theta}_{max} \leq \dot{\theta}_L \tag{42}$$

Therefore, the fuel consumed during any attitude maneuver is

$$W = \left(\frac{4KT}{I_{sp}}\right) \dot{\theta}_{max} \tag{43}$$

where the limit on $\dot{\theta}_{max}$ as established in Equation (42) is $\dot{\theta}_L$. The proportional term in Equation (43) is the quantity either updated by the ODAACS Program or not subject to large changes throughout the course of the mission. By adjusting $\dot{\theta}_L$, a boundary on the fuel consumed in an attitude maneuver can be established, thus providing fuel management.

One possible criterion for fuel management is to restrict the rate of fuel consumption to assure availability for the entire mission. The criterion for fixed mission times can be stated:

$$\frac{\text{Fuel Remaining}}{\text{Mission Time Remaining}} = \text{Allowable Fuel Consumption Rate} = \text{Constant}$$

The rate limit ($\dot{\theta}_L$) is adjusted downward if fuel is being consumed faster than the allowable rate or upward if the rate is slower than allowable. If it is decided to lengthen the mission after the mission has begun, the criterion establishes a lower allowable fuel consumption and decreases the rate limit accordingly. However, information would have to be available on the time history of attitude changes throughout the mission. If the rate limit is lowered, the response time increases because a longer time is spent drifting at the

rate limit. This type fuel management is most applicable to long mission time unmanned satellites with an active attitude control system.

7.3 Future Work. With the performance of the basic ODAACS control concept now established, a logical extension of the effort is the design of the complete three axis control program. The basic problem involved in this design is whether the control programs for each individual axis should exercise their control by operating on each axis sequentially or simultaneously. The solution of this problem must consider the effects of inertial cross-coupling between axes.

Some restriction on the class of applications to be investigated will have to be imposed since a perfectly general investigation will be an extremely large task, most of which would be incidental to the basic problem of designing the "best" three axis control program with a reasonable hardware implementation. During the program design stage the hardware requirements would be rigidly defined. Once defined, the hardware development would be completed and a series of tests of the actual control system in a real or simulated environment conducted.

The scope and direction of any future work would be better defined by consultation with the agencies responsible for application and research in the field of attitude control of space vehicles.